DEPARTMENT OF MATHEMATICS

RESEARCH COMPENDIUM 2023

SRI CHANDRASEKHARENDRA SARASWATHI VISWA MAHAVIDYALAYA

(Deemed to be University u/s 3 of UGC act 1956)

(Accredited with "A" Grade by NAAC)

ENATHUR, KANCHIPURAM - 631 561.


Cabell's Directories
Journal TOCs
EBSCO
ULAKBİM TR DİZİN
ProQuest
Scopus
ELSEVIER
zbMATH
the first resource for mathematics

RESEARCH COMPENDIUM
2023
Contents

	Matematika. Mekhanika. Komp'yuternye Nauki, 33(1), 2023, 119–129.	
9.	**Varadha Raj Manivannan, Victor Anandam,** "A Perturbed Averaging Operator on Finite Graphs"– Linear Algebra and its Applications, 680, 2023, 208-219.	101

ACYCLIC DISTANCE 2 DOMINATION NUMBER OF A GRAPH

N. Saradha

Department of Mathematics, SCSVMV

Abstract

A distance-2 dominating set D⊆V of a graph G is a acyclic distance-2 dominating set if the induced sub graph <V-D> is a acyclic. The acyclic distance-2 dominating number is the minimum cardinality of a acyclic distance-2 dominating set. In this paper, we defined the notion of acyclic distance - 2 domination in graph. We got many bounds on acyclic distance - 2 domination number. Exact values of this new parameter are obtained for some standard graphs. Nordhaus - Gaddum type results are also obtained for this new parameter.

Key words: Distance k-domination, Distance 2-domination, Acylic domination, Split distance 2-Domination, Non split distance 2-domination

1. Introduction

All graphs considered here are simple, finite, connected and undirected. Let n and m denote the order and size of a graph G. We use the terminology of [6]. Let Δ ((δ)) denote the maximum (minimum) degree and ⌊ ⌋(⌈ ⌉) the greatest (least) integer less (greater) than or equal to x. The concept of domination in graphs was introduced by Ore[2]. A set D ⊆ V(G) is said to be a dominating set of G, if every vertex in V(G)\D is adjacent to some vertex in D. The cardinality of a minimum dominating set in G is called the domination number of G and is denoted by γ(G). The problem of finding a minimal distance k-dominating set was considered by Slater[8] with special reference to communication networks while the distance k-dominating set was defined by Henning et al.[7]. For an integer k ≥ 1, a set D ⊆ V(G) is a distance k-dominating set of G, if every vertex in V(G)\D is within distance k from some vertex v ∈ D. The minimum cardinality among all distance k-dominating sets of G is called the distance k-domination number of G and is denoted by γ_k(G). The minimal distance - 2 dominating set in a graph G is a distance - 2 dominating set that contains no distance - 2 dominating set as a proper subset. The distance - 2 open neighborhood of a vertex $v \in V$ is the set, ($N_{\leq 2}(v)$), of vertices within a distance of two from (v). A distance - 2 dominating set of a graph G is a split distance - 2 dominating set if the induced sub graph < V-D > is disconnected. The split distance - 2 domination number $\gamma_{s\leq 2}(G)$ is the minimum cardinality of a minimal split distance - 2 dominating set. A distance -2 dominating set D ⊆ V of a graph G is a non-split distance -2

dominating set if the induced sub graph is connected. The non-split distance -2 domination number $\gamma_{ns\leq 2}(G)$ is the minimum cardinality of a nonsplit distance -2 dominating set. A set $S \subseteq V(G)$ is called an acyclic set if G[S] contains no cycles. The concept of acyclic domination was i ntroduced by Hedetniemi et al. [15]. A set $S \subseteq V(G)$ is called an acyclic dominating set of G if it is both acyclic and dominating. The minimum cardinality of an acyclic dominating set in a graph G is called the acyclic domination number of G, denoted by $\gamma_a(G)$.

2. Acyclic Distance 2-Domination

Definition 2.1 A distance-2 dominating set $D \subseteq V$ of a graph G is a acyclic distance-2 dominating set if the induced sub graph <V-D> is a acyclic. The acyclic distance-2 dominating number is the minimum cardinality of acyclic distance-2 dominating set and is denoted by $\gamma_{a\leq 2}(G)$.

Definition 2.2 The minimal acyclic distance-2 dominating set in a graph G is acyclic distance-2 dominating set that contains no acyclic distance-2 dominating set as a proper subset.

Example 2.3

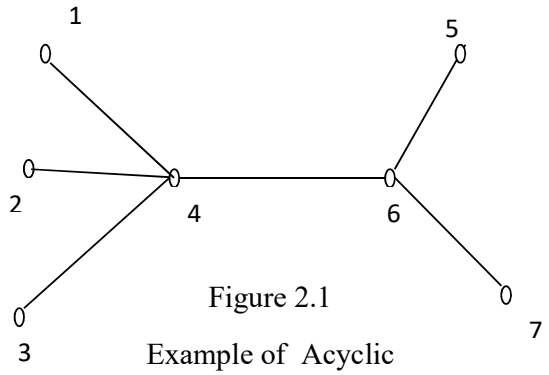

Figure 2.1

Example of Acyclic Distance 2-Domination

Here D={4} , <V-D>={1,2,3,5,6,7}

$\gamma_{a\leq 2}(G)=1$

Observation 2.4

1. For any path P_n, for $n\geq 2$

$$\gamma_{a\leq 2}(P_n)=\left\lceil \frac{n}{5} \right\rceil$$

2. For any cycle C_n, for $n\geq 3$

$$\gamma_{a\leq 2}(C_n)=\left\lceil \frac{n}{5} \right\rceil$$

3. For any complete graph K_n, for $n\geq 3$

$$\gamma_{a\leq 2}(K_n)=n-2$$

4. For any star graph $K_{1,m}$, for $m\geq 1$

$$\gamma_{a\leq 2}(K_{1,m})=1$$

5. For any wheel graph W_n, for $n\geq 2$

$$\gamma_{a\leq 2}(W_n)=2$$

6. For any friendship graph F_n, for $n\geq 2$

$$\gamma_{a\leq 2}(F_n)=1$$

7. For any complete bipartite graph $K_{m,n}$, for $m<n$; $n,m\geq 1$

$$\gamma_{a\leq 2}(K_{n,m})=m-1$$

Theorem 2.5 For any graph G, $\gamma_{\leq 2}(G) \leq \gamma_{a\leq 2}(G)$

Proof

Every acyclic distance-2 dominating set of G is a distance-2 dominating set of G,

We have $\gamma_{\leq 2}(G)\leq\gamma_{a\leq 2}(G)$

Theorem 2.6 For any graph G, $\gamma_{a\leq 2}(G)\leq\gamma_a(G)$

Proof

Every acyclic dominating set of G is a acyclic distance-2 dominating set of G,

We have $\gamma_{a\leq 2}(G)\leq\gamma_a(G)$

Proposition 2.7

For any graph G,

$\gamma_{a\leq 2}(G)= \gamma_{ns\leq 2}(G)=\gamma_{s\leq 2}(G) =\gamma_s(G)=\gamma(G)=\gamma_{\leq 2}(G)$ if and only if G is a star graph $K_{1,m}$,for $m>1$.

Proposition 2.8

For any graph G,

$\gamma_{a\leq 2}(G)=\gamma_{s\leq 2}(G)=\gamma_s(G)=\gamma(G)=\gamma_{\leq 2}(G)$ if and only if G is a friendship graph F_n.

Theorem 2.9 For any graph G , $\gamma_{a\leq 2}(G)=P-\Delta(G)$ if and only if G is a star graph $K_{1,m}$ for $m>1$, where p is number of vertices.

Theorem 2.10 Let G be any connected graph of order greater than or equal to 3, then

$\gamma_{a\leq 2}(G)\leq n-1$, where n is the number of vertices.

Theorem 2.12 For any graph G, $\gamma_{a\leq 2}(G)\leq n-\Delta(G)$

Theorem 2.13 For any tree Tn, $\gamma_{a\leq 2}(G)\leq n-p$ where n is number of vertices and P is number of end vertices.

Note 2.14 For any tree T_n , which is a star graph

$\gamma_{a\leq 2}(G)=n-p$ where n is number of vertices and P is number of end vertices.

Nordhas - Gaddum Type Results

Theorem 2.15 Let G be a graph such that G and $\overline{G}$ have no isolates. Then ,

$\gamma_{a\leq 2}(G)+\gamma_{a\leq 2}(\overline{G})\leq 2(n-1)$

$\gamma_{a\leq 2}(G).\gamma_{a\leq 2}(\overline{G})\leq (n-1)^2$

Proof

The results follow from Theorem 2.10.

3. Conclusion In general, the concept of dominating sets in graph theory finds wide applications in different types of communication networks. Identification of a dominating set, which is fault tolerant, will be useful in the central location theory. Thus in this paper, we defined the notion of acyclic distance - 2 domination in graphs. We obtained many bounds on acyclic distance - 2 domination number. Exact values of this new parameter are obtained for some standard graphs. Nordhaus - Gaddum type results are also obtained for this new parameter. They play very vital role in Coding theory, Computer science, Operations Research, Switching Circuits, and Signal Processing Electrical Networks etc.

References

[1] E.J.Cockayne, S.T.Hedetniemi (1977), Towards a Theory of Domination in Graphs, Networks. vol.7, pp.247-261.

[2] Ore, O.(1962),Theory of Graphs. American Mathematical Society colloq. Publ., Providence, R1, 38.

[3] Domke G.S., Dunbar J.E. and Markus, L.R (2004), The Inverse domination number of a graph, Ars. Combin 72, pp.149-160.

[4] P. Fraisse(1988), A note on distance dominating cycles. Discrete Math. 71, pp.89-92.

[5] A. Hansberg, D. Meierling, and L. Volkmann (2007), Distance domination and distance irredundance in graphs. Electronic J.Combin. 14, #R35.

[6] Harary. F (1969) Graph Theory, Addison – Wesley Reading Mars.

[7] Haynes, T.W., Hedetniemi .S.T. and Slater.P.J (1998), Domination in Graphs: Advanced Topics, Marcel Dekker Inc. New York, U.S.A.

[8] Haynes, T.W., Hedetniemi .S.T. and Slater.P.J (1998)b, Fundamentals of domination in Graphs, Marcel Dekkel Inc. New York, U.S.A.

[9] M.A. Henning, O.R. Oellermann and H.C. Swart (1991), Bounds on distance domination parameters. J.Combin. Inform. System Sci 16, pp.11-18.

[10] V.R. Kulli (2010), Theory of domination in graphs. Vishwa International Publications, Gulbarga, India.

[11] V. R. Kulli (2012), Advances in domination theory Vishwa International Publications, Gulbarga, India.

[12] D. Meierling and L.Volkmann (2005), A lower bound for the distance k-domination number of trees, Result. Math. 47, pp.335- 339.

[13] Randy Davila, Caleb Fast, Michael A. Henning and Franklin Kenter (2015), Lower bounds on the distance domination number of a Graph. arXiv:1507.08745v1 [math.co] 31.

[14] F. Tian and J.M.Xu (2009), A note on distance domination numbers of graphs. Australasian j. Combin. 43, pp.181-190.

[15] S.M. Hedetniemi, S.T. Hedetniemi, D.F. Rall, Acyclic domination, Discrete Math. 222 (2000) 151–165.

An $M^{[X]}/G^{(1,K)}/1$ queue with unreliable server and Bernoulli vacation

P. Nagarajan*

Department of Mathematics,
SCSVMV University,
Enathur, Kanchipuram-631561, India
Email: nagarajandixit@gmail.com
*Corresponding author

R. Kalyanaraman

Department of Mathematics,
Annamalai University,
Annamalai Nagar-608002, India
Email: r.kalyan24@rediff.com

Abstract: A Poisson arrival queue with batch arrival, service in a batch of variable size with a minimum of '1' and a maximum of 'K' customers is considered. After completion of service to the customers the server takes on Bernoulli vacation, also during the service of customers the server may breakdown. The supplementary variable technique is applied. The probability generating function of number of customers in the queue at different server states, mean queue size, and probability of server being idle are obtained. Some particular models are deduced. The amenability of the numerical treatment of this study is carried out. The numerical results are given in the form of tables and figures.

Keywords: Poisson process; batch arrival; batch service; Bernoulli vacation; unreliable server; supplementary variable technique; operating characteristics.

Reference to this paper should be made as follows: Nagarajan, P. and Kalyanaraman, R. (2023) 'An $M^{[X]}/G^{(1,K)}/1$ queue with unreliable server and Bernoulli vacation', *Int. J. Mathematics in Operational Research*, Vol. 25, No. 4, pp.492–510.

Biographical notes: P. Nagarajan completed his PhD in Mathematics from the Annamalai University in 2017. He is currently working as a Senior Assistant Professor at the Department of Mathematics, SCSVMV Deemed to be University, Enathur, Kanchipuram. His research interest includes queueing theory.

R. Kalayanaraman obtained his PhD in the field of queueing theory from Annamalai University. He is currently working as a Professor of Mathematics at the Department of Mathematics, Annamalai University, Chidambaram, Tamil Nadu. He has published more than hundred papers in national and international journals.

This paper is a revised and expanded version of a paper entitled '$M^{[X]}/G^{(1,K)}/1$ queue with unreliable server and with Bernoulli vacation' presented at 8th International Conference on Mathematics and Computing (ICMC-2022), VIT, Vellore, Tamil Nadu, India, 6–8 January 2022.

1 Introduction

Several researchers have studied queueing systems with batch arrival and general batch service. The essential fundamentals of bulk queues are explained in Chaudhry and Templeton (1983). Finite capacity queue, general service with batches and queue length dependent service rates has been analysed by Gupta and Banerjee (2018). An infinite buffer queueing system with versatile bulk-service rule under batch-size-dependent service policy has been studied by Pradhan (2020).

The vacation policies are studied for the purpose of effective utilisation of the server's idle time for secondary jobs. It is well known that the queues with vacation are more important in day to day life. Heavy traffic situations encountered in computers, communication, manufacturing, and production systems are modelled as queueing systems with vacation. The batch arrival general service queue with server vacation has been analysed in detail by Baba (1986). A batch arrival general service queue with balking, startup and with vacation has been analysed in detail by Nithya and Haridass (2020). A batch arrival queue with random vacation policy and with heterogeneous repeated services has been studied by Kalita and Choudhury (2021). The vacation queueing models have been analysed by several researchers (Baba and Dshalalow, 1986; Ke, 2007; Jain and Upadhyaya, 2009; Balasubramanian and Arumuganathan, 2011; Jeyakumar and Senthilnathan, 2016; Kumar et al., 2021).

In everyday life, people can easily see the occurrences of server breakdowns for different reasons. So the queuing models which incorporate the assumption of server breakdown are most suitable for the real-life scenario. A survey on queues with interruption has been done by Krishnamoorthy et al. (2014). An extensive analysis of a batch arrivals queue with general retrial time, breakdowns, repairs and reserved time has been done by Zirem et al. (2018). Batch arrival and fixed batch service queue with different server's interruptions and its application in energy consumption has been studied by Yuvarani and Vijayalakshmi (2020). Batch arrival Poisson queue with breakdown and repairs has been discussed by Rajan et al. (2020). Yu and Tang (2022) have investigated a renewal input bulk arrival queue with a fault-tolerant server, in which the server can keep working with a low service rate even if the partial failure occurs and only when there are no customers in the system, the partial failure can be removed.

Some authors have incorporated the server breakdown on the vacation queuing model. Also, the vacation queueing model with the unreliable server under different environmental assumptions has been studied. The steady state analysis of an $M^{[X]}/G/1$ queueing system with the server operates under N policy, single vacation and with breakdown is carried out by Ke and Lin (2008) in their article. A batch arrival queue with a Bernoulli schedule vacation, with delayed repair and with a standby server is analysed by Rehab et al. (2012). An $M/G/1$ unreliable server, Bernoulli vacation queue with two phases of service has been investigated by Choudhury and Deka (2012).

Kalyanaraman and Nagarajan (2016) have analysed a Poisson queue with batch arrival and batch service where they have assumed that the server may take a vacation and the server may break down. Usually the unreliable server is considered with the assumption that the repair to the server starts immediately after the server breaks down. It is quite natural that as a result of a sudden breakdown, the server may have to wait for a random time (known as delay time) for repair to start in a real scenario. An unreliable bulk queueing model with optional services, Bernoulli vacation schedule and balking is studied by Kumar (2018). A non-Markovian single server batch arrival queueing system with multi-stage of service, service interruptions and deterministic server vacation has been discussed by Vignesh et al. (2018). Jiang and Xin (2019) have presented a more detailed analysis of a single server queueing system with working breakdowns and delaying repair under a Bernoulli-schedule-controlled policy for taking repair. Batch arrival general service queue and optional service, vacation under randomised policy is studied by Singh et al. (2018). Saggou et al. (2019) have derived the probability generating function of the joint probability of system size and the server state of an $M^{[X]}$/G/1 queue with breakdowns, repair, Bernoulli vacation, two delays and geometric loss. Singh et al. (2019) have analysed a bulk queue with additional optional service, vacation and unreliable server. Batch arrival, batch service queue with server breakdown without interruption and controllable arrivals during multiple adaptive vacations has been considered by Jeyakumar and Rameshkumar (2019). Ayyappan and Karpagam (2019) have analysed a batch arrival queue and the server selects customers for service with a minimum of 'a' and a maximum of 'b', in addition to that the server breakdown and immediate repair takes place with a standby server and single vacation. The unreliable bulk arrival queueing system with overloading service, variant arrival rate, close down under multiple vacation policy has been considered by Ayyappan and Nirmala (2021). Fixed batch service queue, unreliable server and with vacation has got attention by Choudhary and Sharma (2022).

In real life situation, one faces the following situation quite often. In manufacturing industries, after the approval, the products are permitted for transportation to the customer shops in bulk via trucks. It is well known that a truck may be loaded with a minimum of 1 and a maximum of K items for transportation service at a time. After transporting the products, if no batches are available for transportation, the truck is used for other work, or the truck may undergo maintenance (vacation period). During the service period (transportation period), the truck may break down and the repair may be started immediately after an occurrence of server break down. The above real life situation can be modelled as queueing system, that triggers us to discuss a batch arrival with a single server where a server provides service for batch customers of variable size with a minimum of '1' and a maximum of 'K' (i.e., $M^{[X]}/G^{(1,K)}/1$ queue) with an unreliable server and with Bernoulli vacation.

The rest of this paper is organised as follows. Section 2 describes the proposed model and its mathematical analysis by finding its probability generating function for the number of customers in the queue. In Section 3, an expression for the mean queue size is derived. Some interesting models as particular cases are deduced in Section 4. In Section 5, the feasibility of implementation of numerical study is carried out for specific environments. Finally, Section 6 contains a brief conclusion.

2 Description of the model and analysis

The arrival process is a Poisson with rate $\lambda > 0$, the customer arrives in batches of variable size X, where X is a random variable with probability $P\{X = j\} = C_j$, whose probability generating function is defined by

$$C(z) = \sum_{j=1}^{\infty} C_j z^j.$$

The server provides service for a batch of customers whose size is a random variable with minimum batch size 1 and maximum size $K(> 0)$ and the service time distribution of each batch is generally distributed with distribution function $G(x)$. After completion of service the server takes a vacation of random duration with probability p or stays in the system with probability $1 - p$ independent of the number of customers in the queue. The vacation period is a random variable with a general probability distribution function $B(x)$. In addition the server may break down during the service of customers. The number of breakdowns are assumed to occur according to a Poisson process with rate 'α'. When the server breaks down, the customer who is in the service will be interrupted and he has to wait at the head of the queue, and the repair of the server will be started immediately. The duration of the repair period is generally distributed with the distribution function $H(x)$.

The supplementary variable technique is used for the analysis. The supplementary variables are elapsed service time, elapsed vacation time, elapsed repair time. We define the following conditional probabilities for the analysis purpose:

- $\mu(x) = \frac{g(x)}{1-G(x)}$ is the conditional probability that the completion of service during the interval $(x, x + dx]$, given that the elapsed service time is 'x'
- $\beta(x) = \frac{b(x)}{1-B(x)}$is the conditional probability that the completion of vacation during the interval $(x, x + dx]$, given that the elapsed vacation time is 'x'
- $\gamma(x) = \frac{h(x)}{1-H(x)}$is the conditional probability that the completion of repair during the interval $(x, x + dx]$ given that the elapsed repair time is 'x'.

The Markov process related to this model is $\{(N(t), S(t)) : t \geq 0\}$ where $N(t)$ be the number of customers in the queue and $S(t)$ be the supplementary variable at time 't'defined as:

$$S(t) = \begin{cases} S_1(t), & \text{Elapsed service time,} \\ S_2(t), & \text{Elapsed vacation time,} \\ S_3(t), & \text{Elapsed repair time.} \end{cases}$$

We define the following probabilities for different server states.

- $P_n(t, x)$ = P {at time 't', there are 'n' customers in the queue (excluding the customer in service) and the elapsed service time is 'x'}
- $V_n(t, x)$ = P {at time 't', there are 'n' customers in the queue and the elapsed vacation time is 'x'}

- $R_n(t,x) = P$ {at time 't', there are 'n' customers in the queue and the elapsed repair time is 'x'}
- $Q_n(t) = P$ {at time 't', there are 'n' customer in the queue and the server is idle}.

Using infinitesimal argument, the system of differential – difference equations for the model are obtained as

$$\frac{dP_0(x)}{dx} = -(\lambda + \mu(x) + \alpha)P_0(x), \tag{1}$$

$$\frac{dP_n(x)}{dx} = -(\lambda + \mu(x) + \alpha)P_n(x) + \lambda \sum_{j=1}^{n} C_j P_{n-j}(x), \text{ for } n = 1, 2, ..., \tag{2}$$

$$\frac{dV_0(x)}{dx} = -(\lambda + \beta(x))V_0(x), \tag{3}$$

$$\frac{dV_n(x)}{dx} = -(\lambda + \beta(x))V_n(x) + \lambda \sum_{j=1}^{n} C_j V_{n-j}(x), \quad \text{for } n = 1, 2, ..., \tag{4}$$

$$\frac{dR_0(x)}{dx} = -(\lambda + \gamma(x))R_0(x), \tag{5}$$

$$\frac{dR_n(x)}{dx} = -(\lambda + \gamma(x))R_n(x) + \lambda \sum_{j=1}^{n} C_j R_{n-j}(x), \quad \text{for } n = 1, 2, ..., \tag{6}$$

$$\begin{aligned} 0 = -\lambda Q + \int_0^\infty R_0(x)\gamma(x)dx \\ + \int_0^\infty V_0(x)\beta(x)dx + (1-p)\int_0^\infty P_0(x)\mu(x)dx \end{aligned} \tag{7}$$

with the boundary conditions

$$\begin{aligned} P_0(0) = (1-p)\int_0^\infty \sum_{j=1}^{K} P_j(x)\mu(x)dx + \int_0^\infty \sum_{j=1}^{K} V_j(x)\beta(x)dx \\ + \int_0^\infty \sum_{j=1}^{K} R_j(x)\gamma(x)dx + \lambda Q, \end{aligned} \tag{8}$$

$$\begin{aligned} P_n(0) = (1-p)\int_0^\infty P_{n+K}(x)\mu(x)dx + \int_0^\infty V_{n+K}(x)\beta(x)dx \\ + \int_0^\infty R_{n+K}(x)\gamma(x)dx, \quad \text{for} \quad n = 1, 2, ..., \end{aligned} \tag{9}$$

$$V_n(0) = p\int_0^\infty P_n(x)\mu(x)dx, \text{ for } n = 0, 1, ..., \tag{10}$$

$$R_n(0) = \alpha\int_0^\infty P_{n-1}(x)dx, \quad \text{for} \quad n = 1, 2, ..., \tag{11}$$

$$R_0(0) = 0 \tag{12}$$

and the normalisation condition

$$Q + \int_0^\infty \sum_{n=0}^{\infty} [P_n(x) + V_n(x) + R_n(x)]dx = 1. \tag{13}$$

For the analysis purpose, the following probability generating functions are defined:

$$P(x,z) = \sum_{n=0}^{\infty} P_n(x)z^n, \quad V(x,z) = \sum_{n=0}^{\infty} V_n(x)z^n,$$

and

$$R(x,z) = \sum_{n=0}^{\infty} R_n(x)z^n, \quad C(z) = \sum_{j=1}^{\infty} C_j z^j.$$

Multiplying equation (2) by z^n, applying $\sum_{n=1}^{\infty}$, and adding with equation (1), lead to

$$\frac{\partial P(x,z)}{\partial x} + (\lambda - \lambda C(z) + \mu(x) + \alpha)P(x,z) = 0. \tag{14}$$

Imitation of such procedure yields

$$\frac{\partial V(x,z)}{\partial x} + (\lambda - \lambda C(z) + \beta(x))V(x,z) = 0 \text{ and} \tag{15}$$

$$\frac{\partial R(x,z)}{\partial x} + (\lambda - \lambda C(z) + \gamma(x))R(x,z) = 0. \tag{16}$$

Solution of above equation (14) is

$$P(z) = \frac{[1 - G^*(a)]A}{az^K - a(1 - p + pB^*(m))G^*(a) - \alpha z[1 - G^*(a)]H^*(m)}. \tag{17}$$

Similar procedure yields

$$V(z) = \frac{apG^*(a)[1 - B^*(m)]A}{m\{az^K - a(1 - p + pB^*(m))G^*(a) - \alpha z[1 - G^*(a)]H^*(m)\}} \text{ and} \tag{18}$$

$$R(z) = \frac{\alpha z[1 - G^*(a)][1 - H^*(m)]A}{m\{az^K - a(1 - p + pB^*(m))G^*(a) - \alpha z[1 - G^*(a)]H^*(m)\}}. \tag{19}$$

Let $S(z)$ be the probability generating function of number of customers in the queue independent of the server state.

Addition of equations (17), (18), and (19), leads to

$$S(z) = P(z) + V(z) + R(z). \tag{20}$$

Now

$$S(z) = \frac{\{[m + \alpha z(1 - H^*(m)](1 - G^*(a)) + apG^*(a)[1 - B^*(m)]\}A}{m\{az^K - a(1 - p + pB^*(m))G^*(a) - \alpha z[1 - G^*(a)]H^*(m)\}} \tag{21}$$

where

$$A = (1-p)\int_0^\infty \sum_{n=1}^{K}(z^K - z^n)P_n(x)\mu(x)dx + \int_0^\infty \sum_{n=1}^{\mathrm{K}}(z^K - z^n)V_n(x)\beta(x)dx$$
$$+ \int_0^\infty \sum_{n=1}^{K}(z^K - z^n)R_n(x)\gamma(x)dx + (z^K - 1)\lambda Q.$$

Let $S(z) = \frac{I_1 A}{m I_2}$.

Where

$$I_1 = [m + \alpha z^K(1 - H^*(m))][1 - G^*(a)] + apG^*(a)[1 - B^*(m)] \text{ and}$$
$$I_2 = az^K - a(1 - p + pB^*(m))G^*(a) - \alpha z[1 - G^*(a)]H^*(m).$$

Notice that $Q + S(1) = 1$ implies $Q = 1 - S(1)$. Since $S(1) = 0/0$, apply l'Hôpital rule twice. This gives

$$S(1) = \left\{\frac{I_1' A'}{m' I'_2}\right\}_{z=1}$$

where

$$I_1'|_{z=1} = -\lambda E(X)\{[1 - G^*(a)][1 + \alpha E(R)] + p\alpha G^*(\alpha)E(V)\},$$
$$I_2'|_{z=1} = \alpha K - \lambda E(X)[1 - G^*(\alpha)] - \alpha\lambda pE(X)E(V)G^*(\alpha)$$
$$- \alpha[1 - G^*(\alpha)][1 + \lambda E(R)E(X)],$$

$$A'|_{z=1} = (1-p)\int_0^\infty \sum_{n=1}^{K}(K - n)P_n(x)\mu(x)dx + K\lambda Q$$
$$+ \int_0^\infty \sum_{n=1}^{K}(K - n)V_n(x)\beta(x)dx + \int_0^\infty \sum_{n=1}^{K}(K - n)R_n(x)\gamma(x)dx,$$

and

$$Q = \left.\frac{m' I'_2 - I_1' A'}{m' I'_2}\right|_{z=1}.$$

3 Mean queue size

In this section mean queue size is calculated. Let us differentiate $S(z)$ with respect to z and substitute $z = 1$ to get the mean queue size.

Differentiation of equation (21) with respect to z, gives

$$S'(z) = \frac{mI_2[I_1'A + I_1A'] - I_1A[m'I_2 + I_2'm]}{[mI_2]^2}.$$

Substituting $z = 1$, we get $S'(1) = 0/0$.

Usage of l'Hôpital rule four times gives

$$S'(1) = \left.\frac{2\{m'I_2'[I_1'A'' + I_1''A'] - I_1'A'[m''I_2' + I_2''m']\}}{6[m'I_2']^2}\right|_{z=1},$$

$$\begin{aligned}
I_1''|_{z=1} &= -2\lambda^2E^2(X)[1 + \alpha E(R)][G^{*\prime}(\alpha)] + [1 - G^*(\alpha)][-\lambda E(X(X-1)) \\
&\quad - 2\alpha\lambda E(R)E(X) - \alpha(\lambda^2E^2(X)E(R^2) + \lambda EX(X-1)E(R))] \\
&\quad + 2p\lambda^2E^2(X)G^*(\alpha)E(V) + 2p\alpha\lambda^2E^2(X)G^{*\prime}(\alpha)E(V) \\
&\quad - p\alpha\lambda EX(X-1)G^*(\alpha)E(V) - p\alpha\lambda^2E^2(X)G^*(\alpha)E(V^2),
\end{aligned}$$

$$\begin{aligned}
I_2''|_{z=1} &= \alpha K(K-1) - 2\lambda KE(X) - \lambda E(X(X-1)) + \lambda E(X(X-1))G^*(\alpha) \\
&\quad + 2p\lambda^2E^2(X)E(V)G^*(\alpha) - 2\lambda^2E^2(X)G^{*\prime}(\alpha) \\
&\quad + 2\alpha p\lambda^2E^2(X)E(V)G^{*\prime}(\alpha) \\
&\quad - p\alpha[\lambda^2E^2(X)E(V^2) + \lambda E(V)E(X(X-1))]G^*(\alpha) \\
&\quad - 2\alpha\lambda E(X)G^{*\prime}(\alpha) \\
&\quad - 2\alpha\lambda E(X)[1 - G^*(\alpha)]E(R) - 2\alpha\lambda^2G^{*\prime}(\alpha)E(R)E^2(X) \\
&\quad - \alpha[1 - G^*(\alpha)][\lambda^2E^2(X)E(R^2) + \lambda EX(X-1)E(R)],
\end{aligned}$$

$$\begin{aligned}
A''|_{z=1} &= (1-p)\int_0^\infty \sum_{n=1}^{K} (K(K-1) - n(n-1))P_n(x)\mu(x)dx \\
&\quad + \int_0^\infty \sum_{n=1}^{K} (K(K-1) - n(n-1))V_n(x)\beta(x)dx \\
&\quad + \int_0^\infty \sum_{n=1}^{K} (K(K-1) - n(n-1))R_n(x)\gamma(x)dx + (K(K-1))\lambda Q,
\end{aligned}$$

and

$$Q = \left.\frac{m'I_2' - I_1'A'}{m'I_2'}\right|_{z=1}.$$

4 Some particular models

In this section a few specific cases are deduced by applying known probability distributions to various general probability distributions of random variables such as batch size, service time, vacation time, and repair time.

4.1 Case 1: $M^{[X]}/M^{(1,K)}/1$ queue with unreliable server and with Bernoulli vacation

Here it is assumed that

$$G(x) = 1 - e^{-\mu x}; \quad B(x) = 1 - e^{-\beta x}; \quad H(x) = 1 - e^{-\gamma x}.$$

Also assume that batch arrival size random variable X follows geometric distribution with probability $C_n = (1-s)^{n-1}s$ for $n \geq 1$, where $s = 1 - t$.

The probability generating function of number of customers in the queue independent of the server state is derived as follows.

$$S(z) = \frac{\{[m(\gamma+m)+\alpha z m]a(\beta+m)+ap\mu m(\gamma+m)\}A}{\left[\begin{array}{c} m\{az^K(\mu+a)(\beta+m)(\gamma+m)-a[(1-p)(\beta+m)+p\beta]\mu(\gamma+m) \\ -\alpha z a\gamma(\beta+m)\} \end{array}\right]}$$

where

$$A = (1-p)\int_0^\infty \sum_{n=1}^{K}(z^K - z^n)P_n(x)\mu(x)dx + \int_0^\infty \sum_{n=1}^{K}(z^K - z^n)V_n(x)\beta(x)dx + \int_0^\infty \sum_{n=1}^{K}(z^K - z^n)R_n(x)\gamma(x)dx + (z^K-1)\lambda Q$$

with $m = \lambda - \lambda C(z)$, $a = \lambda - \lambda C(z) + \alpha$.

The mean queue size is

$$S'(1) = \left.\frac{2\{m'I_2[I_1'A'' + I_1''A'] - I_1'A'[m''I_2' + I_2''m']\}}{6[m'I_2']^2}\right|_{z=1}$$

where

$$I_1'|_{z=1} = -\frac{\lambda}{s\beta\gamma(\mu+\alpha)}[\alpha(\gamma+\alpha)\beta + \alpha p\mu\gamma],$$

$$I_2'|_{z=1} = \frac{\alpha K s\beta\gamma(\mu+\alpha) - \lambda\alpha\beta\gamma - \alpha\lambda p\mu\gamma - \alpha^2(\gamma s+\lambda)\beta}{s\beta\gamma(\mu+\alpha)},$$

$$A'|_{z=1} = (1-p)\int_0^\infty \sum_{n=1}^{K}(Kz^{K-1} - nz^{n-1})P_n(x)\mu(x)dx + \int_0^\infty \sum_{n=1}^{K}(Kz^{K-1} - nz^{n-1})V_n(x)\beta(x)dx + \int_0^\infty \sum_{n=1}^{K}(Kz^{K-1} - nz^{n-1})R_n(x)\gamma(x)dx + (Kz^{K-1})\lambda Q,$$

$$I_1''|_{z=1} = \{2\lambda^2\mu(\alpha+\gamma)\beta^2\gamma - \alpha\beta^2(\mu+\alpha)[2\lambda(1-s)\gamma^2 + 2\alpha\lambda s\gamma + 2\alpha\lambda\gamma(1-s) + 2\lambda^2\alpha] + 2p\lambda^2\mu(\mu+\alpha)\beta\gamma^2 - 2p\alpha\lambda^2\mu\beta\gamma^2 - 2p\alpha\lambda(1-s)\mu(\mu+\alpha)\beta\gamma^2 - p\alpha\lambda^2\mu(\mu+\alpha)\gamma^2\}\left\{\frac{1}{s^2\beta^2\gamma^2(\mu+\alpha)^2}\right\},$$

$$
\begin{aligned}
I_2''|_{z=1} = \{&\alpha K(K-1)s^2\beta^2\gamma^2(\mu+\alpha)^2 + \beta^2\gamma^2(\mu+\alpha)[-2\lambda Ks(\mu+\alpha) \\
&- 2\lambda(1-s)(\mu+\alpha) + 2\lambda(1-s)\mu] \\
&+ \beta\gamma^2[2p\lambda^2\mu(\mu+\alpha) + 2\lambda^2\mu\beta - 2\alpha p\lambda^2\mu] \\
&+ \gamma^2[-\alpha p\mu(2\lambda^2 + 2\lambda(1-s)\beta)(\mu+\alpha) \\
&+ 2\alpha\lambda\mu\beta^2 s] - 2\alpha^2\beta^2\lambda s\gamma(\mu+\alpha) + 2\alpha\lambda^2\beta^2\mu\gamma \\
&- \alpha^2\beta^2[2\lambda^2 + 2\lambda(1-s)\gamma](\mu+\gamma)\} \left\{\frac{1}{s^2\beta^2\gamma^2(\mu+\alpha)^2}\right\},
\end{aligned}
$$

$$
\begin{aligned}
A''|_{z=1} = (1-p)&\int_0^\infty \sum_{n=1}^{K}(K(K-1) - n(n-1))P_n(x)\mu(x)dx \\
&+ \int_0^\infty \sum_{n=1}^{K}(K(K-1) - n(n-1))V_n(x)\beta(x)dx \\
&+ \int_0^\infty \sum_{n=1}^{K}(K(K-1) - n(n-1))R_n(x)\gamma(x)dx + K(K-1)\lambda Q, \text{ and}
\end{aligned}
$$

$$
Q = \left.\frac{m'I_2' - I_1'A'}{m'I_2'}\right|_{z=1}.
$$

4.2 Case 2: $M^{[X]}/G^{(1,K)}/1$ queue with unreliable server, without vacation

Here the probability generating function of the number of customers in the queue independent of the server state is derived by assuming $p = 0$.

$$
S(z) = \frac{[m + \alpha z(1 - H^*(m)](1 - G^*(a))A}{m\{az^K - aG^*(a) - \alpha z[1 - G^*(a)]H^*(m)\}}
$$

where

$$
\begin{aligned}
A = &\int_0^\infty \sum_{n=1}^{K}(z^K - z^n)P_n(x)\mu(x)dx + \int_0^\infty \sum_{n=1}^{K}(z^K - z^n)V_n(x)\beta(x)dx \\
&+ \int_0^\infty \sum_{n=1}^{K}(z^K - z^n)R_n(x)\gamma(x)dx + (z^K - 1)\lambda Q
\end{aligned}
$$

with $m = \lambda - \lambda C(z)$, $a = \lambda - \lambda C(z) + \alpha$.

The mean queue size is

$$
S'(1) = \left.\frac{2\{m'I_2[I_1'A'' + I_1''A'] - I_1'A'[m''I_2' + I_2''m']\}}{6[m'I_2']^2}\right|_{z=1},
$$

$$
I_1'|_{z=1} = -\lambda E(X)[1 - G^*(a)][1 + \alpha E(R)],
$$

$$
I_2'|_{z=1} = \alpha K - \lambda E(X)[1 - G^*(\alpha)] - \alpha[1 - G^*(\alpha)][1 + \lambda E(R)E(X)],
$$

$$A'|_{z=1} = \int_0^\infty \sum_{n=1}^{K} (K-n)P_n(x)\mu(x)dx + \int_0^\infty \sum_{n=1}^{K}(K-n)V_n(x)\beta(x)dx + \int_0^\infty \sum_{n=1}^{K}(K-n)R_n(x)\gamma(x)dx + K\lambda Q,$$

$$I_1''|_{z=1} = -2\lambda^2E^2(X)[1+\alpha E(R)][G^{*\prime}(\alpha)] + [1-G^*(\alpha)][-\lambda E(X(X-1)) - 2\alpha\lambda KE(R)E(X) - \alpha(\lambda^2E^2(X)E(R^2) + \lambda E(X(X-1))E(R))],$$

$$I_2''|_{z=1} = \alpha K(K-1) - 2\lambda KE(X) - \lambda EX(X-1) + \lambda EX(X-1)G^*(\alpha) - 2\lambda^2E^2(X)G^{*\prime}(\alpha) - 2\alpha\lambda E(X)G^{*\prime}(\alpha) - 2\alpha\lambda E(X)[1-G^*(\alpha)]E(R) - \alpha[1-G^*(\alpha)][\lambda^2E^2(X)E(R^2) + \lambda E(X(X-1))E(R)], - 2\alpha\lambda^2G^{*\prime}(\alpha)E(R)E^2(X),$$

$$A''|_{z=1} = \int_0^\infty \sum_{n=1}^{K}(K(K-1)-n(n-1))P_n(x)\mu(x)dx + \int_0^\infty \sum_{n=1}^{K}(K(K-1)-n(n-1))V_n(x)\beta(x)dx + \int_0^\infty \sum_{n=1}^{K}(K(K-1)-n(n-1))R_n(x)\gamma(x)dx + K(K-1)\lambda Q, \text{ and}$$

$$Q = \left.\frac{m'I_2' - I_1'A'}{m'I_2'}\right|_{z=1}.$$

4.3 Case 3: $M^{[X]}/G/1$ queue with breakdown and with Bernoulli vacation

Here the probability generating function corresponding to the number of customers in the queue independent of the server state is derived by assuming $K = 1$.

$$S(z) = \frac{\{[m+\alpha z(1-H^*(m))(1-G^*(a)) + apG^*(a)[1-B^*(m)]\}A}{m\{az - a(1-p+pB^*(m))G^*(a) - \alpha z[1-G^*(a)]H^*(m)\}}$$

where $A = (z-1)\lambda Q$, $m = \lambda - \lambda C(z)$, $a = \lambda - \lambda C(z) + \alpha$.

The mean queue size is derived as

$$S'(1) = \left.\frac{2\{m'I_2[I_1'A'' + I_1''A'] - I_1'A'[m''I_2' + I_2''m']\}}{6[m'I_2']^2}\right|_{z=1},$$

$$I_1'|_{z=1} = -\lambda E(X)\{[1-G^*(a)][1+\alpha E(R)] + p\alpha G^*(\alpha)E(V)\},$$

$$I_2'|_{z=1} = \alpha - \lambda E(X)[1-G^*(\alpha)] - \alpha\lambda pE(x)E(V)G^*(\alpha) - \alpha[1-G^*(\alpha)][1+\lambda E(R)E(X)],$$

$$A'|_{z=1} = \lambda Q,$$

$$
\begin{aligned}
I_1''|_{z=1} &= -2\lambda^2E^2(X)[1+\alpha E(R)][G^{*\prime}(\alpha)] + [1-G^*(\alpha)][-\lambda E(X(X-1)) \\
&\quad - 2\alpha\lambda E(R)E(X) - \alpha(\lambda^2E^2(X)E(R^2) + \lambda E(X(X-1))E(R))] \\
&\quad + 2p\lambda^2E^2(X)G^*(\alpha)E(V) + 2p\alpha\lambda^2E^2(X)G^{*\prime}(\alpha)E(V) \\
&\quad - p\alpha\lambda E(X(X-1))G^*(\alpha)E(V) - p\alpha\lambda^2E^2(X)G^*(\alpha)E(V^2), \\
I_2''|_{z=1} &= -2\lambda E(X) - \lambda EX(X-1) + \lambda EX(X-1)G^*(\alpha) \\
&\quad + 2p\lambda^2E^2(X)E(V)G^*(\alpha) - 2\lambda^2E^2(X)G^{*\prime}(\alpha) \\
&\quad + 2\alpha p\lambda^2E^2(X)E(V)G^{*\prime}(\alpha) - p\alpha[\lambda^2E^2(X)E(V^2) \\
&\quad + \lambda E(V)E(X(X-1))]G^*(\alpha) - 2\alpha\lambda E(X)G^{*\prime}(\alpha) \\
&\quad - 2\alpha\lambda E(X)[1-G^*(\alpha)]E(R) - 2\alpha\lambda^2G^{*\prime}E(R)E^2(X) \\
&\quad - \alpha[1-G^*(\alpha)][\lambda^2E^2(X)E(R^2) + \lambda EX(X-1)E(R)], \\
A''|_{z=1} &= 0,
\end{aligned}
$$

and

$$
Q = \left.\frac{m'I_2' - I_1'A'}{m'I_2'}\right|_{z=1}.
$$

5 Numerical results

In this section, illustrative numerical results of the operating characteristics of model in the particular cases are obtained.

For the model in case 1, the numerical results are obtained by assuming $\mu = 15, \gamma = 16,\ \beta = 15, p = 0.01, s = 0.7$ and varying the values of λ from 1 to 10. Also, the numerical results are presented in the form of Tables and Figures for the values of α from 1 to 5 and $K = 2, 3$.

For the model in case 2, the numerical results are calculated by assuming $\mu = 15, \gamma = 16, \beta = 15, s = 0.7$ and varying the values of λ from 1 to 10. Also, the numerical results are presented in the form of Tables and Figures for the values of α from 1 to 5 and fixing $K = 2, 3$.

For the model in case 3, the numerical results are calculated by assuming $\mu = 15, \gamma = 16, \beta = 15, s = 0.9$ and varying the values of λ from 1 to 10. Also, the numerical results are presented in the form of Tables and Figures for the values of α from 1 to 5 and fixing $K = 1$.

Tables 1 and 2 exhibit the probabilities of server being idle for increasing values of λ from 1 to 10 and α from 1 to 5, and for the values of $K = 2, K = 3$ respectively. From Tables 1 and 2, it is observed that the probability of server being idle decreases as average arrival rate increases from 1 to 10. Also the probability of server being idle decreases as breakdown rate increases from 1 to 5.

Figures 1 and 2 indicate the behaviour of the mean queue size for $K = 2, K = 3$ respectively when λ varies from 1 to 10 and α from 1 to 5. From Figures 1 and 2, it is observed that the mean queue size increases as average arrival rate increases from 1 to 10. Also the mean queue size increases as breakdown rate increases from 1 to 5.

Table 1 Probability of server being idle when $K = 2$: ($\mu = 15$, $\gamma = 16$, $\beta = 15$, $p = 0.01$, $s = 0.7$)

λ	α				
	1	*2*	*3*	*4*	*5*
1	0.8378	0.8337	0.8299	0.8264	0.8230
2	0.6954	0.6880	0.6810	0.6744	0.6682
3	0.5709	0.5606	0.5509	0.5418	0.5332
4	0.4633	0.4506	0.4387	0.4275	0.4170
5	0.3716	0.3569	0.3433	0.3305	0.3184
6	0.2950	0.2789	0.2639	0.2498	0.2366
7	0.2328	0.2156	0.1995	0.1845	0.1704
8	0.1843	0.1663	0.1495	0.1339	0.1192
9	0.1487	0.1303	0.1131	0.0971	0.0821
10	0.1256	0.1070	0.0897	0.0735	0.0583

Table 2 Probability of server being idle when $K = 3$: ($\mu = 15$, $\gamma = 16$, $\beta = 15$, $p = 0.01$, $s = 0.7$)

λ	α				
	1	*2*	*3*	*4*	*5*
1	0.8073	0.8044	0.8018	0.7994	0.7972
2	0.6383	0.6331	0.6283	0.6239	0.6198
3	0.4912	0.4841	0.4776	0.4716	0.4660
4	0.3655	0.3569	0.3491	0.3418	0.3351
5	0.2607	0.2510	0.2421	0.2339	0.2264
6	0.1764	0.1659	0.1563	0.1475	0.1393
7	0.1122	0.1013	0.0912	0.0820	0.0735
8	0.0680	0.0568	0.0465	0.0371	0.0285
9	0.0432	0.0321	0.0219	0.0125	0.0039
10	0.0378	0.0269	0.0169	0.0078	0.0000

Figure 1 Mean queue size when $K = 2$: ($\mu = 15, \gamma = 16, \beta = 15, p = 0.01, s = 0.7$) (see online version for colours)

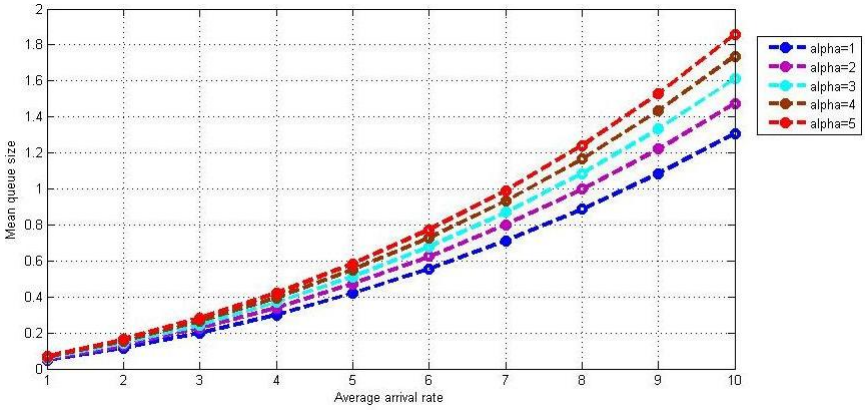

Figure 2 Mean queue size when $K = 3$: $(\mu = 15, \gamma = 16, \beta = 15, p = 0.01, s = 0.7)$ (see online version for colours)

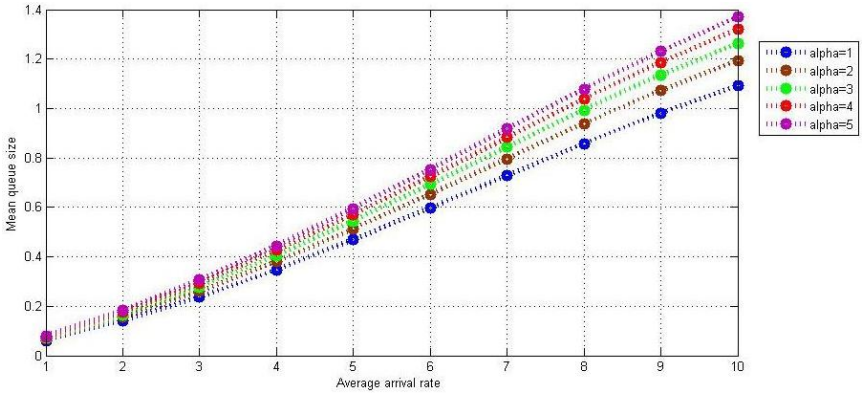

Table 3 Probability of server being idle when $K = 2$: $(\mu = 15, \gamma = 16, \beta = 15, s = 0.7)$

λ	α				
	1	*2*	*3*	*4*	*5*
1	0.8385	0.8344	0.8306	0.8270	0.8236
2	0.6960	0.6885	0.6814	0.6748	0.6686
3	0.5715	0.5611	0.5513	0.5422	0.5336
4	0.4639	0.4511	0.4392	0.4280	0.4174
5	0.3724	0.3577	0.3440	0.3311	0.3191
6	0.2961	0.2800	0.2648	0.2507	0.2374
7	0.2343	0.2170	0.2009	0.1858	0.1716
8	0.1861	0.1681	0.1512	0.1355	0.1207
9	0.1510	0.1325	0.1152	0.0991	0.0840
10	0.1282	0.1095	0.0921	0.0759	0.0607

Table 4 Probability of server being idle when $K = 3$: $(\mu = 15, \gamma = 16, \beta = 15, s = 0.7)$

λ	α				
	1	*2*	*3*	*4*	*5*
1	0.8081	0.8052	0.8025	0.8001	0.7978
2	0.6388	0.6335	0.6287	0.6242	0.6201
3	0.4915	0.4843	0.4777	0.4717	0.4661
4	0.3657	0.3570	0.3491	0.3417	0.3350
5	0.2608	0.2511	0.2421	0.2338	0.2262
6	0.1766	0.1660	0.1564	0.1475	0.1392
7	0.1126	0.1016	0.1564	0.0821	0.0735
8	0.0685	0.0572	0.0469	0.0374	0.0286
9	0.0440	0.0327	0.0224	0.0130	0.0042
10	0.0388	0.0278	0.0177	0.0085	0.0000

Tables 3 and 4 display the probabilities of server being idle for the values of $K = 2, K = 3$ respectively when λ varies from 1 to 10 and α from 1 to 5. From Tables 3 and 4, it is observed that the probability of server being idle decreases as average arrival rate increases from 1 to 10. Also the probability of server being idle decreases as breakdown rate increases from 1 to 5.

Figure 3 Mean queue size when $K = 2 : (\mu = 15, \gamma = 16, \beta = 15, s = 0.7)$ (see online version for colours)

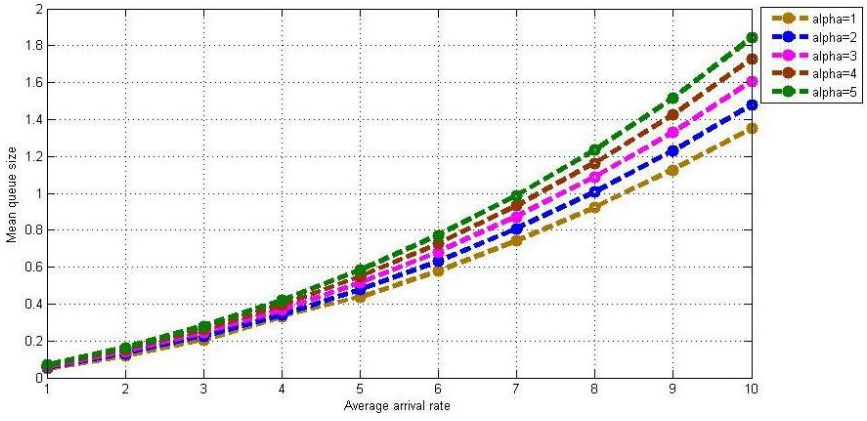

Figure 4 Mean queue size when $K = 3 : (\mu = 15, \gamma = 16, \beta = 15, s = 0.7)$ (see online version for colours)

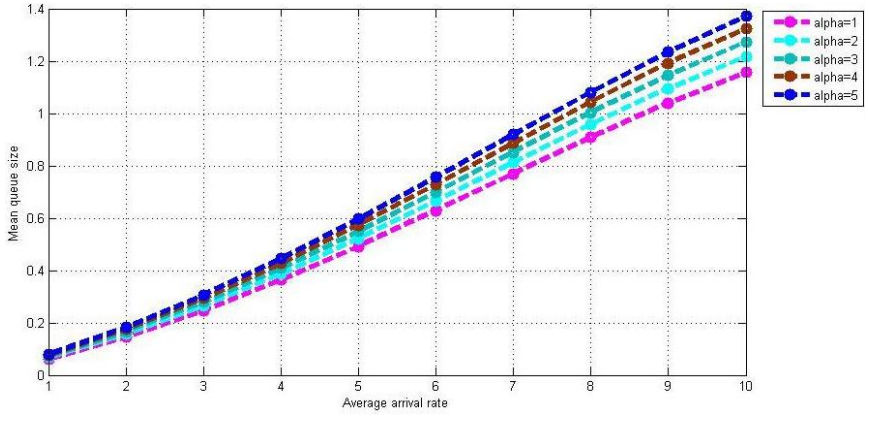

Figures 3 and 4 exhibit the mean queue size for $K = 2, K = 3$ respectively λ varies from 1 to 10 and α from 1 to 5. From Figures 3 and 4, it is observed that the mean queue size increases as average arrival rate increases from 1 to 10. Also the mean queue size increases as breakdown rate increases from 1 to 5.

Table 5 shows the probabilities of server being idle for $K = 1$ when λ varies from 1 to 10 and α from 1 to 5. From Table 5, it is observed that for $K = 1$ the probability of server being idle decreases when λ varies from 1 to 10 and also decreases when α varies from 1 to 5.

Table 5 Probability of server being idle when $K = 1$: ($\mu = 15$, $\gamma = 16$, $\beta = 15$, $p = 0.01$, $s = 0.9$)

λ	α				
	1	*2*	*3*	*4*	*5*
1	0.9280	0.9238	0.9195	0.9153	0.9110
2	0.8553	0.8467	0.8381	0.8294	0.8208
3	0.7814	0.7682	0.7550	0.7418	0.7285
4	0.7061	0.6883	0.6704	0.6524	0.6343
5	0.6295	0.6068	0.5840	0.5610	0.5380
6	0.5515	0.5238	0.4959	0.4678	0.4396
7	0.4721	0.4391	0.4059	0.3725	0.3389
8	0.3912	0.3528	0.3142	0.2752	0.2359
9	0.3087	0.2648	0.2205	0.1757	0.1305
10	0.2248	0.1750	0.1248	0.0740	0.0227

Also from Figure 5, it is inferred that for $K = 1$ the mean queue size decreases when λ varies from 1 to 10 and α from 1 to 5. Figure 5 clearly shows that the mean queue size increases as average arrival rate increases from 1 to 10. Also the mean queue size increases as breakdown rate increases from 1 to 5.

Figure 5 Mean queue size when $K = 1 : (\mu = 15, \gamma = 16, \beta = 15, p = 0.01, s = 0.9)$ (see online version for colours)

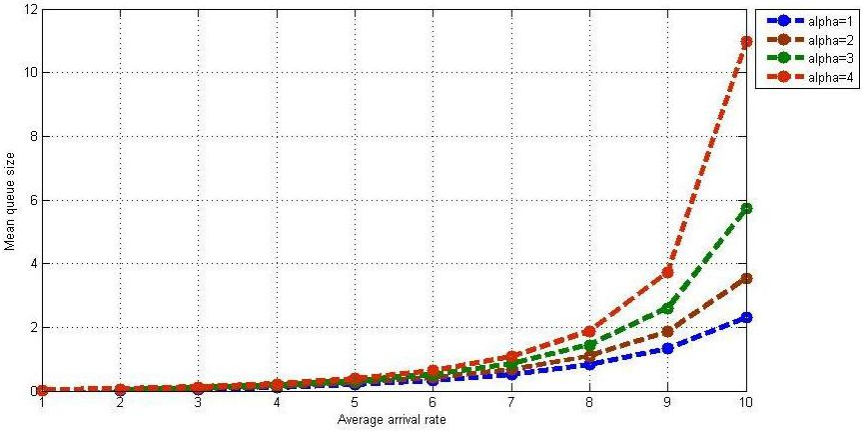

In nutshell, the probability of server being idle decreases when average arrival rate increases from 1 to 10 and breakdown rate increases from 1 to 5. Similarly mean queue size increases when average arrival rate increases from 1 to 10 and break down rate increases from 1 to 5.

Analytical findings are clearly supported by numerical illustrations. The numerical results obtained show that the parameter values exhibit the model's performance measures as well as its effectiveness.

6 Conclusions

In this paper, a single server batch arrival and batch service queue with Bernoulli vacation, and with unreliable server was completely analysed. The probability generating functions for number of customers in the queue at various server state were obtained. From the probability generating function a compact formula for mean queue size was derived. Some particular models were deduced by assuming particular known probability distribution to general probability distributions. Numerical results were obtained for particular cases by assuming particular values to the parameters. The model can be extended further by taking the breakdown period as generally distributed random variable. Finally, we hope that the queueing model concerned is well applicable to real life scenario and having noteworthy applications in manufacturing and transportation system, etc. by taking suitable distributions depending upon the situations.

Acknowledgements

The authors express their heartiest gratitude to the anonymous referees and the Chief Editor for their unified valuable suggestions, which assisted in fine-tuning the shape of this paper to its present format. Also, the first author records his gratitude to his employer for supporting and encouraging his research efforts.

References

Ayyappan, G. and Karpagam, S. (2019) 'An $M^{[X]}/G^{(a,b)}/1$ queueing system with server breakdown and repair, standby server, and single vacation', *International Journal of Mathematics in Operational Research*, Vol. 14, No. 2, pp.221–235.

Ayyappan, G. and Nirmala, M. (2021) 'Analysis of unreliable bulk queueing system with overloading service, variant arrival rate, close down under multiple vacation policy', *International Journal of Operational Research*, Vol. 42, No. 3, pp.371–399.

Bacot, J.B. and Dshalalow, J.H. (2001) 'A bulk input queuing system with batch gated service and multiple vacation policy', *Mathematical and Computer Modeling*, Vol. 34, pp.873–886.

Baba, Y. (1986) 'On the $M^X/G/1$ queue with vacation time', *Operations Research Letters*, Vol. 5, No. 2, pp.93–98.

Balasubramanian, M. and Arumuganathan, R. (2011) 'Steady state analysis of a bulk arrival general bulk service queueing system with modified M-vacation policy and variant arrival rate', *International Journal of Operational Research*, Vol. 1, No. 4, pp.380–407.

Chaudhry, M.L. and Templeton, J.G.C. (1983) *A First Course in Bulk Queues*, Wiley-Interscience Publication, New York.

Choudhary, A. and Sharma, D.C. (2022) 'Analysis of Markovian queue model with unreliable service station and a vacation after fixed services', *International Journal of Mathematics in Operational Research*, Vol. 21, No. 3, pp.411–428.

Choudhury, G. and Deka, M. (2012) 'A single server queuing system with two phases of service subject to server break down and Bernoulli vacation', *Applied Mathematical Modeling*, Vol. 36, No. 12, pp.6050–6060.

Gupta, G. and Banerjee, A. (2018) 'On $M/G(a;b)/1/n$ queue with batch size and queue length dependent service', *International Conference on Mathematics and Computing*, Springer, pp.249–262.

Jain, M. and Upadhyaya, S. (2009) 'Optimal repairable $M^{[X]}/G/1$ queue with multi-optional services and Bernoulli vacation', *International Journal of Operational Research*, Vol. 7, No. 1, pp.109–132.

Jeyakumar, A. and Senthilnathan, B. (2016) 'Steady state analysis of bulk arrival and bulk service queueing model with multiple working vacations', *International Journal of Mathematics in Operational Research*, Vol. 9, No. 3, pp.375–394.

Jeyakumar, S. and Rameshkumar, E. (2019) 'A study on $M^{[X]}/G^{(a,b)}/1$ queue with server breakdown without interruption and controllable arrivals during multiple adaptive vacations', *International Journal of Mathematics in Operational Research*, Vol. 15, No. 2, pp.137–155.

Jiang, T. and Xin, B. (2019) 'Computational analysis of the queue with working breakdowns and delaying repair under a Bernoulli-schedule-controlled policy', *Communications in Statistics – Theory and Methods*, Vol. 48, No. 4, pp 1–16.

Kalita, P. and Choudhury, G. (2021) 'Analysis of batch arrival single server queue with random vacation policy and two types of general heterogeneous repeated service', *International Journal of Operational Research*, Vol. 42, No. 2, pp.131–162.

Kalyanaraman, R. and Nagarajan, P. (2016) 'Bulk arrival, fixed batch service queue with unreliable server and with Bernoulli vacation', *International Journal of Applied Engineering Research*, Vol. 11, No. 1, pp.421–429.

Ke, J.C. (2007) 'Operating characteristic analysis of M^X/G/1 system with variant vacation policy and balking', *Applied Mathematical Modeling*, Vol. 31, No. 7, pp.1321–1337.

Ke, J.C. and Lin, C.H. (2008) 'Maximum entropy approach for batch-arrival queue under policy with an un-reliable server and single vacation', *Journal of Computational and Applied Mathematics*, Vol. 221, No. 1, pp.1–15.

Krishnamoorthy, A., Pramod, P.K. and Chakravarthy, S.R. (2014) 'Queues with interruptions: a survey', *TOP: An Official Journal of the Spanish Society of Statistics and Operations Research*, Vol. 22, No. 1, pp.290–320, Sociedad de Estadística e Investigación Operativa, Springer.

Kumar, R., Ghosh, S. and Banik, A.D. (2021) 'Numerical study on transient behavior of finite bulk arrival or service queues with multiple working vacations', *International Journal of Mathematics in Operational Research*, Vol. 18, No. 3, pp.384–403.

Kumar, B. (2018) 'Unreliable bulk queueing model with optional services, Bernoulli vacation schedule and balking', *International Journal of Mathematics in Operational Research*, Vol. 12, No. 3, pp.293–316.

Nithya, R.P. and Haridass, M. (2020) 'Stochastic modelling and analysis of maximum entropy of M^X/G/1 queuing system with balking, startup and vacation interruption', *International Journal of Services and Operations Management*, Vol. 37, No. 3, pp.343–371.

Pradhan, S. (2020) 'On the distribution of an infinite-buffer queueing system with versatile bulk-service rule under batch-size-dependent service policy: $M/Gn(a,Y)/1$', *International Journal of Mathematics in Operational Research*, Vol. 16, No. 3, pp.407–434.

Rajan, B.S., Ganesan, V. and Rita, S.. (2020) 'Batch arrival Poisson queue with breakdown and repairs', *International Journal of Mathematics in Operational Research*, Vol. 17, No. 3, pp.424–435.

Rehab, F., Khalaf, K.C.M., and Cormac, A.L. (2012) 'On an $M^{[X]}$ / G /1 queuing system with random breakdowns, server vacations, delay times and a standby server', *International Journal of Operational Research*, Vol. 15, No. 1, pp 30–47, Inderscience Enterprises Ltd.

Saggou, H., Sadeg, I., Ourbih-Tari, M. and Bourennane, E.B. (2019) 'The analysis of unreliable $M^{[X]}/G^{(1,K)}/1$ queuing system with loss, vacation and two delays of verification'. *Communications in Statistics - Simulation and Computation*, Vol. 48, No. 5, pp.1366–1381.

Singh, C.J., Kaur, S. and Jain, M. (2019) 'Analysis of bulk queue with additional optional service, vacation and unreliable server', *International Journal of Mathematics in Operational Research*, Vol. 14, No. 4, pp.517–540.

Singh, C.J., Kumar, B. and Kaur, S. (2018) 'M^X/G/1 state dependent arrival queue with optional service and vacation under randomized policy', *International Journal of Industrial and Systems Engineering*, Vol. 29, No. 2, pp.252–272.

Vignesh, P., Srinivasan, S., and Sundari, S.M. (2018) 'Analysis of a non-Markovian single server batch arrival queueing system of compulsory three stages of services with fourth optional stage service, service interruptions and deterministic server vacations', *International Journal of Operational Research*, Vol. 34, No. 1, pp.28–53.

Yu, M. and Tang, Y. (2022) 'Analysis of a renewal batch arrival queue with a fault-tolerant server using shift operator method', *Oper. Res. Int. J.*, Vol. 22, No. 3, pp.2831–2858.

Yuvarani, C. and Vijayalakshmi, C. (2020) 'Analysis of multistage $M^{[X]}/G^K/1$ queue with different server's interruptions and its application in energy consumption', *International Journal of Ambient Energy*, Vol. 41, No. 6, pp.691–698.

Zirem, D., Boualem, M., Adel-Aissanou, K. and Aissani, D. (2018) 'Analysis of a single server batch arrival unreliable queue with balking and general retrial time', *Quality Technology and Quantitative Management*, Vol. 16, No. 6, pp.672–695.

RESEARCH ARTICLE | MAY 09 2023

Effects of heat and mass transmission with radiation on MHD nanofluid flow past over an oscillating plate using chemical reaction

S. Sarala; E. Geetha ✉; M. Mageswari; ... et. al

AIP Conference Proceedings 2707, 030011 (2023)
https://doi.org/10.1063/5.0143693

Effects Of Heat And Mass Transmission With Radiation On MHD Nanofluid Flow Past Over An Oscillating Plate Using Chemical Reaction

S.Sarala[1,2, a)] , E.Geetha [3,b)], M.Mageswari[4,c)] M.Radha Madhavi[5, d)]

[1]*Sri Chandrasekharendra Saraswathi Viswa Maha Vidyalaya, Enathur, Kanchipuram-631561, Tamilnadu, India,*
[2]*Department of Mathematics, Aarupadai Veedu Institute of Technology, Vinayaka Missions Research Foundation, Chennai-603104, Tamilnadu, India,*
[3]*Department of Mathematics, Sri Chandrasekharendra Saraswathi Viswa Maha Vidyalaya, Enathur, Kanchipuram- 631561, Tamilnadu, India*
[4] *Department of Mathematics, Govt.College of Engineering, Bargur-635104, Krishnagiri District, Tamilnadu, India*
[5]*Department Of Mathematics, Koneru Lakshmaiah Education Foundation, Vaddeswaram-522302, Andhra Pradesh, India.*

[a)] *saralashun@gmail.com*
[b)] *Corresponding author : geethamuthu06@gmail.com*
[c)]*dr.mageswari.abhi@gmail.com*
[d)] *mrmadhavi5@gmail.com*

Abstract. *The existing study of the paper using chemical reaction examines the consequences of thermal and mass transferal on MHD Alumina nanofluid energy passed over an oscillatory plate by radiation. Using similarity transformations, the governing equations are reformed into dimensionless equations and solved through Laplace Transformation. The effects of parameters in radiation (R), Schmidt number (Sc), Prandtl number (Pr), magnetic parameter (M), chemical Reaction Parameter (K_c), solid volume fraction (ϕ), thermal Grashof number (Gr), mass Grashof number (Gc), phase angle (ω) are scrutinized in velocity, temperature, and concentration forms. The depicted charts are shown the enhancement of the velocity, temperature, and concentration. It observes that an increment of magnetohydrodynamic diminishes the velocity, an increment of thermal and mass Grashof number stand out towards the increase through the velocities, and increasing radiation reduces a temperature. An increment of Schmidt number diminishes the concentration of the Alumina nanofluid. The Concentration of the fluid decreases as an increment of chemical reactive parameters. The increment in time directs to increase the Nusselt number along with the Sherwood number. The skin friction Coefficient improvements with accumulative values of mass grashof number and radiation.*

1. INTRODUCTION

Nanofluids has several engineering application in heat transfer for maximal thermal conductivity. Heat and mass transfer occur on invertors, turbines, space engines, power creators, pumps, refrigeration loops, steel rotators, satellites, etc. It is highly significant in industry innovations. The convection and radiation influence is a vital application in vapor producers of power plants with load changes. Nowadays convective heat transfer with applied magnetic field study is popular in various fields. In MHD flows, hall current effects in Ohm's law are considered when a durable magnetic field is applied. It is neglected for smaller values. Chemical compound responses are categorized as similar and dissimilar based on solid volume fraction. In this paper, a first-order chemical reaction is considered. Due to cross-transmission, heat and mass transmission concerned each other. Based on concentration and temperature, the heat transmission is termed as the Dufour effect and Soret effect respectively. In real life, people prefer white colour clothes instead of black for less amount of heat absorption and to keep the body cool. The

1st International Conference on Essence of Mathematics and Engineering Applications
AIP Conf. Proc. 2707, 030011-1–030011-14; https://doi.org/10.1063/5.0143693
Published by AIP Publishing. 978-0-7354-4516-1/$30.00

car radiators are coated with black colour which emits a lot of heat. If you pour the water, it will reduce the heat. Here water is acted as a coolant. In thermal properties, Aluminium is frequently used in thermal conductivity, convective heat transmission coefficient, and heat transference coefficient. In this paper, aluminum oxide nanofluid using chemical response is considered.

Biswas et al. [1] has performed the numerical investigation of variation in different dimensionless parameters. Das et al. [2] mentioned the scope and features of those magnetic nanofluids. He also focused on the application of nanofluids based on their specific usage. Datta et al. [3] have applied the finite volume method for resolving equations. He generated the ANSYS Fluent code for finding values and calculated the dynamic viscosity of the nanofluid and Brinkman model. Mahanthesh et al. [4], provided base fluid and Copper nanofluids values. Mahbubul et al. [5] examined the optimum dispersion of nanoparticles. He measured current conductivity and viscidness by the ultra-sonication procedure. Misra et al. [6] were sightseen the controls of warmness and quantity transfer on porous blood vessels Variations of parameters were executed generated the graphs with tables.

Exhausting chemical reaction, Muthukumaraswamy et al. [7] evaluated the Hartmann number with hall parameter and rotation parameter. Oahimire et al. [8] conferred using chemical reactions in three dimensional fluid flow. Rout et al.[9] has computed and analyzed the thermal energy transmission and has taken variable temperature as a boundary condition. Srinivas et al. [10] have used thermosolutal nanofluid and applied the Gauss-Siedel iteration method to solve the governing equation. In his calculation of values, he used C-programming code. Swarnalathamma et al.[11] has studied the Eyring-Powel Nanofluid through an Isothermal Sphere with thermal slip effect. Rajput et al. [12] had examined the Hall effect in a porous plate with chemical reactive and radiation. This technique is applied in rocket science and missile technology. Venkateswarlu et al. [13] has studied the oscillating plate with steady frequency and applied the perturbation method to solve the governing equation. Zubair Akba et al. [14] analyzed metallic nanoparticles.

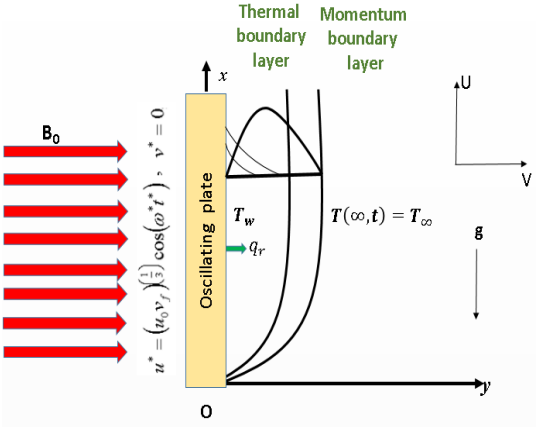

FIGURE 1. The physical model and coordinate system

The physical model is shown in Figure 1. The effects of MHD nanofluid movement of an incompressible viscid fluid past an oscillating vertical using chemical reaction and radiation have not been studied in all the above-cited papers. In this paper, alumina-water is used.

To the author's knowledge, no studies have been found in literature, to study the effects of heat and mass transfer on MHD nanofluid flow past over an oscillating plate with radiation and chemical reaction.

2. MATHEMATICAL ANALYSIS

Using chemical reaction and thermal radiation, the viscid flow of an incompressible concentrative Al_2O_3 nanofluid past an oscillating perpendicular plate has been considered. The $x^* o y^*$ plane is taken and $z^* = 0$. At the time $t^* \le 0$, the plate and fluid are at the same temperature T_∞. The plate has oscillated alongside the x^*

axis and the y^* axis is usual for the remaining axes. Near the plate, the temperature value is expected T_∞. The velocity $u^* = (u_0 v_f)^{\left(\frac{1}{3}\right)} \cos(\omega^* t^*)$ is started oscillating and the temperature surges to T_w . The uniform magnetic field B_0 is applied uniformly equivalent to the z^* axis. At the normal direction to the plate, the radiative heat flux q_r is handled. Thermo-physical properties of the base fluid and nanofluid are tabulated in Table 1.

TABLE 1. Thermo-physical properties of water and Alumina nanoparticles.

Physical Properties	ρ (kg / m^3)	$C_p\,(J/KgK)$	K(W / mK)	$\beta\times10^3\,(K^{-1})$	φ	$\sigma\ (s/m)$
Water / Base fluid	997.1	4179	0.613	21	0.0	5.5 x 10^{-6}
Al_2O_3 (Alumina)	3970	765	40	0.85	0.15	35 x 10^6

The mass transfer concentration coefficient ranges from 0.01 to 0.1in Alumina nanofluid. The equation of continuity is $\nabla \cdot \vec{F} = 0$ where u^*, v^*, w^* denotes the elements of velocity F. It provides w^*=0 inflow which is satisfied by the plate everywhere. The external velocity varies inversely–linear with the distance along the surface which is known as Pseudo similarity. The velocity resemblance variables are reserved as the essential resemblance variables. It is denoted by η. The water-based Al_2O_3 nanoparticles are taken as a fluid. The water and the Alumina nanoparticles stayed which are in current symmetry. *Z** and t* direct the movement of the fluid. The flow is far off since the plate without disruption is considered.

The Boussinesq's approximation governing equations are as follows for unstable flow:

$$\rho_{nf}\frac{\partial u^*}{\partial t^*} = \mu_{nf}\frac{\partial^2 u^*}{\partial z^{*2}} + g(\rho\beta)_{nf}(T-T_\infty) + g(\rho\beta^*)_{nf}(C^*-C^*_\infty) + \sigma_{nf}B_0^2\left(v^*-u^*\right) \tag{1}$$

$$\rho_{nf}\frac{\partial v^*}{\partial t^*} = \mu_{nf}\frac{\partial^2 v^*}{\partial z^{*2}} - \sigma_{nf}B_0^2\left(v^*+u^*\right) \tag{2}$$

$$(\rho c_p)_{nf}\frac{\partial T}{\partial t^*} = k_{nf}\frac{\partial^2 T}{\partial z^{*2}} - \frac{\partial q_r}{\partial z^*} \tag{3}$$

$$\frac{\partial C^*}{\partial t^*} = D\frac{\partial^2 C^*}{\partial z^{*2}} - K_1(C^*-C^*_\infty) \tag{4}$$

where u* is the primary velocity and v* is the secondary velocity.

The initial and boundary conditions of the projected problem are specified by:

$$\begin{aligned} &u^*=0, && v^*=0, \quad T=T_\infty, && C^*=C^*_\infty && \text{for all } z^*, t^* \le 0 \\ &u^*=(u_0 v_f)^{\left(\frac{1}{3}\right)}\cos(\omega^* t^*), && v^*=0, \quad T=T_w, && C^*=C^*_w, && \text{for all } t^*>0 \\ &u^*\to 0, && v^*\to 0, \quad T\to T_\infty && C^*\to C^*_\infty && \text{at } z^*\to\infty \end{aligned} \tag{5}$$

The following set of non-dimensional quantities are introduced below

$$U=\frac{u^*}{(u_0 v_f)^{\left(\frac{1}{3}\right)}}, \qquad V=\frac{v^*}{(u_0 v_f)^{\left(\frac{1}{3}\right)}}, \qquad Z=z^*\left(\frac{u_0}{v_f^2}\right)^{\left(\frac{1}{3}\right)}$$

$$\omega=\omega^*\left(\frac{v_f}{u_0^2}\right)^{\left(\frac{1}{3}\right)}, \qquad M^2=\frac{\sigma_f B_0^2}{\rho_f}\left(\frac{v_f}{u_0^2}\right)^{\left(\frac{1}{3}\right)} \qquad R=\frac{16\,a^*\,\sigma_f T_\infty^{\,3}}{k_f}\left(\frac{v_f^{\,2}}{u_0}\right)^{\left(\frac{1}{3}\right)}$$

$$\theta=\frac{T-T_\infty}{T_w-T_\infty}, \qquad C=\frac{C^*-C^*_\infty}{C^*_w-C^*_\infty}, \qquad K_c=K_1\left(\frac{v_f}{u_0^2}\right)^{\left(\frac{1}{3}\right)}$$

$$Gr=\frac{g\,\beta_f(T_w-T_\infty)}{u_0} \qquad Gc=\frac{g\,\beta_f^*(C^*_w-C^*_\infty)}{u_0}, \qquad \mathrm{Pr}=\frac{\mu c_p}{k_f},$$

The local radiant for the case of an optically thin gray gas is expressed by

$$\frac{\partial q_r}{\partial z^*} = -4a^* \sigma_f \left(T_\infty^4 - T^4\right) \tag{6}$$

It is assumed that the temperature differences within the flow are sufficiently small such that T^4 may be expressed as a linear function of the temperature. This is accomplished by expanding T^4 in a Taylor series about T_∞ and neglecting higher-order terms, thus

$$T^4 \cong 4T_\infty^3\ T - 3T_\infty^4 \tag{7}$$

By using equations, dimensionless parameter equation (3) simplifies to

$$(\rho\, c_p)_{nf} \frac{\partial T}{\partial t'} = k_{nf} \frac{\partial^2 T}{\partial z^{*2}} + 16a^* \sigma T_\infty^3 (T_\infty - T) \tag{8}$$

By using the dimensionless parameter, equations Eq. (1), Eq. (2), and Eq. (3) lead to,

$$L_1 \frac{\partial U}{\partial t} = L_3 \frac{\partial^2 U}{\partial Z^2} + L_4\left(V - U\right) + L_2 Gr.\theta + L_7 Gc.C \tag{9}$$

$$L_1 \frac{\partial V}{\partial t} = L_3 \frac{\partial^2 V}{\partial Z^2} - L_4\left(U + V\right) \tag{10}$$

$$L_5 \frac{\partial \theta}{\partial t} = L_6 \frac{1}{\Pr} \frac{\partial^2 \theta}{\partial Z^2} - \frac{R}{\Pr}\theta \tag{11}$$

Where

$$L_1 = (1-\phi) + \phi\left(\frac{\rho_s}{\rho_f}\right)$$

$$L_2 = (1-\phi) + \phi\left(\frac{(\rho\beta)_s}{(\rho\beta)_f}\right)$$

$$L_3 = \frac{1}{(1-\phi)^{2.5}}$$

$$L_4 = 1 + \frac{3(\sigma-1)\phi}{(\sigma+2)-(\sigma-1)\phi}, \qquad \sigma = \frac{\sigma_s}{\sigma_f}$$

$$L_5 = (1-\phi) + \phi\left(\frac{(\rho c_p)_s}{(\rho c_p)_f}\right)$$

$$L_6 = \left[\frac{k_s + 2k_f - 2\phi(k_f - k_s)}{k_s + 2k_f + \phi(k_f - k_s)}\right]$$

$$L_7 = (1-\phi) + \phi\left(\frac{(\rho\beta^*)_s}{(\rho\beta^*)_f}\right)$$

Where R is the radiation parameter, Pr is the Prandtl number, Gr is the thermal Grashof number, and Gr approximates the ratio of the buoyancy force to the viscous force acting. Large R signifies a large radiation effect while R→0 corresponds to zero radiation effect.

The corresponding initial and boundary conditions are represented by Eq. (12),

$$\begin{aligned} & U = 0, && V = 0, \quad \theta = 0,\ C = 0 \quad for\ all \quad Z, t \le 0 \\ t > 0: \quad & U = Cos(\omega t), && V = 0, \quad \theta = 1,\ C = 1 \quad at \quad Z = 0 \\ & U \to 0, && V \to 0,\ \theta \to 0,\ C \to 0 \ at \ Z \to \infty \end{aligned} \tag{12}$$

$$Let\ F = U + iV \tag{13}$$

The newest governing equations are

$$L_1 \frac{\partial F}{\partial t} = L_3 \frac{\partial^2 F}{\partial Z^2} - L_4 b_1 F + L_2 Gr\,\theta + L_7 Gc\ C \tag{14}$$

$$L_5\frac{\partial\theta}{\partial t}=L_6\frac{1}{\Pr}\frac{\partial^2\theta}{\partial Z^2}-\frac{R}{\Pr}\theta \tag{15}$$

$$\frac{\partial C}{\partial t}=\frac{1}{Sc}\frac{\partial^2 C}{\partial Z^2}-K_c.C \tag{16}$$

The newest initial and boundary conditions are,

$$\begin{aligned} &F=0\,, && \theta=0\,, && C=0 && for\ all\ Z,t\le 0\\ t>0:\ &F=Cos\left(\omega t\right), && \theta=1\,, && C=1 && at\quad Z=0\\ &F\to 0\,, && \theta\to 0, && C\to 0 && at\quad Z\to\infty \end{aligned} \tag{17}$$

3. SOLUTION PROCEDURE

The solution is written in the combination of exponential and complementary error functions. It is denoted by the Eq.(18)

$$erfc(x)=1-erf\,(x) \tag{18}$$

The Laplace transform is used in RLC circuit analysis, to solve both ordinary and partial differential equations. The dimensionless equations Eq. (14), Eq.(15), and Eq. (16) with conditional equations Eq. (17) are solved by Laplace transformation. The outcomes are termed as follows

$$\begin{aligned} F=&\frac{\exp(i\omega t)}{4}\begin{pmatrix}\exp(2\eta\sqrt{g(b_2+i\omega)t})\ erfc\left(\eta\sqrt{g}+\sqrt{(b_2+i\omega)t}\right)\\ +\exp(-2\eta\sqrt{g(b_2+i\omega)t})\ erfc\left(\eta\sqrt{g}-\sqrt{(b_2+i\omega)t}\right)\end{pmatrix}\\ &+\frac{\exp(-i\omega t)}{4}\begin{pmatrix}\exp(2\eta\sqrt{g(b_2-i\omega)t})\ erfc\left(\eta\sqrt{g}+\sqrt{(b_2-i\omega)t}\right)\\ +\exp(-2\eta\sqrt{g(b_2-i\omega)t})\ erfc\left(\eta\sqrt{g}-\sqrt{(b_2-i\omega)t}\right)\end{pmatrix}\\ &+\frac{c}{2d}\left(\exp\left(2\eta\sqrt{gb_2t}\right)erfc\left(\eta\sqrt{g}+\sqrt{b_2t}\right)+\exp\left(-2\eta\sqrt{gb_2t}\right)erfc\left(\eta\sqrt{g}-\sqrt{b_2t}\right)\right)\\ &-\frac{c.\exp(dt)}{2d}\begin{pmatrix}\exp\left(2\eta\sqrt{g(b_2+d)t}\right)erfc\left(\eta\sqrt{g}+\sqrt{(b_2+d)t}\right)\\ +\exp\left(-2\eta\sqrt{g(b_2+d)t}\right)erfc\left(\eta\sqrt{g}-\sqrt{(b_2+d)t}\right)\end{pmatrix}\\ &+\frac{e}{2f}\left(\exp\left(2\eta\sqrt{gb_2t}\right)erfc\left(\eta\sqrt{g}+\sqrt{b_2t}\right)+\exp\left(-2\eta\sqrt{gb_2t}\right)erfc\left(\eta\sqrt{g}-\sqrt{b_2t}\right)\right)\\ &-\frac{e.\exp(ft)}{2f}\begin{pmatrix}\exp\left(2\eta\sqrt{g(b_2+f)t}\right)erfc\left(\eta\sqrt{g}+\sqrt{(b_2+f)t}\right)\\ +\exp\left(-2\eta\sqrt{g(b_2+f)t}\right)erfc\left(\eta\sqrt{g}-\sqrt{(b_2+f)t}\right)\end{pmatrix}\\ &-\frac{c}{2d}\left(\exp\left(2\eta\sqrt{abt}\right)erfc\left(\eta\sqrt{a}+\sqrt{bt}\right)+\exp\left(-2\eta\sqrt{abt}\right)erfc\left(\eta\sqrt{a}-\sqrt{bt}\right)\right)\\ &+\frac{c.\exp(dt)}{2d}\begin{pmatrix}\exp\left(2\eta\sqrt{a(b+d)t}\right)erfc\left(\eta\sqrt{a}+\sqrt{(b+d)}\right)\\ +\exp\left(-2\eta\sqrt{a(b+d)t}\right)erfc\left(\eta\sqrt{a}-\sqrt{(b+d)t}\right)\end{pmatrix}\\ &-\frac{e}{2f}\begin{pmatrix}\exp(2\eta\sqrt{Sc.K_c.t})\ erfc\left(\eta\sqrt{Sc}+\sqrt{K_c.t}\right)\\ +\exp(-2\eta\sqrt{Sc.K_c.t})\ erfc\left(\eta\sqrt{Sc}-\sqrt{K_c.t}\right)\end{pmatrix}\\ &+\frac{e.\exp(ft)}{2f}\begin{pmatrix}\exp(2\eta\sqrt{Sc.(K_c+f)}\ erfc\left(\eta\sqrt{Sc}+\sqrt{(K_c+f)t}\right)\\ +\exp(-2\eta\sqrt{Sc.(K_c+f)}\ erfc\left(\eta\sqrt{Sc}-\sqrt{(K_c+f)t}\right)\end{pmatrix}\end{aligned} \tag{19}$$

$$\theta=\frac{1}{2}\left(\exp(2\eta\sqrt{abt})\ erfc\left(\eta\sqrt{a}+\sqrt{bt}\right)+\exp(-2\eta\sqrt{abt})\ erfc\left(\eta\sqrt{a}-\sqrt{bt}\right)\right) \tag{20}$$

$$Where \quad a=\frac{L_5\,\mathrm{Pr}}{L_6},\ b=\frac{R}{L_5\,\mathrm{Pr}},\ b_1=M^2(1+i),\ b_2=\frac{L_4 b_1}{L_1},\ c=\frac{L_2 Gr}{L_1-L_3 a},\ d=\frac{L_3 ab-L_4 b_1}{L_1-L_3 a},\ e=\frac{L_7.Gc}{L_1-L_3.Sc},\ f=\frac{L_3.Sc.K_c-L_4.b_1}{L_1-L_3.Sc},\ g=\frac{L_1}{L_3}$$

$$C=\frac{1}{2}\left(\exp(2\eta\sqrt{K_c.Sc.t}\ \ erfc\left(\eta\sqrt{Sc}+\sqrt{K_c t}\right)+\exp(-2\eta\sqrt{K_c Sc.t})\ erfc\left(\eta\sqrt{Sc}-\sqrt{K_c t}\right)\right) \tag{21}$$

For measuring shear stress is expressed as skin friction (τ) at the plate.it is specified by

$$C_f=-\left(\frac{\partial F}{\partial z}\right)_{z=0} \tag{22}$$

The rate of temperature transmission is expressed by way of a Nusselt number (Nu). It has been specified by

$$Nu=-\left(\frac{\partial \theta}{\partial Z}\right)_{Z=0} \tag{23}$$

Among moving fluid and a solid body, heat transfer is calculated using the Nusselt number.

The ratio of mass transfer is expressed as a Sherwood number (Sh). It is specified by

$$Sh=-\left(\frac{\partial C}{\partial Z}\right)_{Z=0} \tag{24}$$

The velocity F has computed and represented by Eq. (19). Using the below formula, the complex error function is detached from real (U) and imaginary (V) parts separately. Real and imaginary parts are differentiated with initial conditions for calculating the Skin friction coefficient.

$$erf(a+ib)=erf(a)+\frac{\exp(-a^2)}{2a\pi}\left[1-\cos(2ab)+i\sin(2ab)\right]+\frac{\exp(-a^2)}{\pi}\sum_{n=1}^{\infty}\frac{\exp\left(\frac{-n^2}{4}\right)}{n^2+4a^2}\left[f_n(a,b)+ig_n(a,b)\right]+\in(a,b)$$

Where $f_n=2a-2a\cosh(nb)\cos(2ab)+n\sinh(nb)\sin(2ab)$

$g_n=2a\cosh(nb)\sin(2ab)+n\sinh(nb)\cos(2ab)$

$|\in(a,b)|\approx 10^{-16}|erf(a+ib)|$

4. RESULTS AND DISCUSSION

Like the fluid flow, the numerical values are analyzed for several variables Gr, Gc, Sc, φ , ω , Pr, M, t, K_c, and R with chemical reactions. Constant temperature and constant concentration are considered.

4.1 ANALYSIS OF VELOCITY PROFILES

In Figure 2. An increment M value decreased in Primary velocity U with $\omega = \pi/2$, t=0.2, Pr=0.71, R=1, Sc=0.6, K_c =1, Gr=5, GC=7, $\varphi = 0.15$.

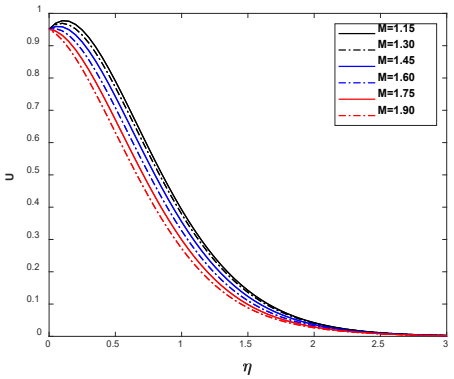

FIGURE 2. Primary Velocity profile for different M

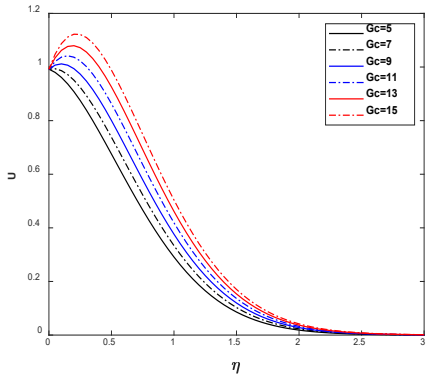

FIGURE3. Primary Velocity profile for different Gc

The increment of Gc increased the primary velocity U in Figure 3. The increment of Prandtl number values increases both velocities are displayed in Figure 4 and Figure 13. The impact of the increase of time (t) increases the primary velocity in Figure 5. The velocity profile of thermal Grashof number (Gr) is depicted in Figure 6. The increment of the velocity of the fluid in primary velocity by an increment in Gr. An increment by chemical compound response decreases the primary velocity in Figure 7.

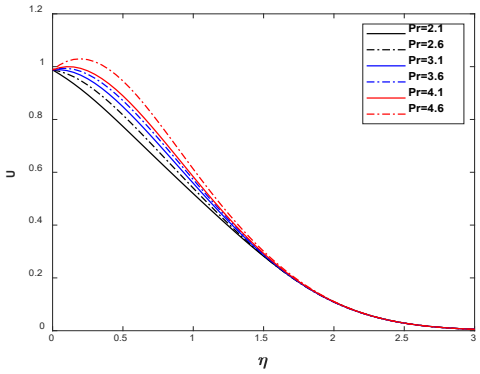

FIGURE 4. Primary Velocity profile for different Pr

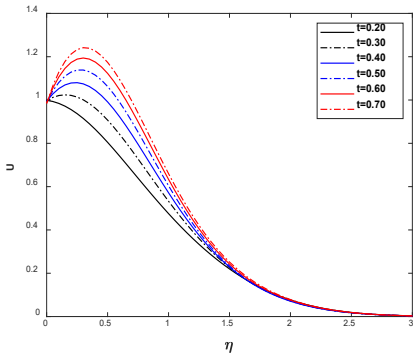

FIGURE 5. Primary Velocity profile for different t

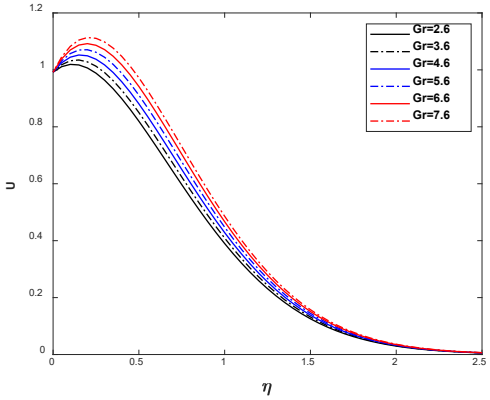

FIGURE 6. Primary velocity profile for different Gr

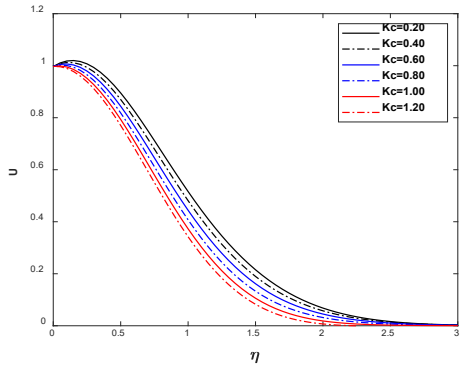

FIGURE 7. Primary velocity profile for different K_c

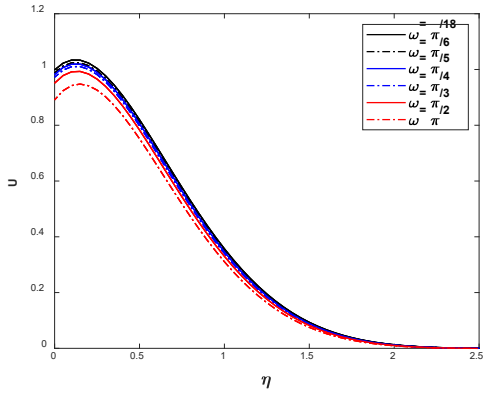

FIGURE 8. Primary velocity profile for different ω

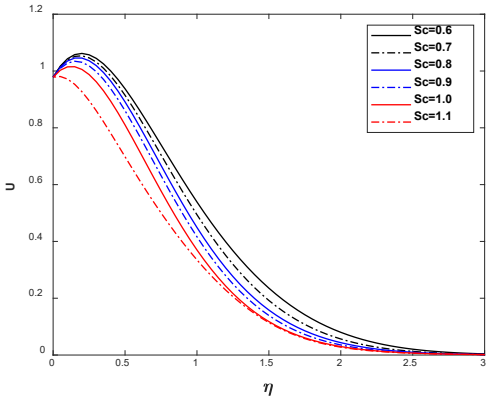

FIGURE 9. Primary velocity profile for different Sc

The phase angle ω ranges from π/18 to π/2 reduced the U in Figure 8. The increment of Schmidt number decreases the Primary velocity in Figure9. There is an improvement in the velocity that outcomes of Sc within the

boundary layer. The increment of solid volume fraction φ reduces the primary velocity U in Figure 10. The density of fluid raises once more alumina particles are mixed into the water and the fluid transforms into denser.

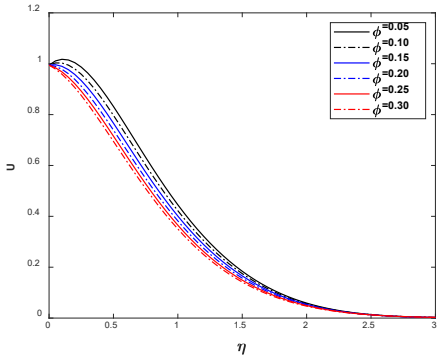

FIGURE 10. Primary velocity profile for different φ

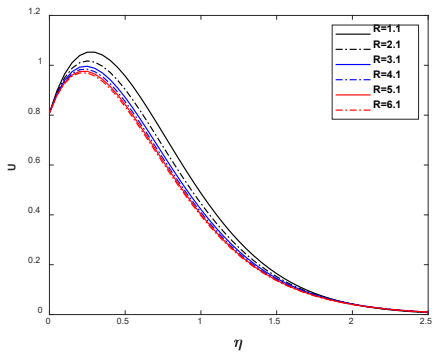

FIGURE 11. Primary velocity profile for different R

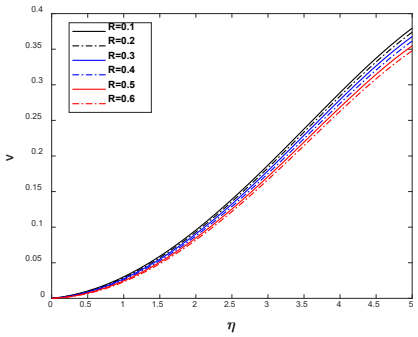

FIGURE 12. Secondary velocity profile for different R

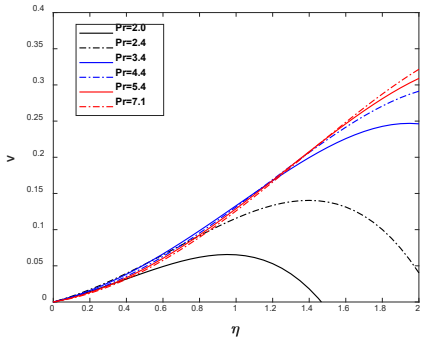

FIGURE 13. Secondary velocity profile for different Pr

With the increasing R-value, the influence at both velocities is decreased and depicted in Fig.11 and Fig.12.

4.2 ANALYSIS OF TEMPERATURE PROFILES

The thermal transmission rate is existed high in the air compared with water. So temperature increases while decreasing the Pr. The thermal diffusivity increment shows the way to a decline in the Pr. Thermal diffusion has a propensity to reduce the fluid temperature. The temperature values of various Pr has presented in Figure 14.

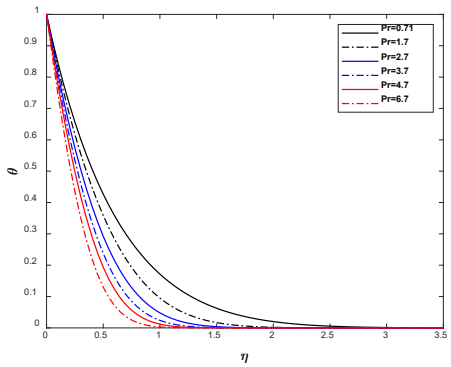

FIGURE.14. Temperature profile for different pr

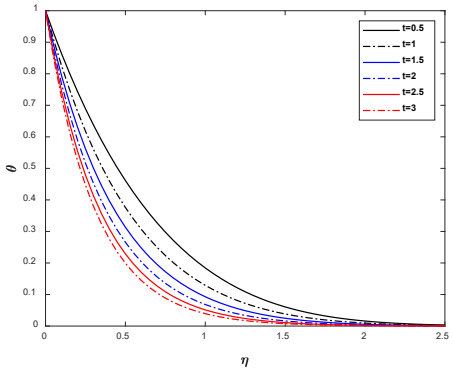

FIGURE.15. Temperature profile for different t

The temperature profile of the set of values of t has presented in Figure 15. This one has been created the temperature of Alumina nanofluid decreased by an increment of t.

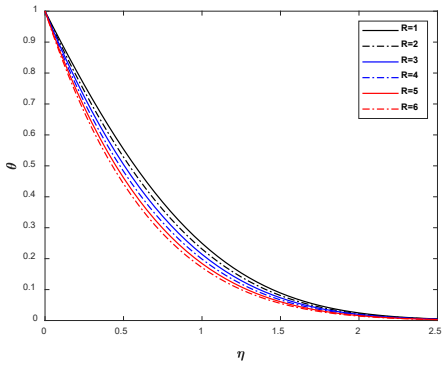

FIGURE.16. Temperature profile for different R.

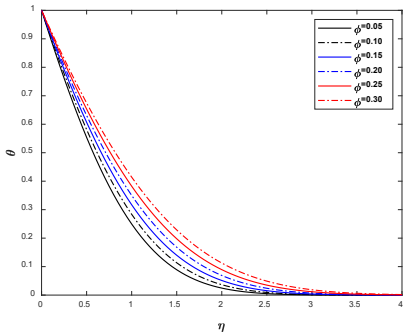

FIGURE.17. Temperature profile for different φ

Dissimilar values of temperature are presented in Figure 16. and Figure 17. for a set of R and φ.It has been generated decrement of heat in Alumina nanofluid if the raise of values of R. A temperature profile by different values of solid volume fraction has been displayed in Figure 18. It has been initiated heat increases with Alumina by an increment of solid volume fraction.

4.3 ANALYSIS OF CONCENTRATION PROFILES

In Figure 18. , the concentration values of various values of Sc and Kc=2 at time t=0.2 are depicted explicitly. The values of Sc decrease If the concentration values raises. The concentration values rise by reduction of chemical compound response are presented in Fig.18.This one is also perceived that in Fig.19, the concentration values increase of drop-in time.

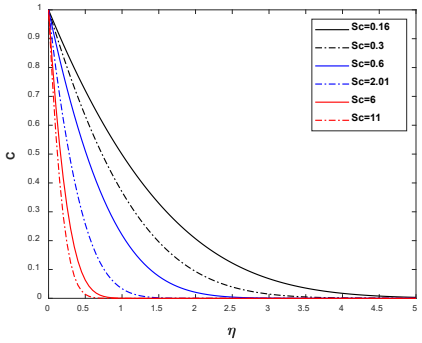

FIGURE.18. Concentration profile for different Sc

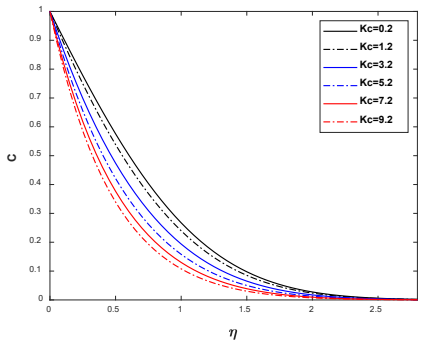

FIGURE.19. Concentration profile for different Kc

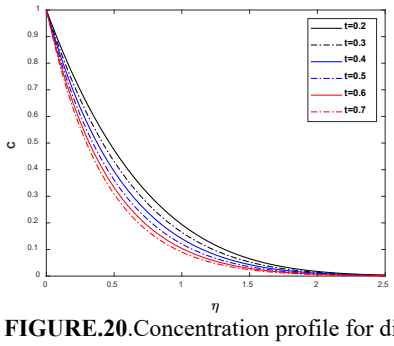

FIGURE.20.Concentration profile for different t

4.4 ANALYSIS OF PARAMETERS OF NUSSELT NUMBER, SHERWOOD NUMBER, SKIN FRICTION COEFFICIENT

At numerical impressions in solid volume fraction, R, Pr,t on thermal transfer coefficients are computed and itemized in Table.2. The particle size $\varphi = 0.15$ has been considered for the Nusselt number investigation.

TABLE 2. Variants in Nusselt Number

t	Pr	φ	R	Nu
0.3	0.71	0.05	1	1.2306
0.4	0.71	0.05	1	1.3377
0.5	0.71	0.05	1	1.4405
1.0	**1.1**	0.05	1	1.9705
1.0	**3.1**	0.05	1	2.1874
1.0	**5.1**	0.05	1	2.8103
0.1	0.71	**0.05**	1	1.0022
0.1	0.71	**0.09**	1	0.9447
0.1	0.71	**0.13**	1	0.8917
0.2	0.71	0.05	**0.8**	1.0728
0.2	0.71	0.05	**2.4**	1.4202
0.2	0.71	0.05	**4.0**	1.7265

TABLE 3. Variants in Sherwood number

t	Kc	Sc	Sh
0.6 **3.6** **5.6**	2	0.6	1.7544 4.1570 5.1846
0.5	**0.4** **0.8** **1.2**	0.6	1.0432 1.2021 1.3517
0.8	1.0	**1.2** **7.6** **8.4**	1.8073 4.5484 4.7818

TABLE 4. Comparison of Sherwood number

Kc	Sc	t	Sherwood number Ref[9].	Present Study
1.5	0.6	0.5	0.7298	1.4584
0.5	0.3 2.0	0.5	0.4253 1.0982	0.7664 1.9789
0.5	0.6	0.5 1.0	0.6015 0.9241	1.0839 1.2780

The various value of the Schmidt number, Sherwood numbers are calculated and listed in Table.3, and also increasing Schmidt number value. Sherwood's number is increasing for various amounts of Sc and K_c. This one

stands displayed in Figure 22. and Figure 23. The comparison values of the Sherwood number are increased for increasing parameters in Ref[9]. But in Table 4. the present study Sherwood numbers are increasing with respective parameters positively.

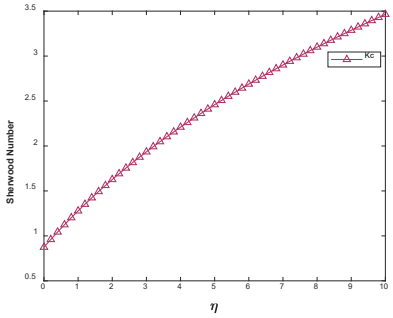

FIGURE 21. Sherwood number for different K_c

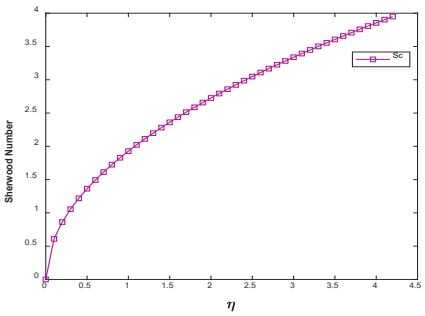

FIGURE 22.Sherwood number for different Sc

TABLE 5. Variations in Skin friction coefficient values on Primary Velocity (U) and Secondary Velocity (V)

t	φ	Pr	R	M	Gr	Gc	ω	Sc	K_c	C_f (Primary)	C_f (Secondary)
0.05										0.9322	0.0883
0.10	0.15	0.71	1.0	1.0	3.0	3.0	π/6	0.6	1.0	0.7671	0.2018
0.15										0.6100	0.3384
	0.13									0.7434	0.2142
0.1	**0.15**	0.71	1.0	1.0	3.0	3.0	π/7	0.6	1.0	0.7677	0.1997
	0.17									0.7888	0.1873
		3.0								1.1238	0.1014
0.2	0.15	**5.0**	1.0	1.0	3.0	3.0	π/4	0.6	1.0	1.1233	0.1132
		6.0								1.1178	0.1310
			1.0							0.4197	0.5601
0.2	0.15	0.71	**1.5**	1.0	3.0	3.0	π/3	0.6	1.0	0.4526	0.6458
			2.0							0.4788	0.6794
				1.0						0.8077	1.0169
0.25	0.15	2	1.3	**1.2**	3.0	5.0	π/8	0.6	1.0	0.6623	1.0702
				1.4						0.6349	1.0852
					1.0					-0.1484	1.2805
0.3	0.15	2.0	1.1	1.0	**11.0**	8	π/12	0.6	1.0	0.4244	3.1189
					21.0					0.9971	4.9574
						2.0				1.8744	0.4233
0.2	0.15	2.0	1.0	0.5	5	**8.0**	π/6	0.6	1.0	1.1120	0.7725
						16.0				0.0956	1.2382
							π/9			1.0769	0.0400
0.2	0.15	4.0	1.0	1	4.0	4.0	**π/6**	0.6	1.0	1.0693	0.0514
							π/3			1.0300	0.1164
								0.6		0.8868	0.0478
0.1	0.15	3.0	1.0	1	3.0	6.0	π/4	**0.7**	1.0	0.9091	0.1039
								0.8		0.9260	0.1915
									1.0	0.6657	0.7322
0.2	0.15	2.0	1.0	1	4	6	π/3	0.6	**2.0**	0.7763	0.9989
									3.0	0.8275	0.9417

The skin friction coefficient values are listed for numerous thermal Grashof number Gr, Mass Grashof number Gc, Magnetic parameter M, nanoparticle volume fraction φ, t, Pr, R, Sc,ω, K_c in Table 5. The skin friction

coefficient values are increased by cumulative values as to Schmidt number, chemical compound response for both velocities.

CONCLUSION

The major concept of this paper is to acquire the exact solution and to find the influences of the Hotness in addition to Mass Transmission of the unstable free convective Alumina nanofluid stream above an oscillating platter with the existence of radiative energy and MHD using chemical compound response. The probe of chemical compound response in an oscillating plate and Alumina nanofluid flow, the highlights of concluding remarks have been summarized as followed

- An increment of the phase angle, magnetic parameter, the volume of solid fraction, radiation, directs to drop in the primary velocity.
- The rise of radiation and the Prandtl parameter indicates the decrease in the secondary velocity.
- The radiation parameter, volume of solid fraction, and Prandtl number are increased by diminishing the heat. But increasing solid volume indicates an increase in heat.
- Nusselt number rises through increment of time, radiation, Prandtl number also it declines range of solid volume fraction size.
- The Increment of time, Schmidt number, and chemical compound response direct raise the Sherwood number.
- An increment of phase angle and Magnetic parameter give way to the reduction of Skin friction coefficient values.

NOMENCLATURE

List of symbols

B_0	Constant applied magnetic field (Wbm^{-2})
C_p	Specific heat at constant pressure ($J\,kg^{1}\,K^{-1}$)
C_f	Coefficient of Skin Friction
E	Electric field (kJ)
F	Complex Function
g	Gravity acceleration ($m\,s^{2}$)
Gr	Thermal Grashof number
Gc	Mass Grashof number
K_c	Chemical Reaction Parameter.
M	Dimensionless magnetic field parameter
m	Hall Parameter
Nu	Nusselt Number
n	Dimensionless frequency
Pr	Prandtl number
$\overline{q_w}$	Dimensional heat flux from the plate
$t^{\ddot{}}$	Time(s)
t	Dimensionless time (s)
T	Local temperature of the nanofluid (K)
T_w	Wall temperature (K)
T_∞	The temperature of the ambient nanofluid (K)
$u^{\ddot{}}, v^{\ddot{}}, w^{\ddot{}}$	Velocity components along $x^{\ddot{}}, y^{\ddot{}}, z^{\ddot{}}$ axes
U, V, W	Dimensionless velocity components
x, y, z	Cartesian coordinates

Greek symbols

α	Thermal diffusivity ($m^2 s^{-1}$)
β	Thermal expansion coefficient (K^{-1})
β^*	Mass expansion coefficient
ε	Dimensionless small quantity (<<1)
φ	Solid volume fraction of the nanoparticles
ρ	Density
k	Thermal conductivity ($m^2 s^{-1}$)
μ	Dynamic viscosity (Pa s)
ϑ	Kinematic viscosity ($m^2 s^{-1}$)
θ	Dimensionless temperature
η	Pseudo-similarity variable
ω	Phase angle
σ	Electrical conductivity ($m^2 s^{-1}$)

Superscript

$-$	Dimensional quantities

Subscripts

f	Fluid
nf	Nanofluid
s	Solid

ACKNOWLEDGMENTS

I thank Dr.E.Geetha, Assistant Professor, Department of mathematics, Sri Chandrasekharendra Saraswathi Viswamaha Vidyalaya, Enathur, Kanchipuram for the valuable suggestions and motivation for improving the manuscript.

REFERENCES

1. Biswas, R. & Ahmmed, S. F. Effects of Hall Current and Chemical Reaction on Magnetohydrodynamics Unsteady Heat and Mass Transfer of Casson Nanofluid Flow Through a Vertical Plate. *J. Heat Transfer* 140, 1–12 (2018).
2. Das, S., Jana, R. N. & Makinde, O. D. Magnetohydrodynamic free convective flow of nanofluids past an oscillating porous flat plate in a rotating system with thermal radiation and hall effects. *J. Mech.* 32, 197–210 (2016).
3. Datta, A., Kumar, S. & Halder, P. Heat Transfer and Thermal Characteristics Effects on Moving Plate Impinging from Cu-Water Nanofluid Jet. *J. Therm. Sci.* 29, 182–193 (2020).
4. Mahanthesh, B., Gireesha, B. J. & Gorla, R. S. R. Heat and mass transfer effects on the mixed convective flow of chemically reacting nanofluid past a moving/stationary vertical plate. *Alexandria Eng. J.* 55, 569–581 (2016).
5. Mahbubul, I. M., Elcioglu, E. B., Amalina, M. A. & Saidur, R. Stability, thermophysical properties and performance assessment of alumina–water nanofluid with emphasis on ultrasonication and storage period. *Powder Technol.* 345, 668–675 (2019).
6. Misra, J. C. & Adhikary, S. D. MHD oscillatory channel flow, heat and mass transfer in a physiological fluid in presence of chemical reaction. *Alexandria Eng. J.* 55, 287–297 (2016).

7. Muthucumaraswamy, R. & Jeyanthi, L. Hall effects on MHD flow past an infinite vertical plate in the presence of rotating fluid of variable temperature and mass diffusion with first-order chemical reaction. *ARPN J. Eng. Appl. Sci.* 10, 9596–9603 (2015).
8. Oahimire, J. I. & Olajuwon, B. I. Effect of Hall current and thermal radiation on heat and mass transfer of a chemically reacting MHD flow of a micropolar fluid through a porous medium. *J. King Saud Univ. - Eng. Sci.* 26, 112–121 (2014).
9. Rout, P. K., Sahoo, S. N. & Dash, G. C. Effect of heat source and chemical reaction on MHD flow past a vertical plate with variable temperature. *J. Nav. Archit. Mar. Eng.* 13, 101–110 (2016).
10. Srinivas & Kishan, N. Chemical Reaction Effects on MHD Nanofluid Flow of a Convection Slip in a Saturated Porous Media Over a Radiating Stretching Sheet with Heat Source/Sink. *Asian Res. J. Math.* 2, 1–15 (2017).
11. Swarnalathamma, B. V. Heat and Mass Transfer on MHD flow of Nanofluid with thermal slip effects. 13, 13705–13726 (2018).
12. U S Rajput & Gaurav Kumar. Effects Of Radiation, Chemical Reaction And Porosity Of The Medium On Mhd Flow Past An Oscillating Plate With Heat And Mass Transfer. (2017).
13. Venkateswarlu, B. & Satya Narayana, P. V. Chemical reaction and radiation absorption effects on the flow and heat transfer of a nanofluid in a rotating system. *Appl. Nanosci.* 5, 351–360 (2015).
14. Zubair Akbar, M., Ashraf, M., Farooq Iqbal, M. & Ali, K. Heat and mass transfer analysis of unsteady MHD nanofluid flow through a channel with moving porous walls and medium. *AIP Adv.* 6, (2016).

Volume 05, No.01, June 2023 ISSN- 2395-3497

नवीन अन्वेषण

Naveen Anveshan

A Journal of the Multidisciplinary Subjects

An Official Publication of
Pandit S.N.Shukla University Shahdol, (M.P.)

Volume 05, No.01, June 2023 ISSN- 2395-3497

Contents

Volume 05, No.01, June 2023 ISSN- 2395-3497

नवीन अन्वेषण
Naveen Anveshan

A Journal of the Multidisciplinary Subjects

An Official Publication of
Pandit S.N.Shukla University, Shahdol, (M.P.)

SKIN FRICTION ANALYSIS OF PARABOLIC MOTION EFFECTS ON VERTICAL PLATE WITH VARIABLE TEMPERATURE AND UNIFORM MASS FLUX

E. Geetha
Department of Mathematics, Sri Chandrasekharendra Saraswathi Viswa Mahavidyalaya Enathur, Kanchipuram 631561, India
Email: geethamuthu06@gmail.com

ABSTRACT: The effects of a uniform mass flux on a parabolic starting vertical plate with varying temperature are shown in this paper. The momentum, energy, and mass equations from Bousseinq's equations are taken into consideration here and converted into linear partial differential equations utilizing non-dimensional quantities. Laplace transform is used to solve the governing equations. Graphical analyses of the velocity profiles is performed for a variety of parameters, including time, thermal Grashof number, mass Grashof number, Schmidt number, and Prandtl number. For increasing levels of time, thermal Grashof number, or mass Grashof number, it has been observed that velocity increases. It is observed that when t grows, the values of shear stress drop, and when the mass Grashof number increases, the values of shear stress decrease. The shear stress is obtained for various values of thermal Grashof number, mass Grashof number, Schmidt number, Prandtl number, and time.

Key words: Parabolic, vertical plate, constant mass flux, variable temperature, Shear stress.

INTRODUCTION

There are many technical applications for the unstable natural convection flow of a viscous fluid up a vertical plate, which is a classic problem in fluid mechanics and heat transfer. Since it is essential for a variety of applications, including the cooling of electronic devices by fans, the cooling of nuclear reactors during emergency shutdown, the exposure of solar central receivers to wind current, and chemical catalytic reactions, the study of convective flow, heat transfer, and mass transfer has been an active area of research.

Siegel[1] examined transient free convection from a vertical plate. The transition of vertical natural convection flows in water was researched by Joshi et al[2]. A semi-infinite rapidly heated vertical plate's boundary layer evolution was explored by Patterson et al. [3]. The transient free convection flow past an infinite vertical plate with periodic temperature variation was examined by Das et al[4]. Schetz et al.[5] discussed unstable natural convection near a doubly-infinite vertical plate. Illingworth[6] has investigated the advection of a gas near an

infinite flat plate in a laminar flow. Elder [7] has researched laminar free convection in a vertical slit. The transient free convection around vertical plates and spherical cylinders has been researched by Goldstein [8].

Alan Shapiro et al.[9] have explored the Prandtl number dependence of unsteady natural convection along a vertical plate in a stably stratified fluid. The effects of magneto hydrodynamic flow past a vertical plate with varying surface temperature have been examined by Abbas[10]. Saravana et al. [11] evaluated the impact of mass transfer on MHD viscous flow via an impulsively begun infinite vertical plate with constant mass flux. The effects of mass transfer on flow past an impulsively initiated infinite vertical plate with constant mass flux have been studied by Soundalgekar et al. [12]. The heat and mass transport via natural convection in a porous media has been explored by Bejan and Khair[13]. Vajravelu et al.[14] examined the unsteady convective boundary layer flow of a viscous fluid at a vertical surface with changeable fluid parameters. Elbashbeshy[15] has investigated the movement of heat and mass along a vertical plate with a fluctuating surface temperature and concentration when a magnetic field is present. The unstable free convection on a vertical cylinder with variable heat and mass flux has been explored by Ganesan and Rani [16]. The implications of mass transfer on the transient free convective flow of a dissipative fluid down a semi-infinite vertical plate with continuous heat flux have been explored by Gokhale and Samman [17]. Somers [18] investigated the theoretical underpinnings of coupled thermal and mass transfer from a vertical flat plate. Takhar et al.'s [19] studied of transient free convection across a semi-infinite vertical plate with varying surface temperature.

Soundalgekar et al.[20] examined the impact of mass transfer and heat sources on the flow through an accelerated infinite vertical plate. The precise solution of the effects of mass transfer on flow through an abruptly began infinite vertical plate with constant mass flux has been studied by Das et al. [21]. Satyanarayana et al.[22] studied the effects of radiation and mass transfer on a moving vertical plate with varying temperature and viscous dissipation. Using the Crank-Nicolson finite difference approach, Abd el-nabyet al[23] investigated the effects of radiation on unsteady free convective flow past a semi-infinite vertical plate with fluctuating surface temperature. Sahin Ahmed et al.[24] explored the Laplace Technique on Magneto Hydrodynamic Radiating and Chemically Reacting Fluid over an Infinite Vertical Surface. The MHD free convective flow across an exponentially accelerated vertical plate with variable temperature and variable mass diffusion has been explored by Vijaya et al. [25]. The literature has not yet explored the impact of natural convective heat and mass transfer of an incompressible fluid flowing past a parabolic-started vertical plate with variable

temperature and uniform mass flux.

This study aims to investigate the impact of a laminar free convective flow of an incompressible fluid past on a vertical plate begun at a parabolic angle and subjected to a constant mass flux as the temperature of the plate varies. The laplace transform approach is used to solve the governing equations.

MATHEMATICAL FORMULATION

The unsteady flow of a viscous incompressible fluid past a parabolic starting infinite vertical plate with changing temperature and uniform mass flux was investigated in this paper. The fluid under consideration here is gray and absorbs-emits radiation, but it is not a scattering medium. The x-axis runs vertically up the plate, whereas the y-axis runs normal to the plate. At first, it is assumed that the plate and fluid are both at the same temperature T_∞ and have the same concentration C'_∞ level at all spots. The plate is given a parabolic motion in its own plane with velocity $u = u_0 t'^2$ at time t' > 0. Simultaneously, the plate temperature rises linearly with time t', and mass flux flows uniformly from the plate.

Then by usual Boussinesq's approximation, the unsteady flow is governed by the following set of equations.

$$\frac{\partial u}{\partial t'} = g\beta(T - T_\infty) + g\beta^*(C' - C'_\infty) + \nu\frac{\partial^2 u}{\partial y^2} \qquad (1)$$

$$\rho C_p \frac{\partial T}{\partial t'} = k\frac{\partial^2 T}{\partial y^2} \qquad (2)$$

$$\frac{\partial C'}{\partial t'} = D\frac{\partial^2 C'}{\partial y^2} \qquad (3)$$

With the following initial and boundary conditions

$$u = 0,\ T = T_\infty,\ C' = C'_\infty, \quad \text{for all } y,\ t' = 0.$$

$$t' > 0,\ u = u_0 t'^2,\ T = T_\infty + (T_w - T_\infty)At',\ \frac{\partial C'}{\partial y} = -\frac{j''}{D} \text{ at } y = 0 \qquad (4)$$

$$u \to 0, T \to T_\infty, C' \to C'_\infty \text{ as } y \to \infty$$

On introducing the following non – dimensional quantities:

$$U = u\left(\frac{u_0}{v^2}\right)^{1/3}, t = \left(\frac{u_0^2}{v}\right)^{1/3} t', Y = y\left(\frac{u_0}{v^2}\right)^{1/3}, \theta = \frac{T - T_\infty}{T_W - T_\infty}, C = \frac{C' - C_\infty'}{\frac{j'' v^{2/3}}{D u_0^{1/3}}},$$

$$Gr = \frac{g\beta(T - T_\infty)}{(v u_0)^{1/3}}, Gc = \frac{g\beta^* \left(\frac{j'' v^{2/3}}{D u_0^{1/3}}\right)}{(v u_0)^{1/3}}, \Pr = \frac{\mu C_p}{k}, Sc = \frac{v}{D}, A = \left(\frac{u_0^2}{v}\right)^{1/3}$$

In equations (1) to (4) leads to

$$\frac{\partial U}{\partial t} = Gr\theta + GcC + \frac{\partial^2 U}{\partial Y^2} \quad (6)$$

$$\frac{\partial \theta}{\partial t} = \frac{1}{\Pr}\frac{\partial^2 \theta}{\partial Y^2} \quad (7)$$

$$\frac{\partial C}{\partial t} = \frac{1}{Sc}\frac{\partial^2 C}{\partial Y^2} \quad (8)$$

The initial and boundary conditions in non dimensional quantities are

$U = 0, \theta = 0, C = 0$ For all Y, $t \leq 0$

$$t > 0, \quad U = t^2, \theta = t, \frac{\partial C}{\partial Y} = -1 \quad \text{at } Y = 0 \quad (9)$$

$$U \to 0, \theta \to 0, C \to 0 \text{ As } Y \to \infty$$

METHODS OF SOLUTIONS

The dimensionless governing equations (6) to (8) and the corresponding initial and boundary conditions (9) are tackled using Laplace transform technique.

The solutions to the unstable linear coupled partial differential equations of a viscous flow have been derived in terms of exponential and complementary error functions using the laplace transform approach.

$$C = 2\sqrt{t}\,t\left[\frac{\exp(-\eta^2 Sc)}{\sqrt{\pi}\sqrt{Sc}} - \eta\, erfc(\eta\sqrt{Sc})\right] \tag{10}$$

$$\theta = t\left[(1+2\eta^2 \Pr)erfc(\eta\sqrt{\Pr}) - \frac{2\eta\sqrt{\Pr}}{\sqrt{\pi}}\exp(-\eta^2 \Pr)\right] \tag{11}$$

$$U = \frac{t^2}{3}\left[(3+12\eta^2+4\eta^4)erfc(\eta) - \frac{\eta}{\sqrt{\pi}}(10+4\eta^2)\exp(-\eta^2)\right]$$
$$-at^2\left[\begin{array}{l}(3+12\eta^2+4\eta^4)erfc(\eta)-(3+12\eta^2\Pr+4\eta^4(\Pr)^2)erfc(\eta\sqrt{\Pr}) \\ -\frac{\eta}{\sqrt{\pi}}(10+4\eta^2)\exp(-\eta^2)+\frac{\eta\sqrt{\Pr}}{\sqrt{\pi}}(10+4\eta^2\Pr)\exp(-\eta^2\Pr)\end{array}\right]$$
$$-bt\sqrt{t}\left[\begin{array}{l}\frac{4}{\sqrt{\pi}}(1+\eta^2)\exp(-\eta^2)-\eta(6+4\eta^2)erfc(\eta) \\ -\frac{4}{\sqrt{\pi}}(1+\eta^2 Sc)\exp(-\eta^2 Sc)+\eta\sqrt{Sc}(6+4\eta^2 Sc)erfc(\eta\sqrt{Sc})\end{array}\right] \tag{12}$$

Where $a = \dfrac{Gr}{6(1-\Pr)}, b = \dfrac{Gc}{3\sqrt{Sc}(1-Sc)}$

Skin friction

The boundary layer produces a drag force on the plate due to the viscous stresses which are developed at the wall. The viscous stress at the surface of the plate is given by

$$\tau = -\left(\frac{\partial u(y,t)}{\partial y}\right)_{y=0} \tag{13}$$

$$\tau = \frac{-1}{2\sqrt{t}}\left[\frac{t^2}{3}\left(\frac{-16}{\sqrt{\pi}}\right) - \frac{Grt^2}{6(1-\Pr)}\left(\frac{-16}{\sqrt{\pi}}\right)(1-\sqrt{\Pr}) - \frac{Gct\sqrt{t}}{3\sqrt{Sc}(1-Sc)}\left(-6+6\sqrt{Sc}\right)\right]$$

RESULTS AND DISCUSSION

To get a better understanding of the flow regime's mechanics, we investigated the effects of thermal Grashof number Gr, mass Grashof number Gc, Prandtl number Pr, Schmidt number Sc, and time t on velocity, temperature, concentration profiles, and skin friction. Throughout the discussion, we consider Gr = Gc = 5 >0 (plate cooling), i.e., free convection current transport heat away from the plate into the boundary layer, t=0.2, Pr=0.71 (air), Sc = 0.16.

The influence of the Prandtl number Pr (Pr = 0.71, 2.0, 7.0) on the velocity profiles at t=0.2 is seen in Figure 1. It is observed that when Pr grows, velocity decreases. This is consistent with the physical reality that the thickness of the thermal boundary layer decreases as Pr increases. Figure 2 depicts the effects of time t on the velocity profile in the presence of air (Pr = 0.71). It is noted that as the value of t increases, so does the velocity.

Figure 3 depicts the effect of various Schmidt numbers Sc (Sc = 0.16, 0.6, 2.01) on the velocity profile in the presence of air (Pr = 0.71) at time t = 0.2. Sc here denotes the relative efficacy of momentum and mass transmission via diffusion. Furthermore, as Sc increases in magnitude, the momentum barrier layer shrinks. Figure 4 depicts the influence of velocity in the presence of air (Pr = 0.71) at time t = 0.2 for various values of thermal Grashof number Gr and mass Grashof number Gc. The velocity increases with increasing thermal or mass Grashof number. This is because buoyancy force increases fluid velocity and the value of Gr or Gc.

Tables 1 and 2 demonstrate the influence of skin friction for various values of thermal Grashof number Gr, mass Grashof number Gc, Prandtl number Pr, Schmidt number Sc, and time t. Table 1 illustrates the effect of skin friction in the presence of air (Pr = 0.71) and Table 2 shows the effect of skin friction in the presence of water (Pr = 7.0). In both tables, we see that skin friction increases as the mass Grashof number increases and skin friction increases as the Schmidt number increases. Skin friction reduces as time t increases.

CONCLUSION

The transient free convection viscous flow past over a parabolic starting infinite vertical plate with fluctuating temperature, generated by a uniform mass flux, has been mathematically analyzed. For the momentum, energy, and mass conservation equations, dimensionless governing equations are developed, and solutions are achieved using the laplace transform approach. The study found that as time t grows, so does the velocity, concentration, and temperature of the plate. While the temperature and velocity of the plate increase, Pr drops and the Schmidt number decreases.

The velocity of the plate increases as the thermal Grashof number Gr or the mass Grashof number Gc increases. Skin friction increases with rising value of mass Grashof number Gc or Schmidt number Sc, but the pattern reverses in time t.

REFERENCES

1. Siegel,R., (1958), Transient free convection from a vertical flat plate, Trans. ASME, 80, 347 – 359.
2. Joshi,Y. Gebhart,B.,(1987), Transition of vertical natural flows in water, J.Fluid Mech.,179,407 – 438.
3. Patterson, J.C. Graham, T.Schopf, W.and Armfield, S.W., (2002), Boundary layer development on a semi – infinite suddenly heated vertical plate, J. Fluid Mech., 453, 39-55.
4. Das, U.N. Deka, R.K. andSoundalgekar, V.M.,(1999), Transient free convection flow past an infinite vertical plate with periodic temperature variation,J.Heat Transfer, 12, 1091-1094.
5. Schetz, J.A. Eichlorn, R., (1962), Unsteady natural convection in the vicinity of a doubly – infinite vertical plate, Trans. ASME J. Heat transfer, 84, 334-338.
6. Illlingworth, C.R., (1950), Unsteady laminar flow of a gas near an infinite flat plate,Proc. Cambridge philos. Soc., 46, 603-613.
7. Elder,J.W., (1965), Laminar free convection in a vertical slot,J.Fluid Mech., 23, 77-98.
8. Goldstein, R.J. Briggs, D.G., (1964), Transient free convection about vertical plate and circular cylinders, Trans. ASME: J.Heat transfer, 86,490-500.
9. Alan Shapiro, EvgeniFedorovich, (2004),Prandtl number dependence of unsteady natural convection along a vertical plate in a stably stratified fluid, Int. J. of Heat and mass transfer, 47, 4911-4927.
10. Abbas, I.A.Palani, G., (2010),The effects of magneto hydrodynamic flow past a vertical plate wuth variable surface temperature, Applied Mathematics and Mechanics, 31, 329-338
11. Saravana, R. Sreekanth, S. Reddy, H.R., (2011), Mass transfer effects on MHD viscous flow past an impulsively starts infinite vertical plate with constant mass flux, Advances in applied science research, 2, 221-229
12. Soundalgekar, V.M. Das, U.N. Ray,S.N., (1996), Mass transfer effects on flow past an impulsively started infinite vertical plate with constant mass flux, Int. J. of Heat and mass transfer, 31, 163-167.
13. Bejan, A. Khair, K.R., (1985),Heat and mass transfer by natural convection in a porous medium, Int. J. of Heat and mass transfer, 28, 900-918.
14. Vajravelu, K. Prasad, K.V. Chin-on Ng.,(2013), Unsteady convective boundary layer flow of a viscous fluid at a vertical surface with variable fluid properties, Non- linear analysis: Real world applications,14, 455-464.

15. Elbashbeshy,E.M.A.,(1997), Heat and mass transfer along a vertical plate with variable surface temperature and concentration in the presence of magnetic field, Int. J. Engg. Sci., 34,515-522.
16. Ganesan, P. and Rani, H.P., (2000), unsteady free convection MHD flow past a vertical cylinder with mass transfer, Int. J. Ther. Sci., 39, 265-272.
17. Gokhale, M.Y. and Al Samman, F.M., (2003),Effects of mass transfer on the transient free convection flow of a dissipative fluid along a semi-infinite vertical plate with constant heat flux, Int. J. Heat and mass transfer, 46, 999-1011.
18. Somers, E.V., (1956), Theoretical considerations of combined heat and mass transfer from vertical flat plate, J. Appl. Mech., 23, 295-301.
19. Takhar, H.S.Ganeşan, P. Ekambavahar, K.andSoundalgekar, V.M., (1997), Transient free convection past a semi-infinite vertical plate with variable surface temperature. Int. J. Numerical methods Heat fluid flow, 7,280-296.
20. Soundalgekar, V.M.Pohanerkar, S.C and Lahurikar, R.M., (1992), Effects of Heat mass transfer and Heat sources on the flow past an accelerated infinite vertical plate,Forschungimingenieurwesen – Engineering research, 58,63-66.
21. Das, U.N. Ray, S.N. and Soundalgekar, V.M., (1996), Mass transfer effects on flow past an impulsively started infinite vertical plate with constant mass flux – an exact solution, Heat and mass transfer, 31, 163-167.
22. Kesavaiah, D.ch. Satyanarayana, P.V.Gireeshkumar,J. and Venkataramana,S., (2012), Radiation and mass transfer effects on moving vertical plate with variable temperature and viscous dissipation, Int.J.of mathematical Archive, 3(8), 3028-3035.
23. Abd El-Naby, M.A. Elsayed, M.E.Elbarbary and Nader ,Y.A., (2003), Finite difference solution of radiation effect on MHD free convection flow over a vertical plate with variable surface temperature, Journal of applied mathematics, 2, 65-86.
24. Sahin Ahmed, DimbeswarKalita, (2012), Laplace technique on magnetohydrdynamic radiating and chemically reacting fluid over an infinite vertical surface, Int.J.ofsci and tech., 1, 224-233.
25. Vijaya, N.Ramana Reddy, G.V.,(2012), MHD free convective flow past an exponentially accelerated vertical plate with variable temperature and variable mass diffusion. Asian J of Current Engineering and Maths, 1,308-313.

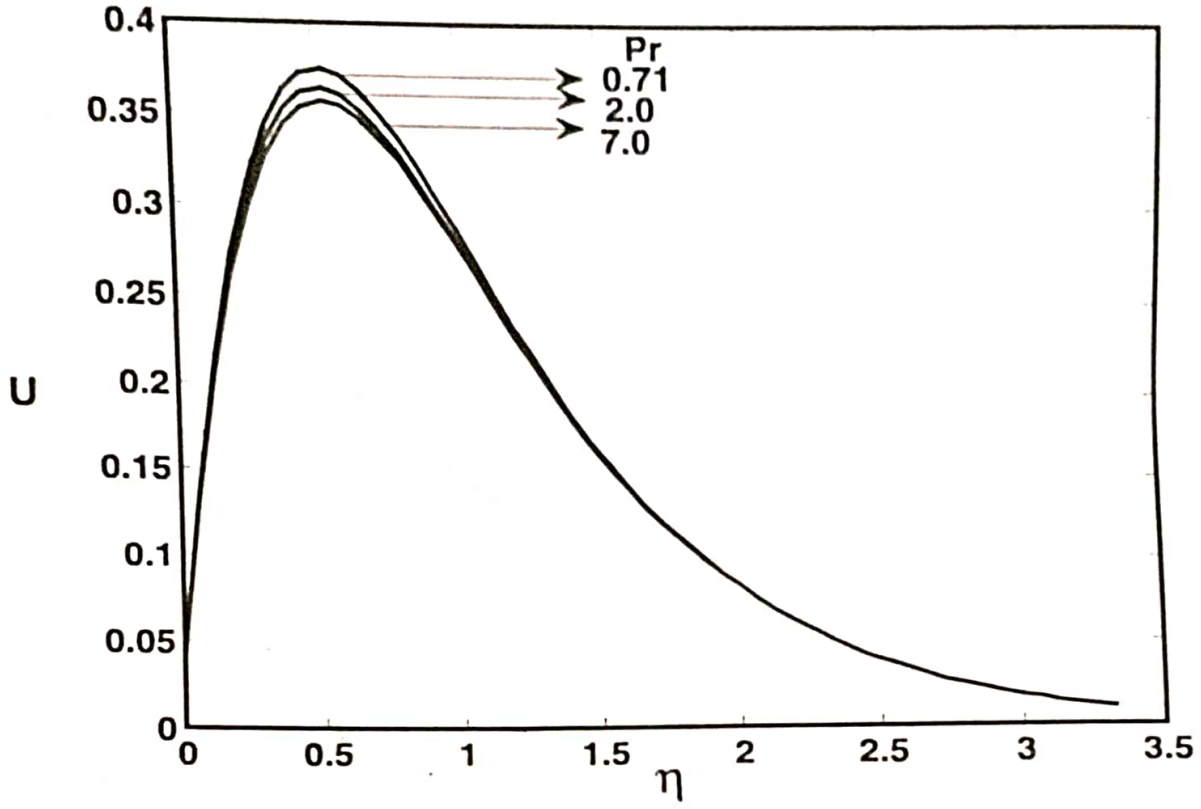

Figure.1. Velocity profiles for different values of Pr

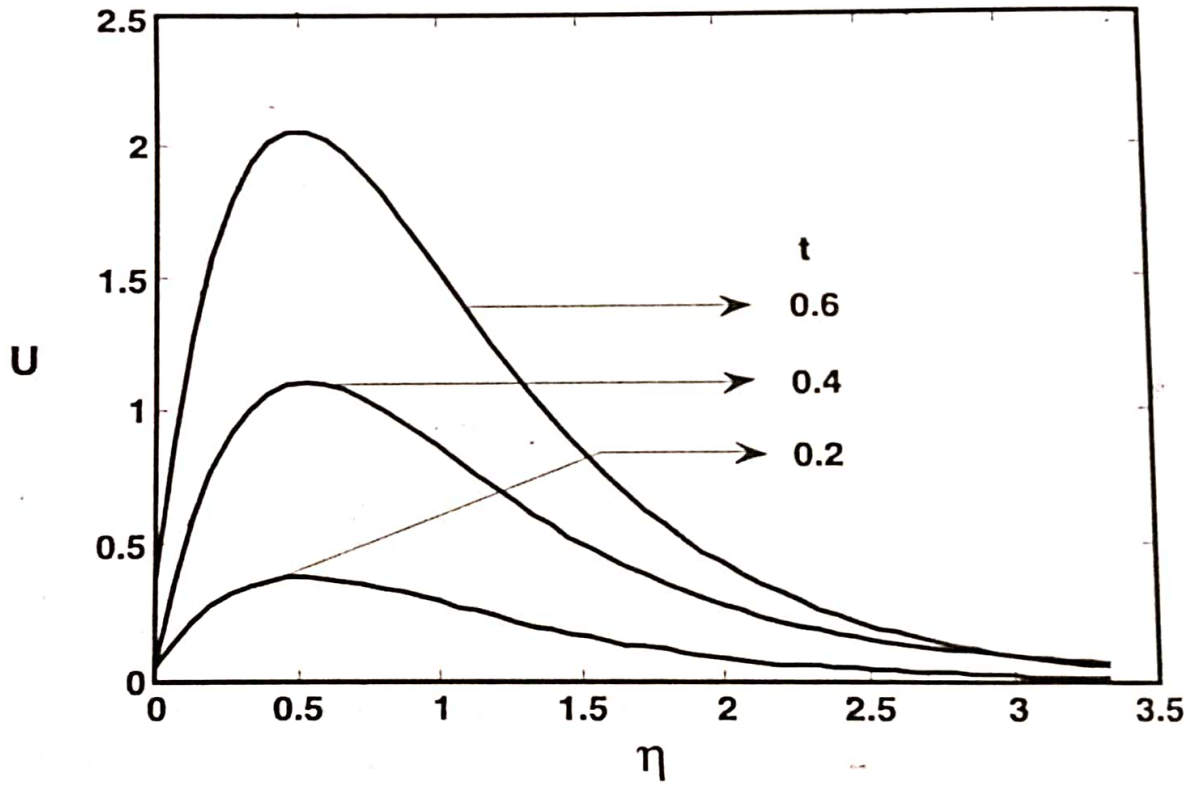

Figure.2. Velocity profiles for different values of t

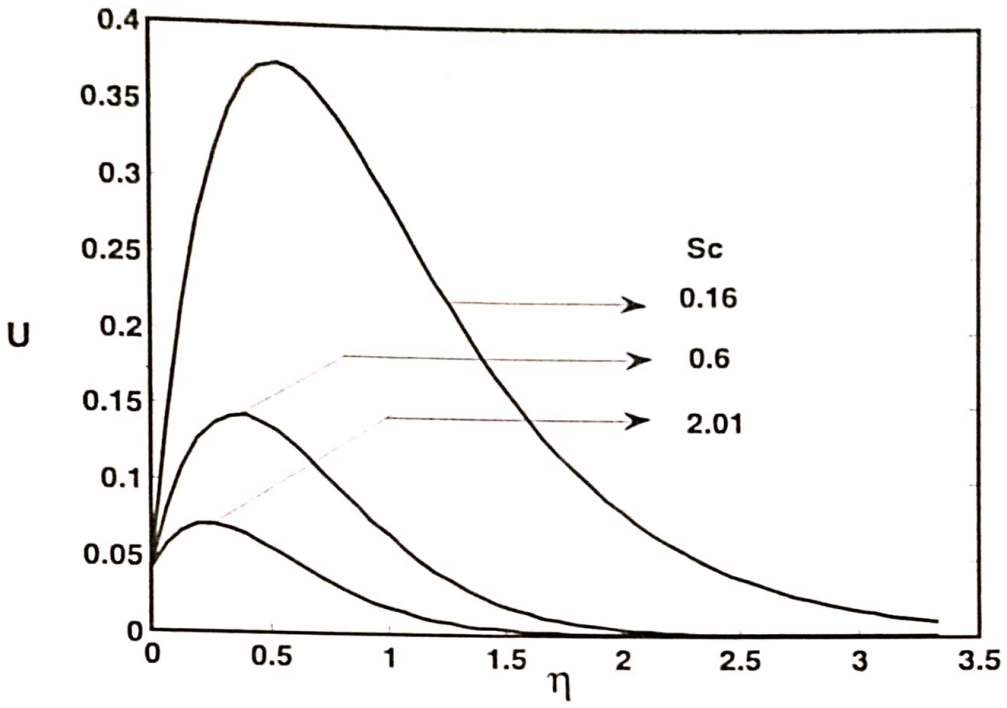

Figure.3. Velocity profiles for different values of Sc

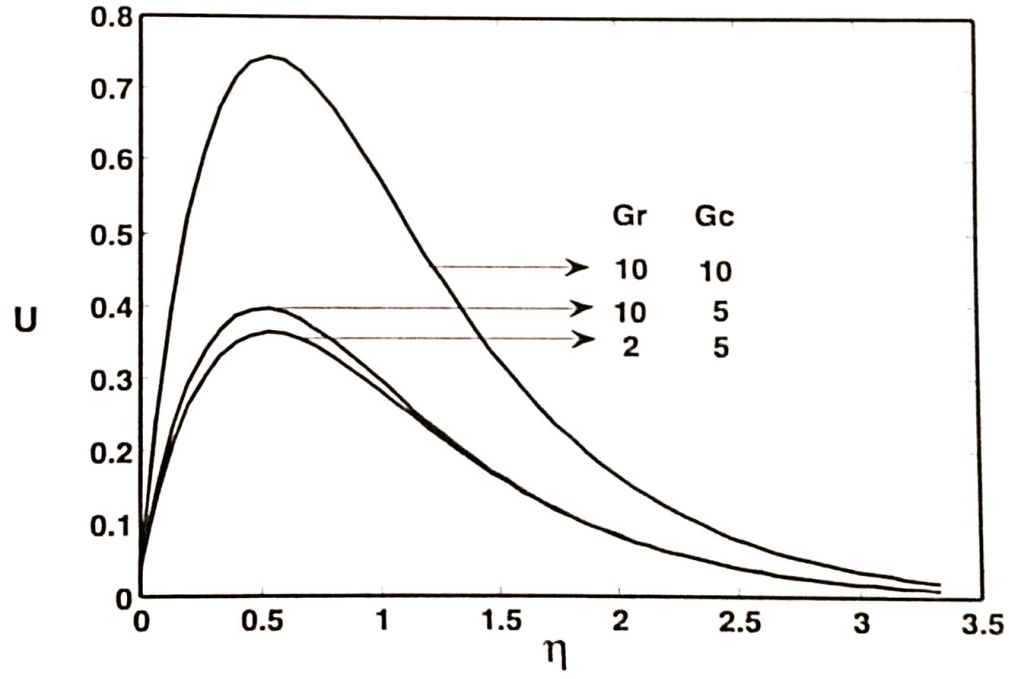

Figure.4. Velocity profiles for different values of Gr and Gc

Table 1 Skin friction profiles for air

T	Gr	Gc	Sc	Pr	τ
0.2	2	5	0.6	0.71	-0.665949
0.2	5	5	0.16	0.71	-1.833723
0.2	5	5	0.6	0.71	-0.775495
0.2	5	5	2.01	0.71	-0.339745
0.2	5	10	0.6	0.71	-1.502981
0.4	5	5	0.6	0.71	-1.590762
0.6	5	5	0.6	0.71	-2.431920

Table 2 Skin friction profiles for water

T	Gr	Gc	Sc	Pr	τ
0.2	2	5	0.6	7	-0.629829
0.2	5	5	0.16	7	-1.743424
0.2	5	5	0.6	7	-0.685196
0.2	5	5	2.01	7	-0.249447
0.2	5	10	0.6	7	-1.412682
0.4	5	5	0.6	7	-1.335357
0.6	5	5	0.6	7	-1.962712

FINDING MINIMUM TASK COMPLETION TIME USING FUZZY CONCEPTS

K. Pramila
Sri Chandrasekharendra Saraswathi ViswaMahavidyalaya
kpramila@kanchiuniv.ac.in

Abstract:-The study of scheduling problem has attracted many researchers in various fields. Fuzzy set theory is a tool to handle uncertainty in scheduling problems. Since in real situations information is imprecise or incomplete, many researchers used fuzzy graph to represent the fuzzy relation. Also efficient scheduling has become essential for manufacturing firms to survive in today's intensely competitive business environment. In this work, a scheduling problem is represented as a fuzzy graph in which the vertices are the tasks and the edges shows the conflict between the tasks. Our aim is to find the minimum task completion time of the scheduling problem which is equivalent to fuzzy chromatic sum of the fuzzy graph which can be achieved by fuzzy coloring.

INTRODUCTION

Fuzzy graph theory is a branch of mathematics that extends traditional graph theory by incorporating the concept of fuzziness. While traditional graph theory deals with crisp, binary relationships between nodes, fuzzy graph theory allows for degrees of membership or uncertainty in these relationships. This field is useful when dealing with situations that involve imprecision, ambiguity, or vagueness.

In classical graph theory, a graph is represented as a set of vertices (nodes) connected by edges (links) that can be either present or absent. In contrast, fuzzy graph theory introduces the concept of fuzzy edges, where the presence of a connection between two nodes is represented by a degree of membership ranging between 0 and 1. A value 1 represents a fully connected edge, while 0 indicates a complete absence of the edge. Any value between 0 and 1 signifies a partial or fuzzy connection.

Fuzzy graph theory provides a framework to analyse and model complex systems where relationships between elements are not clearly defined. It finds applications in various domains, including decision-making, pattern recognition, image processing, artificial intelligence and optimization.

By incorporating fuzziness into graph theory, fuzzy graph theory provides a more flexible and realistic representation of real-world problems. It allows for the modelling and analysis of complex systems that involve uncertain or imprecise data, leading to more accurate decision-making and problem- solving in various domains.

LITERATURE REVIEW

In real life situation some statements cannot be true or cannot be false but it lies between true and false. To solve this discourse, the unused concept of fuzzy set and fuzzy relation terms were introduced by Professor Lofti Asker Zadeh in 1965 [1]. These concepts are widely used in various scientific areas. In between 1970 – 80 these concepts are used in decision making problem which created a big revolution on that time. He described the fuzzy set by its membership function which lies between [0,1].

Now days these concepts are not only used in engineering science but also in medical areas. On this extension, the fuzzy graph was defined by Kaufmann in 1973. But later, ProfessorAzriel Rosenfeld developed the fuzzy graph by using the concept of fuzzy relation on fuzzy set in 1975 [2].

C. Eslahchi and B.N. Onagh introduced the fuzzy graph coloring of fuzzy graph [3] in 2006. There are two different ways of coloring a fuzzy graph. The first type of coloring a fuzzy graph with crisp vertex set and fuzzy edge set and the second type is with fuzzy vertex set and fuzzy edge set. They explained the chromatic fuzzy sum of fuzzy graph in detailed manner by considering the job scheduling problem. On coloring the vertices the minimum sum coloring problem (MSC) has a novel application in scheduling theory. They consider scheduling n jobs on a single machine. To allocate the requirements, the constraints are given by a conflict graph G i.e. the vertices are represented as a processors and the edges are represented as competition on resources, if two vertices are adjacent then the corresponding processors cannot process their jobs simultaneously. The concept of chromatic number of fuzzy graph was introduced by Munoz etal [4] in 2004. They explained a way of approach for obtaining the chromatic number of the coloring function

In [5] and [6] T. Pathinathanetal and SenthilrajSwaminathan gave an model problem for the above concept. The minimum number of colors required for vertex coloring of a graph 'G' is called the chromatic number of G and it is denoted as $\chi(G)$. .

In 2009,Lavanyaetal [7] discussed the total coloring of fuzzy graph. They introduced the concept of total coloring of fuzzy graph by considering the fuzzy vertex set and the fuzzy edge set and defines the total coloring. In 2014, Anjalikishore and Sunitha [9] gave an algorithm to find the chromatic number of crisp graph. Later, this algorithm was developed to find a fuzzy chromatic number of fuzzy graph also.

In this work, we applied graph coloring technique to find the minimum job completion time which is equivalent to fuzzy chromatic sum of the fuzzy graph.

BASIC DEFINITIONS

Definition 1.3.1 [10]:

A fuzzy graph G = (V, σ, μ) is an algebraic structure of non empty set V together with a pair of functions $\sigma : V \to [0,1]$ and $\mu : V \times V \to [0,1]$ such that for all u, v $\in V$, $\mu(u, v) \leq \sigma(u) \wedge \sigma(v)$ and μ is a symmetric fuzzy relation on σ. Here σ(u) and μ(u, v) represents the membership values of the vertex u and of the edge (u, v) in G respectively.

Example:
Consider

Consider $G:(\sigma,\mu)$ is a fuzzy graph with the underlying set V={a,b,c,d} where $\sigma : V \to [0,1]$, $\mu : V \times V \to [0,1]$ are defined as $\sigma(a)=0.2$, $\sigma(b)=0.5$, $\sigma(c)=0.7$, $\sigma(d)=1$; $\mu(a,b)=0.1$, $\mu(b,c)=0.6$, $\mu(a,c)=0.5$, $\mu(c,d)=0.9$, $\mu(d,a)=0.4$.

Fig 1.3.1 Fuzzy Graph G

Definition 1.3.2 [10]:
The fuzzy graph G = (V, σ, μ) the elements V and E called vertices and edges of G, respectively, two vertices x and y in G are called adjacentif (1/2) min {σ(x), σ(y)} ≤ μ(xy).

Definition 1.3.3 [10]:
The edge xy of G is called strong edge if x and y are adjacent otherwise it called weak edge.(i.e) Strong if I (1/2) min {σ(x), σ(y)} ≤ μ(xy)., otherwise weak.

Definition 1.3.4 [10]:
The fuzzy graph G = (V, σ, μ) is called a complete fuzzy graph if μ(uv) ≤ σ(u) ∧ σ(v) for all u, v ∈ V and uv∈ E.

Definition 1.3.5:

Let G = (V, E) be a graph. A vertex – coloring of G is an assignment of a color to each of the vertices of G in such a way that adjacent vertices are assigned different colors. If the colors are chosen from a set of k colors, then the vertex – coloring is called a k – vertex – coloring, abbreviated to k – coloring, whether or not all k colors are used.

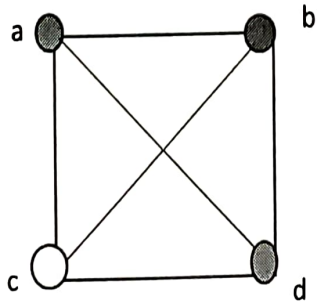

Fig 1.3.2 Fuzzy Graph with 4 coloring

Definition 1.3.6 [3]:

A family $\Gamma = \{\gamma_1, \gamma_2 \ldots \gamma_k\}$ of fuzzy sets on a set V is called a k –fuzzy coloring of $G = (V, \sigma, \mu)$ if

(i) $V\Gamma = \sigma$,
(ii) $\gamma_i \wedge \gamma_j = 0$,
(iii) For every strong edge (x, y) (i.e., $\mu(x, y) > 0$) of G, $\min \{\gamma_i(x), \gamma_j(y)\} = 0$ $(1 \leq i \leq k)$.

Definition1.3.7:
If G has a k – coloring, then G is said to be k – colourable.

Definition 1.3.8:
The smallest k, such that G is k – colourable, is called the chromatic number of G and it is denoted by $\chi(G)$.

Definition 1.3.9:

The minimum number k for which there exist a k – fuzzy coloring is called the fuzzy chromatic number of G, denoted as $\chi^f(G)$.

Definition 1.3.10 [3]:

For a k- fuzzy coloring $\Gamma = \{\gamma_1, \gamma_2, \ldots .., \gamma_k\}$ of a fuzzy graph of G,

- Chromatic fuzzy sum of

G denoted by $\Sigma(G)$ is defined as

$$\Sigma_\Gamma(G) = 1 \sum_{x \in C_1} \theta_1(x) + 2\sum_{x \in C_2} \theta_2(x) + \ldots\ldots\ldots + k \sum_{x \in C_k} \theta_k(x)$$

Where $C_i = \text{supp}\ \gamma_i$ and $\theta_i(x) = \max \{\sigma(x) + \mu(xy)/\ y \in C\}$.

Definition 1.3.11[3]:
The Chromatic fuzzy sum of G denoted by $\Sigma(G)$ is defined as follows

$$\Sigma(G) = \min \{\frac{\Sigma_\Gamma(G)}{\Gamma} \text{ is fuzzy coloring}\}$$

Then, the number of fuzzy coloring of G is finite and so there exists a fuzzy Γ_0 which is called minimum fuzzy coloring of G is such that $\Sigma(G) = \Sigma_{\Gamma_0}(G)$

Algorithm to Find Chromatic Number of a Fuzzy Graph [9]

Step 1: Initialize $k' = 0$.

Step 2: If $|V| = 0$, return $\chi(G) = 0$.

Step 3: Choose a collection of a fuzzy sets $\{\gamma_1, \gamma_2, \ldots\ldots, \gamma_n\}$ where

$\gamma_j(u_i) = \{(u_j, \sigma(u_j))\} \cup \{(u_i, \sigma(u_i)) / \mu(u_i, u_j) = 0, i \neq j\}$

(Where $\cup$ stands for standard fuzzy union), such that

$\mu(u_i, u_m) = 0, u_i, u_m \in \gamma_j^*, i \neq m.$

Step 4: If $\exists$ a subfamily $\Gamma' = \{\gamma_1, \gamma_2, \ldots\ldots, \gamma_k\}$ such that $\gamma_i \wedge \gamma_j = 0$, $i \neq j$, i, j = 1, 2,...., k and $\sum_{j=1}^{k} |\gamma_j^*|$ is maximum , let

$S = V - \cup_{j=1}^{k} \gamma_j^*$.

Step 5: If $|S| \neq 0$,

{

If k = 1, then $\chi(G) = 1$ and Go to step 7

else if $1 < k \leq n$, assign color C_j to γ_j^* and then $\chi(G) = k$ and

Go to step 7.

}

Step 6: While $|S| \neq 0$

Assign color C_j to γ_j^*, j = 1, 2, ...,k and then $\chi(G) = k$.

Let $k' = \chi(G) + k'$.

Put $G = \langle S \rangle$ and Go to step 3.

Step 7: $\chi(G) = k + k'$.

Step 8: End.

Minimum Job Completion Time of a Scheduling Problem

In our daily life, scheduling problems are important. For example, in a manufacturing plant, scheduling jobs to minimize the total time consumption is very much essential for a firm to survive in present competitive business world. The study of scheduling problem has attracted researchers from various fields. Permutation flow shop sequencing problems have long been a topic of interest for the researchers & practitioners in this field. Recently the objective of minimizing total flow time, total completion time if all jobs are available for processing at the beginning, has attracted more attention from researchers.

In scheduling problems, the objective is often to find the minimum job completion time, also known as the make span. The make span refers to the total time required to complete all the jobs in the schedule. The scheduling problem is

typically represented as a set of jobs (j) and a set of machines (M). Each job consists of a sequence of tasks that need to be processed, and each task requires a certain amount of time to be completed on a specific machine. The goal is to find an optimal assignment of tasks to machines such that the make span is minimized.

In real world, everything is uncertain and hence complexity arises in all fields. To overcome this uncertainty, the concept of fuzzy in introduced and many researches are developed for the past decades. Hence in the field of scheduling also fuzzy environment is introduced as the processing times of jobs may be uncertain due to incomplete knowledge or uncertain time.

In this work, minimum job completion of time in a sequencing problem is discussed using fuzzy concepts. Consider scheduling n jobs on a single machine. At any given time, the machine is capable to perform any number of tasks, as long as these tasks are independent or the conflicts between the tasks are less than a number which depends on the choice of the problem. Any of the tasks consume some time of the machine. Let x and y be two tasks with some conflict. Suppose that the machine is capable to perform on x and y simultaneously, in this case, the amount of time that machine spends on x (or y) depends on the individual amount of time which previously was spent on x (or y) together with the measure of the conflict between x and y.

Our goal is to minimize the average response time, or equivalently to minimize the sum of the task completion time. In order to solve this problem a fuzzy graph $\tilde{G} = (X,\sigma,\mu)$, is defined where X is the set of all tasks, $\sigma(x)$ is the amount of the consuming time of the machine for each $x \in X$, and $\mu(xy)$ is the measure of the conflict between the tasks x and y. Finding the minimum value of the job completion time for this pr oblem is equivalent to the chromatic fuzzy sum of $\tilde{G}$.

Finding minimum completion time for scheduling 7 tasks on a single machine

Assumption:

Assume that at any time the machine is capable to perform any number of tasks and these tasks are independent or conflicts between them are less than one.

The time consumption for the tasks is as given below:

For task 1 and 4 is 0.2hrs

For task 3 is 0.5hrs

For task 5 and 7 is 0.4hrs

For task 2 and 6 is 0.7hrs

Also,

Task {(1, 2),(4,5),(5,7)} conflict together with 0.3 hours
Task {(1, 3),(3,4),(5,6)} conflict together with 0.5 hours
Task {(1, 4),(1,5),(2,4),(4,7)} conflict together with 0.8 hours
Task {(6, 7)} is conflict with 0.9 hours

Let $\hat{G}$ = (V, σ, μ) be the fuzzy graph representing the given job scheduling problem where V is the set of all tasks, and σ(x) is the amount of time consumption of machine for each x ϵV and μ(x, y) is the measure of the conflict between the tasks x and y. Then, the job completion time for this problem is equivalent to the chromatic sum of $\hat{G}$.To find the chromatic number, color the fuzzy graph following the colouring technique of fuzzy graph.

The fuzzy graph $\hat{G}$ = (V, σ, μ) is defined as follows:
Let V = {1, 2, 3, 4, 5, 6, 7}

$$\sigma(i) = \begin{cases} 0.2, & for\ i = 1,4 \\ 0.5, & for\ i = 3 \\ 0.4, & for\ i = 5,7 \\ 0.7, & for\ i = 2,6 \end{cases} \quad \mu(i,j) = \begin{cases} 0.3, for\ i,j = \{(1,2),(4,5),(5,7)\} \\ 0.5, for\ i,j = \{(1,3),(3,4),(5,6)\} \\ 0.8, for\ i,j = \{(1,4),(1,5),(2,4),(4,7)\} \\ 0.9, for\ i,j = \{(6,7)\} \end{cases}$$

The conflict graph for the above scheduling problem

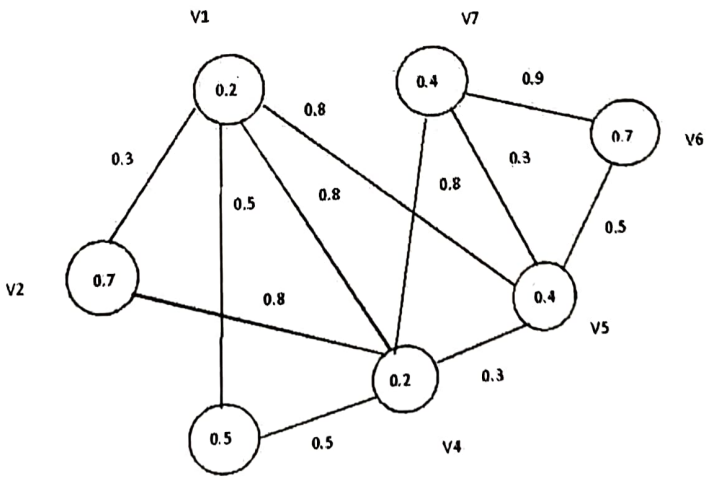

Fuzzy Graph of the Scheduling Problem

Let us find the fuzzy chromatic number of this compatibility graph

Let $_1 = \{\gamma_1, \gamma_2, ..., \gamma_7\}$ be a family of fuzzy set defined on V where,

$$\gamma_1(i) = \begin{cases} 0.5, for\ i = 3 \\ 0, otherwise \end{cases} \quad \gamma_2(i) = \begin{cases} 0.4, for\ i = 5 \\ 0, otherwise \end{cases}$$

$$\gamma_3(i) = \begin{cases} 0.7, for\ i = 6 \\ 0, otherwise \end{cases} \quad \gamma_4(i) = \begin{cases} 0.2, for\ i = 1 \\ 0, otherwise \end{cases}$$

$$\gamma_5(i) = \begin{cases} 0.4, for\ i = 7 \\ 0, otherwise \end{cases} \quad \gamma_6(i) = \begin{cases} 0.2, for\ i = 4 \\ 0, otherwise \end{cases}$$

$$\gamma_7(i) = \begin{cases} 0.7, for\ i = 2 \\ 0, otherwise \end{cases}$$

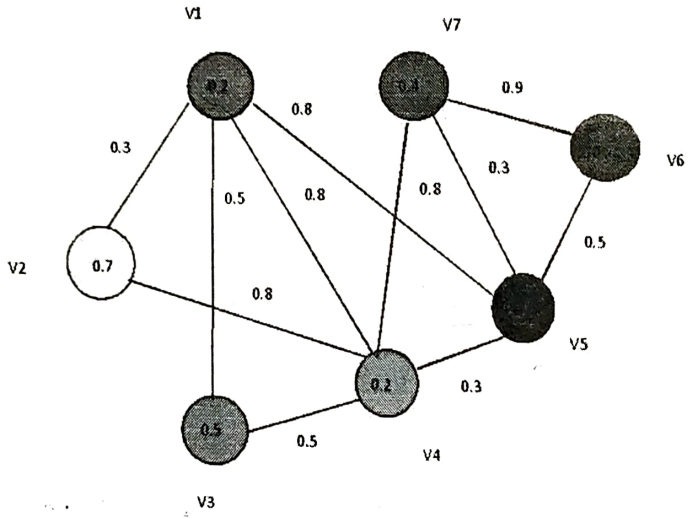

Fig 3.2.4Coloring of the Fuzzy Graph Using $_1$

Vertex	γ_1	γ_2	γ_3	γ_4	γ_5	γ_6	γ_7	Max
1	0	0	0	0.2	0	0	0	0.2
2	0	0	0	0	0	0	0.7	0.7
3	0.5	0	0	0	0	0	0	0.5
4	0	0	0	0	0	0.2	0	0.2
5	0	0.4	0	0	0	0	0	0.4
6	0	0	0.7	0	0	0	0	0.7
7	0	0	0	0	0.4	0	0	0.4

From the above table, we can see that Γ_1 satisfies all the properties of k- fuzzy coloring. Therefore G has 7-coloring and $\chi'(G) = 7$

For this 7- coloring, Γ_1 chromatic number is calculated as follows:

$C_1 = \{1\}, C_2 = \{2\}, C_3 = \{3\}, C_4 = \{4\}, C_5 = \{5\}, C_6 = \{6\}, C_7 = \{7\}$

Then,

$$\theta_1(1) = \max\{0.2+0, 0.2+0\} = 0.2$$
$$\theta_2(2) = \max\{0.7+0, 0.7+0\} = 0.7$$
$$\theta_3(3) = \max\{0.5+0, 0.5+0\} = 0.5$$
$$\theta_4(4) = \max\{0.2+0, 0.2+0\} = 0.2$$
$$\theta_5(5) = \max\{0.4+0, 0.4+0\} = 0.4$$
$$\theta_6(6) = \max\{0.7+0, 0.7+0\} = 0.7$$
$$\theta_7(7) = \max\{0.4+0, 0.4+0\} = 0.4$$

Therefore, the Γ_1 - chromatic sum of G is,

$$\sum_{\Gamma}(G) = 1\sum_{x\epsilon c_1}\theta_1(x) + 2\sum_{x\epsilon c_2}\theta_2(x) + \ldots + k\sum_{x\epsilon c_k}\theta_k(x)$$
$$\sum_{\Gamma_1}(G) = 1(0.2)+2(0.7)+3(0.5)+4(0.2)+5(0.4)+6(0.7)+7(0.4)$$
$$= 12.9$$

We can find another family of fuzzy set defined on V with $\Gamma_2 = \{\gamma_1, \gamma_2, \gamma_3, \gamma_4\}$ where,

$$\begin{cases} 0.2 & \\ 0.7 & \begin{cases} 0.7, for\ i = 2 \\ 0.4, for\ i = 7 \end{cases} \end{cases} \gamma_2$$

$$\gamma_3(i) = \begin{cases} 0.5, for\ i = 3 \\ 0.4, for\ i = 5 \end{cases} \qquad \gamma_4(i) = \begin{cases} 0.2, for\ i = 4 \\ 0, otherwise \end{cases}$$

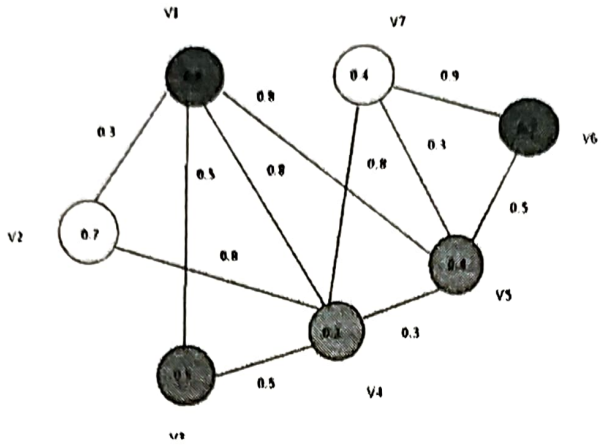

Fig 3.2.5 Coloring of the Fuzzy Graph Using Γ_2

Vertex	γ_1	γ_2	γ_3	γ_4	Max
1	0.2	0	0	0	0.2
2	0	0.7	0	0	0.7
3	0	0	0.5	0	0.5
4	0	0	0	0.2	0.2
5	0	0	0.4	0	0.4
6	0.7	0	0	0	0.7
7	0	0.4	0	0	0.4

Therefore, the Γ_2- chromatic sum of G is,

$\Sigma_{\Gamma_2}(G)$ = 1(0.2+0.7) + 2(0.7+0.4) + 3(0.5+0.4) + 4(0.2)

= 1(0.9)+2(1.1)+3(0.9)+4(0.2) = 6.6

Let $\Gamma_3 = \{\gamma_1, \gamma_2, \gamma_3, \gamma_4\}$ be a family of fuzzy set defined on V where,

$$\gamma_1(i) = \begin{cases} 0.7, for\ i = 2 \\ 0.5, for\ i = 3 \\ 0.7, for\ i = 6 \end{cases} \gamma_2(i) = \begin{cases} 0.4, for\ i = 5 \\ 0, otherwise \end{cases}$$

$$\gamma_3(i) = \begin{cases} 0.2, for\ i = 1 \\ 0.4, for\ i = 7 \end{cases} \gamma_4(i) = \begin{cases} 0.2, for\ i = 4 \\ 0, otherwise \end{cases}$$

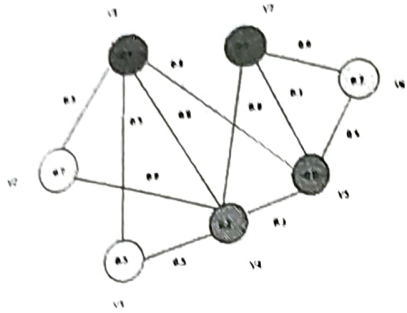

Vertex	γ_1	γ_2	γ_3	γ_4	Max
1	0	0	0.2	0	0.2
2	0.7	0	0	0	0.7
3	0.5	0	0	0	0.5
4	0	0	0	0.2	0.2
5	0	0.4	0	0	0.4
6	0.7	0	0	0	0.7
7	0	0	0.4	0	0.4

Fig 3.2.6 Coloring of the Fuzzy Graph Using Γ_3

From the above table, we can see that $\Gamma_3$statisfied all the properties of k-fuzzy coloring.
Therefore, G has 4 coloring and $\chi(G) = 4$

Therefore, the Γ_3 - chromatic sum of G is,

$$\Sigma_{\Gamma_3}(G) = 1(0.7+0.5+0.7) + 2(0.4) + 3(0.2+0.4) + 4(0.2)$$
$$= 1(1.9) + 2(0.4) + 3(0.6) + 4(0.2)$$
$$= 5.3$$

Let $\Gamma_4 = \{\gamma_1, \gamma_2, \gamma_3\}$ be a family of fuzzy set defined on V where,

$$\gamma_1(i) = \begin{cases} 0.7, for\ i = 2 \\ 0.5, for\ i = 3 \\ 0.4, for\ i = 5 \end{cases} \gamma_2(i) = \begin{cases} 0.2, for\ i = 4 \\ 0.7, for\ i = 6 \end{cases} \gamma_3(i) = \begin{cases} 0.2, for\ i = 1 \\ 0.4, for\ i = 7 \end{cases}$$

Vertex	γ_1	γ_2	γ_3	Max
1	0	0	0.2	0.2
2	0.7	0	0	0.7
3	0.5	0	0	0.5
4	0	0.2	0	0.2
5	0.4	0	0	0.4
6	0	0.7	0	0.7
7	0	0	0.4	0.4

Fig 3.2.7Coloring of the Fuzzy Graph Using Γ_4

From the above table, we can see that $r_4$statisfies all the properties of k-fuzzy coloring.
Therefore, G has 3coloring and $\chi'(G) = 3$
Therefore, the r_4 - chromatic sum of G is,

$$\Sigma_{r_4}(G) = 1(0.7+0.5+0.4) + 2(0.2+0.7) + 3(0.2+0.4) = 1(1.6) + 2(0.9) + 3(0.6) = 5.2$$

RESULT

Therefore, the fuzzy chromatic sum of G is

$$\Sigma(G) = \min\{r_1, r_2, r_3, r_4\} = \min\{12.9, 6.6, 5.3, 5.2\} = 5.2$$

The fuzzy chromatic sum of $\widehat{G}$ is 5.2
Therefore, the minimum time of task completion time of the problem is 5.2hrs.

CONCLUSION

Fuzzy set theory has many applications in all fields including management, medical field, industry, etc., especially in industrial world, its role is very much important. In the competitive business world, processing jobs in optimised time is essential. In this wok, a scheduling problem with seven tasks along with their time consumption is considered. The tasks are independent or conflicts between them are less than one. The aim of the work is to find minimum task completion time, for which the conflict graph of the problem is modelled as a fuzzy graph. The minimum time taken is equivalent to fuzzy chromatic sum of the fuzzy graph. Hence to find the chromatic sum, chromatic number of the graph is found, which is found as three. The fuzzy chromatic sum is 5.2.Hence the minimum task completion time of all tasks is found to be 5.2 hours.

REFERENCES

[1]. L.A. Zadeh, Fuzzy set, Information and Control, Vol 8, 1965, Pg.338 - 335

[2]. A. Rosenfeld, Fuzzy graphs, In: L.A. Zadeh, K.S. Fu and M. Shimura, "Fuzzy Sets and their Application", Academic press, NewYork, 1975.

[3]. Changoz Eslachi and B.N. Onagh, "Vertex Strength of Fuzzy Graph", International Journal of Mathematics and Mathematical Sciences, Pg.1-9 (2006).

[4] Susana Munoz, M. Teresa Ortuno, Javier Yanez, "Coloring Fuzzy Graphs", ELSEVIER, Pg.211-221 (2004)

[5] T. Pathinathan, J. JesinthaRosline, "Application of Fuzzy Graphs in Scheduling Jobs", International Journal of Computing Algorithm, Volume 03, Pg: 34-36, 2014.

[6] Dr.SenthilrajSwaminathan, "Fuzzy Graph Applications of Job Allocation", International Journal of Engineering and Innovative Technology (IJEIT), Volume 01,2012.

[7]. S. Lavanya, R. Sattanathan, "Fuzzy Total Coloring of Fuzzy Graphs", International Journal of Information Technology and Knowledge Management, Volume 02, Pg: 37-39, 2009.

[8]. S. Lavanya and M. Anathanaryanan, "Fuzzy Graph Coloring Using Alpha Cuts", International Journal of Engineering and Applied Science, Volume 04, 2014.

[9]. Anjaly Kishore and M.S. Sunitha, "Chromatic Number of Fuzzy Graphs", Annals of Fuzzy Mathematics and Informatics, Volume 07, Pg: 543-551, 2014.

[10].Nivethana, V. Parvathi, "A Fuzzy Total Colorinng and Chromatic Number of a Complete Fuzzy Graph", Int. J. Emerg. Trends Eng. Dev. Pg:377 - 384, 2013.

[11] VivekRaich ,ShwetaRai, Task Scheduling Problem Using Fuzzy Graph, Oriental Journal of Physical Sciences Vol. 1(1 & 2),16-20 (2016)

applied sciences

MDPI

Article

Comparative Evaluation of Viscosity, Density and Ultrasonic Velocity Using Deviation Modelling for Ethyl-Alcohol Based Binary Mixtures

Radhakrishnan Padmanaban [1], Ahobilam Gayathri [1], Aanantha Iyengar Gopalan [2,*], Dong-Eun Lee [2,3] and Kannan Venkatramanan [1,*]

[1] Faculty of Science, Sri Chandrasekharendra Saraswathi Viswa Mahavidyalaya, Enathur, Kanchipuram 631561, India; padhu.mphil@gmail.com (R.P.); ag@kanchiuniv.ac.in (A.G.)
[2] Intelligent Construction Automation Center, Kyungpook National University, Daegu 41566, Republic of Korea; dolee@knu.ac.kr
[3] School of Architecture, Civil, Environment and Energy, Kyungpook National University, 1370, Sangyeok-dong, Buk-gu, Daegu 702701, Republic of Korea
* Correspondence: algopal99@gmail.com (A.I.G.); kv@kanchiuniv.ac.in (K.V.)

Abstract: This study reports the comparative deviations in experimental viscosity, density and ultrasonic velocity of two new ethanol-based binary liquid mixtures (ethanol + 1-hexanol and ethanol + 1-octanol) at 303.15 K by applying various theoretical models (Hind relation (ηH), Kendall and Monroe relation (ηK-M), Bingham relation (ηB), Arrhenius–Eyring relation (ηAE), Croenauer-Rothfus Kermore relation (ηCRK) and Gambrill relation (ηG)). Typically, the experimental densities are compared with theoretical methods like the Mchaweh–Nasrifar–Mashfeghian model (ρMNM), Hankinson and Thomson model (ρHT), Yamada and Gunn model (ρYG) and Reid et al. (ρR) model. Additionally, the experimental ultrasonic velocities are compared with various theoretical models like the Nomoto relation (UN), Van Dael and Vangeel relation (UIMR), Impedance relation (UIR), Rao's specific velocity relation (UR) and Junjie relation (UJ). The average percentage of deviation (APD) is determined to identify the most suited model that can closely agree to the experimental values of the specified property (viscosity, density and ultrasonic velocity). From the APD values, it may be concluded that the ηK-M model is the most suitable theoretical method for estimating the viscosity for the ethanol + 1-hexanol system, and the Gambrill model is the suitable method for estimating viscosity for ethanol + 1-octanol liquid systems. Similarly, the model of Reid et al. and Jungie's relation are the most suited theoretical models to predict the density and ultrasonic velocity of the binary liquid systems, respectively. Form the experimental data, various molecular interaction properties like adiabatic compressibility, intermolecular free length, free volume, internal pressure, and viscous relaxation time are analysed. The results of this study are expected to be useful in predicting the suitable molecular proportions that can be suited for industrial application (flavouring additive, insecticide, in the manufacture of antiseptics, perfumes for 1-hexanol based mixtures and flavouring, and as an antifoaming agent for 1-octanol based liquid mixtures).

Keywords: molecular binary mixtures; liquid; theoretical models; thermophysical properties; deviation

Citation: Padmanaban, R.; Gayathri, A.; Gopalan, A.I.; Lee, D.-E.; Venkatramanan, K. Comparative Evaluation of Viscosity, Density and Ultrasonic Velocity Using Deviation Modelling for Ethyl-Alcohol Based Binary Mixtures. *Appl. Sci.* **2023**, *13*, 7475. https://doi.org/10.3390/app13137475

Academic Editor: Leonid Burakovsky

Received: 5 May 2023
Revised: 17 June 2023
Accepted: 22 June 2023
Published: 25 June 2023

1. Introduction

Over the last three decades, significant progress has been witnessed in the theoretical understanding of liquid–liquid binary mixtures [1,2], keeping in view that the prediction of the few important properties like density, viscosity, and the excess properties, is related to their engineering performance. Studies on the theoretical modelling of thermodynamic and engineering properties have been carried out on alcohol-based binary/ternary mixtures like water and ethanol [3], 1,3,5-trimethyladamantane + 1,2,3,4-tetrahydronaphthalene + n-octanol and corresponding binary systems [4], n-hexane, ethanol, and cyclopentyl methyl ether [5],

pentanol + ethyl cyclohexane + methyl myristate and corresponding binary systems [6] and ethylene glycol-based ternary mixture [7]. The knowledge of the thermodynamic and transport properties of alcohol-based binary mixtures can be used to develop theoretical models and for the design of new technologies. Importantly, information on the dynamic viscosity of liquid mixtures can be used in chemical engineering calculations involving fluid, heat, and mass transfer [8]. The experimental viscosity data of ethanol-based liquid mixtures (ethanol + 1-hexanol and ethanol + 1-heptanol) have been reported [9]. The viscosity for binary mixtures containing n-hexanol and ethyl valerate or hexyl acetate, as well the details on negative viscosity deviations over the entire composition have been presented [10]. The viscosity of binary systems containing n-hexanol and other related details has been reported [11–14]. The deviation in the viscosity data was correlated with its composition using polynomial models, and details on the interpretation of molecular interactions, as well as on the transport and ultrasound properties of binary liquid solutions are presented [15–21]. Studies on viscosity, a transport property, have been used in terms of modelling and simulation, and the activation energy values as determined by Arrhenius plots have been detailed [22,23]. It has been notified that liquid viscosity is highly affected by the heat and decreases with an increase in temperature [22]. Most liquids have an exponential relationship between temperature and viscosity rather than linear dependence.

Ultrasonic properties and their variation within the composition of the binary mixture are useful to design engineering processes and in chemical and biological industries. Ultrasonic velocity is useful to investigate the molecular interactions between the components of the mixture. The measurement of ultrasonic velocity is the only direct method to determine isentropic compressibility, which then provides further access to the related thermodynamic properties of the liquids and liquid mixtures [24–26]. Ultrasound measurements are one of the most widely used techniques in the investigation of liquids and are essential in the construction and validation of fundamental equations of its state.

The present investigation is focused on the first-time theoretical evaluation of the viscosity, density and ultrasonic properties of two binary liquid mixtures: ethanol + 1-hexanol and ethanol + 1-octanol at 303.15 K, to decide on the deviation of the values of the properties as well to know the average percentage of deviation (APD). In this work, the experimental value of the properties was taken as reference from the literature [27]. The experimental viscosities were compared with various theoretical methods like the Hind relation (ηH) [28], Kendall and Monroe relation (ηK-M) [29], Bingham relation (ηB), Arrhenius–Eyring relation (ηAE), Croenauer–Rothfus Kermore relation (ηCRK) and Gambrill relation (ηG) [30]. Turning to the other study in this work, the experimental densities were compared by deriving the values through theoretical methods like the Mchaweh–Nasrifar–Mashfeghian model (ρMNM) [31], Hankinson and Thomson model (ρHT) [32], Yamada and Gunn model (ρYG) [33] and Reid et al. model (ρR) [34]. Also, this work reports on the comparison of experimental ultrasonic velocities using various theoretical methods like the Nomoto relation (UN) [35], Van Dael and Vangeel relation (Uimr) [36], Impedance relation (UIR) [37], Rao's specific velocity relation (UR) [38] and the Junjie relation (UJ) [39]. The APD was determined to identify the most suited method that agrees with the experimental values. From the experimental values of density, viscosity and ultrasonic velocity, various molecular interaction properties like adiabatic compressibility, intermolecular free length, free volume, internal pressure, viscous relaxation time and their excess properties were analysed.

2. Experimental Details

The binary mixtures were prepared from Analar-grade ethanol (E-Merck chemicals, Darmstadt, Germany), 1-hexanol, and 1-octanol (S.D Fine Chemicals Ltd., India) (27). Ethanol, 1-hexanol, and 1-octanol were purified by the methods described in the literature [40,41]. The binary mixtures of ethanol with 1-hexanol and 1-octanol were prepared by weighing an appropriate volume of each liquid component and were kept in special airtight bottles. All solutions were prepared in a dry bog. Viscosities were determined using a Cannon–Ubbelhode viscometer [27,42] calibrated with triple-distilled water. The

viscometer containing test liquids was kept for about 20 min in a thermostatic water bath and the temperature fluctuation in the viscometer measurement was minimized. The overall experimental uncertainty was estimated to be $\pm 1.5 \times 10^{-3}$. The densities of pure liquids and binary mixtures were measured using a single-stem pycnometer (made of Pyrex glass) with a bulb capacity of 8×10^{-3} dm^3 and with a graduated stem of 5.0×10^{-7} dm^{-3} divisions. The ultrasonic velocities of pure liquids and their mixtures were measured using a single-frequency ultrasonic interferometer operating at 3 MHz with an uncertainty of +0.05% and a temperature (±0.02 K) maintained in a thermostatic water bath [27]. The values of densities and viscosities at 303.15 K were determined precisely up to ± 0.01 kgm^{-3} and $\pm 3 \times 10^{-6}$ Nsm^{-2}, respectively. The Cannon–Ubbelhode viscometer is conceptually simple: the time it takes a volume of solute to flow through a thin capillary is compared to the time for a solvent flow. It turns out that the flow time for either is proportional to the viscosity, and inversely to the density.

The relative viscosity is determined using the ratio $\eta_{rel} = \eta_{soln}/\eta_{solvent}$ (1)

3. Results and Discussions

3.1. Viscosity Studies

The viscosity of a liquid is affected by many factors such as temperature, size, molecular weight, inter-molecular forces and the presence of impurities. Viscosity determination helps in understanding the molecular interactions and properties of binary and ternary liquid systems. It is to be noted that attractive interactions can cause an increase in the viscosity of these systems. Regardless of the fact that viscosities can be used as the base data in a simulation, equipment design, solution theory or molecular dynamics, it is also essential in designing calculations involving heat transfer, mass transfer and fluid flow. The accurate prediction of the viscosities of binary mixtures is considered very important considering the above facts. A large number of viscosity models have been applied, but few reviews have described the application prospects of the models [43,44]. Models that describe the viscosity of liquid mixtures can be classified into two categories: (i) empirical equations using only one adjusting parameter and simple algebraic formulations [28], and (ii) semi-empirical models which are deduced based on different theories, like Eyring's absolute reaction-rate theory, the theory of corresponding states, and molecular dynamic models [45].

Table 1 infers the deviation between the experimental and the literature values for pure components.

Table 1. Experimental values of the viscosity, density and ultrasonic velocity of pure liquids.

Liquid	Density (kg/m^3)		Viscosity ($\times 10^{-3}$ Nsm^{-2})		Ultrasonic Velocity (m/s)	
	Expt [27]	Literature	Expt [27]	Literature	Expt [27]	Literature
Ethanol	783.9	780.5 [46]	1.0090	0.983 [46]	1133.3	1130 [46]
1-Hexanol	807.6	810.0 [47]	3.8951	3.513 [47]	1281.7	1289 [47]
1-Octanol	817.2	803.03 [48]	6.4931	5.9424 [48]	1327.5	1329 [48]
APD of experimental and literature value		0.80%		7.5%		0.3%

The viscosity of the binary liquid mixtures was calculated using the Hind relation, Kendall and Monroe relation, Bingham relation, Arrhenius–Eyring relation, Croenauer–Rothfus Kermore relation and Gambrill relation as detailed below:

Hind relation (η_H)

The following relations were proposed for the evaluation of the viscosity of binary liquid systems by Hind et al. [28]:

$$\eta = x_1^2\eta_1 + x_2^2\eta_2 + 2x_1x_2H_{12} \quad (2)$$

$$H_{12} = \left(\eta - \eta_{calc}^{id}\right)/(2x_1x_2)\eta_{calc}^{id} = x_1^2\eta_1 + x_2^2\eta_2 \quad (3)$$

where x is the mole fraction, η is the viscosity, the subscripts 1 and 2 refer to the components 1 and 2, respectively, and H_{12} refers to cross-pair interactions, which can be obtained from Equation (3).

Kendall and Monroe relation (η_{KM}) [29]

Kendall and Monroe derived an equation for the analysis of viscosity of binary liquid systems based on a zero-adjustable parameter:

$$\eta_m = \left(x_1\eta_1^{1/3} + x_2\eta_2^{1/3}\right)^3 \quad (4)$$

where x_1, x_2 and η_1, η_2 are the mole fraction and viscosity of the pure component, respectively.

Bingham relation (η_B) [30]

Bingham derived an equation for the analysis of viscosity of binary liquid systems based on a zero-adjustable parameter:

$$\eta_m = (x_1\eta_1 + x_1\eta_1) \quad (5)$$

Arrhenius–Eyring relation (η_{AE}) [30]

Arrhenius derived an equation for the analysis of viscosity of binary liquid systems based on a zero-adjustable parameter.

$$log\eta_m = x_1log\eta_1 + x_2log\eta_2 \quad (6)$$

Croenauer–Rothfus Kermore relation (η_{CRK}) [30]:

$$logv_m = \Sigma x_i \log(v_i) \quad (7)$$

Gambrill relation (η_G) [30]:

$$v_m^{1/3} = \Sigma x_i v_i^{1/3} \quad (8)$$

where v_m is the kinematic viscosity of mixture, whereas x_i and v_i are the mole fraction and kinematic viscosity of individual pure liquids.

$$\text{Average Percentage of Deviation(APD)} = \frac{1}{n}\Sigma\frac{(\text{Experimental values} - \text{Theoretical Values})}{Experimental\ Values} \times 100 \quad (9)$$

Tables 2 and 3 present the experimental and theoretical viscosities predicted by various models for binary liquid systems ethanol + 1-hexanol and ethanol + 1-octanol at 303.15 K. Irrespective of the theoretical models, the common prediction is that the relative η increases with the increase in the concentration of 1-hexanol/1-octanol. The η is the minimum at the lower 1-hexanol/1-octanol concentration, and with the concentration range (1.00) η becomes maximum. The increasing frictional forces are expected to arise from the presence of more carbon atoms in the linear chain of alcohol and the molecular layers formed between the lower-carbon and higher-carbon containing alcohol and to be the reason for the increase in values with concentration of the higher-carbon number containing alcohol [22]. From Tables 2 and 3, it can be observed that there are differences in the theoretical values of the viscosities of the ethanol + 1-hexanol and ethanol + 1-octanol binary mixtures at 303.15 K compared to the experimental values. The reason for the difference is ascribed to the limitations and approximation incorporated in these theories. In the ethanol + 1-hexanol binary liquid system, it is observed that the APD, as derived from the theoretical values of η calculated by using various theoretical models (Hind relation, Kendall and Monroe relation, Bingham relation, Arrhenius–Eyring relation, Croenauer–Rothfus Kermore relation and Gambrill relation), follow the trend $\Delta\eta_H = \Delta\eta_B$

> $\Delta\eta_{AE}$ >$\Delta\eta_{CRK}$ > $\Delta\eta_G$ > $\Delta\eta_{KM}$. This study infers that the APD of η is more in the Hind model and Bingham model and less in the Kendall and Monroe model. Furthermore, within Table 2, it can be noticed that the Kendall and Monroe model is the most suitable theoretical model for predicting viscosity for ethanol + 1-hexanol binary liquid systems.

Table 2. Experimental and theoretical viscosity of binary liquid system of Ethanol + 1-Hexanol at 303.15 K.

Mole Fraction of Ethanol	Viscosity (Experimental Values) $\times 10^{-3}$ Nsm^{-2}	Theoretical Viscosity ($\times 10^{-3}$ Nsm^{-2})					
		Hind Relation (η_H)	Kendall and Monroe Relation (η_{KM})	Bingham Relation (η_B)	Arrhenius–Eyring Relation (η_{AE})	Croenauer–Rothfus Kermore Relation (η_{CRK})	Gambrill Relation (η_G)
0.00	3.8951	3.8951	3.8424	3.8951	3.8951	3.8950	4.1085
0.14	3.3639	3.4815	3.2784	3.4815	3.2096	3.2152	3.5068
0.28	2.8872	3.0829	2.7899	3.0829	2.6634	2.6701	2.9834
0.49	2.2414	2.4895	2.1564	2.4895	2.0175	2.0241	2.3057
0.64	1.8073	2.0341	1.7412	2.0341	1.6302	1.6354	1.8616
0.77	1.5088	1.6754	1.4545	1.6754	1.3782	1.3814	1.5546
0.87	1.2795	1.3865	1.2480	1.3865	1.2039	1.2049	1.3330
0.95	1.0933	1.1463	1.0920	1.1463	1.0760	1.0768	1.1675
1.00	1.0090	1.0090	1.0089	1.0090	1.0090	1.0088	1.0784
APD from experimental values		−6.46%	2.32%	−6.46%	5.35%	5.21%	−4.43%

Table 3. Experimental and theoretical viscosity of binary liquid system of Ethanol + 1-Octanol at 303.15 K.

Mole Fraction of Ethanol	Viscosity (Experimental Values) $\times 10^{-3}$ Nsm^{-2}	Theoretical Viscosity ($\times 10^{-3}$ Nsm^{-2})					
		Hind Relation (η_H)	Kendall and Monroe Relation (η_{KM})	Bingham Relation (η_B)	Arrhenius–Eyring Relation (η_{AE})	Croenauer–Rothfus Kermore Relation (η_{CRK})	Gambrill Relation (η_G)
0.00	6.4931	6.4931	6.3727	6.4931	6.4931	6.4930	6.8147
0.13	5.4708	5.7796	5.2978	5.7796	5.0963	5.11579	5.6738
0.24	4.6068	5.1604	4.4692	5.1604	4.1302	4.1588	4.7932
0.33	4.0015	4.6619	3.8686	4.6619	3.4871	3.5194	4.1542
0.55	2.9218	3.4894	2.6733	3.4894	2.3420	2.3707	2.8753
0.70	2.1685	2.6657	2.0006	2.6657	1.7707	1.7871	2.1461
0.81	1.6888	2.0542	1.5818	2.0542	1.4388	1.4459	1.6916
0.89	1.3623	1.5859	1.3039	1.5859	1.2273	1.2295	1.3922
0.96	1.1211	1.2272	1.1146	1.2272	1.0866	1.0871	1.1904
1.00	1.0090	1.0090	1.0089	1.0090	1.0090	1.0089	1.0783
APD from experimental values		−12.41%	3.88%	−12.41%	9.60%	9.19%	−2.93%

Regarding the results derived from the ethanol + 1-octanol binary liquid system, the comparison of the experimental η with the value predicted from various theoretical models is presented in Table 3. Additionally, the details of the APD are given in Table 3 which follows the following trend: $\Delta\eta_H = \Delta\eta_B > \Delta\eta_{AE} > \Delta\eta_{CRK} > \Delta\eta_{KM} > \Delta\eta_G$. From the results,

it can be concluded that the Gambrill model is the most suitable theoretical method for estimating the viscosity for the Ethanol + 1-octanol binary liquid system.

3.2. Density Studies

Density is an important concept because it allows one to determine whether a substance with a specified density will float/sink in a liquid. Specifically, substances with a lesser density than the density of the liquid will float in that liquid. Also, it is an important physical property used in calculating the acoustic and physical properties of a substance such as the molar refraction, dipole moment, boiling temperature and superficial tension.

The density of the binary liquid mixtures, taken for the present study, was calculated using the Mchaweh–Nasrifar–Mashfeghian model (ρ_{MNM}) [31], Hankinson and Thomson model (ρ_{HT}) [32], Yamada and Gunn model (ρ_{YG}) [33] and Reid et al. model (ρ_R) [34] as given by the following details:

Mchaweh–Nasrifar–Mashfeghian model (ρ_{MNM}) [31]

Mchaweh, Nasrifar and Mashfeghian reported the following correlation:

$$\rho_{mix} = \rho_{cmix}\rho_{0mix} \tag{10}$$

where ρ_{mix} is the density of the mixed solution, and ρ_{cmix} is the critical density of the mixture. The critical density of the mixture is calculated with the following equation:

$$\rho_{cmix} = [\sum_{i=1}^{N} x_i \rho_{ci}^{-3/4}]^{-4/3} \tag{11}$$

where x_i is the mole fraction, and ρ_{ci} is the critical density of the ith component.

$$\rho_{0mix} = 1 + 1.169\tau_{mix}^{1/3} + 1.818\tau_{mix}^{2/3} - 2.658\tau_{mix}^{3/3} + 2.161\tau_{mix}^{4/3} \tag{12}$$

where the temperature-dependent variable τ_{mix} is calculated by the following expression:

$$\tau_{mix} = 1 - T_{rmix}/\alpha_{SRK} \tag{13}$$

In the above equation, T_{rmix} is the reduced temperature of the mixed solution and α_{SRK} is the term from the original Soave Redlich–Kwong equation of the state. The reduced temperature of the mixture is defined as

$$T_{rmix} = T/\sum_{i=1}^{N} x_i T_{ci} \tag{14}$$

where T_{ci} is the critical temperature of the ith component. The parameter α_{SRK} is defined in terms of the reduced temperature (T_r):

$$\alpha_{SRK} = \left[1 + m\left(1 - \sqrt{T_{rmix}}\right)\right]^2 \tag{15}$$

$$m = 0.480 + 1.574\omega_{mix} - 0.176\omega_{mix}^2 \tag{16}$$

The acentric factor of the solution ω_{mix} is calculated with the following expression:

$$\omega_{mix} = \sum_{i=1}^{N} x_i \omega_i \tag{17}$$

where ω_i is the acentric factor of the ith component. The acentric factor is a measure of the complexity of the molecule as formed in relation to a molecule with spherical symmetry of a simple fluid for which $\omega = 0$.

Hankinson and Thomson model (ρ_{HT}) [32]

The Hankinson–Thomson model (H-T) [21] is based on the corresponding state principle and is valid for $0.25 < T_r < 0.95$. The density of the pure compound is defined by

$$\rho = \rho_c / \left[V^{(0)}\left(1 - \omega V^{(1)}\right)\right] \tag{18}$$

$$V^{(0)} = 1 - 1.5281\left(1 - T_r\right)^{1/3} + 1.4390\left(1 - T_r\right)^{2/3} - 0.8144(1 - T_r) + 0.19045\left(1 - T_r\right)^{4/3} \tag{19}$$

$$V^{(1)} = \left(-0.296123 + 0.386914T_r - 0.0427258T_r^2 - 0.0480645T_r^3\right)/(T_r - 1.00001) \tag{20}$$

The reduced temperature of the component is defined as

$$T_r = T/T_c$$

Yamada and Gunn model (ρ_{YG}) [33]

The Yamada–Gunn model extended the Racket equation and requires the molecular weight M, the critical density ρ_c, the reduced temperature T_r and the acentric factor ω:

$$\rho = \rho_c \left(0.29056 - 0.08775\omega\right)^{-(1-T_r)^{2/7}} \quad (21)$$

Reid et al. model (ρ_R) [34]

The Reid et al. model proposed an equation also based on the molecular weight, critical density, reduced temperature and acentric factor:

$$\rho = \rho_c \left[1 + 0.85(1 - T_r) + (1.6916 + 0.984\omega)\left(1 - T_r\right)^{1/3}\right] \quad (22)$$

The density values calculated using the Mchaweh–Nasrifar–Mashfeghian model, Hankinson and Thomson model, Yamada and Gunn model and Reid et al. model and their deviations are presented in Tables 4 and 5. In both (ethanol + 1-hexanol and ethanol + 1-octanol) binary liquid systems, it was observed that the deviation of density takes the following order: $\Delta\rho_{MNM} > \Delta\rho_{HT} > \Delta\rho_{YG} > \Delta\rho_R$. This study demonstrated that the APD of the density is more in the Mchaweh–Nasrifar–Mashfeghian model and least in the Reid et al. model, amongst the models used in this work. Also, the theoretical calculations made on the density of binary mixtures using various models gave the conclusion that the density values estimated from Reid et al. [34] are the most suitable ones for predicting the density of both binary mixtures, Ethanol + h-Hexanol and Ethanol + 1-octanol. Thus, it is worth mentioning that the basic assumptions used in the model of Reid et al. [34] and the assumptions applied in that model are well-suited for estimating the closer value of the density for the studied binary mixtures.

Table 4. Experimental and theoretical density of binary liquid system of Ethanol + 1-Hexanol at 303.15 K.

Mole Fraction of Ethanol	Density (Experimental Values) kg/m^3	Theoretical Density (kg/m^3)			
		Mchaweh–Nasrifar–Mashfeghian Model (ρ_{MNM})	Hankinson and Thomson Model (ρ_{HT})	Yamada and Gunn Model (ρ_{YG})	Reid et al. Model (ρ_R)
0.00	807.6	654.2	844.9	839.7	839.2
0.14	805.6	656.6	847.9	842.9	842.2
0.28	802.9	658.8	850.5	845.6	844.7
0.49	798.6	661.5	853.6	848.9	847.8
0.64	794.8	663.3	855.2	850.6	849.5
0.77	791.2	664.4	855.9	851.5	850.4
0.87	787.7	665.1	856.1	851.8	850.7
0.95	785.7	665.5	856.0	851.8	850.7
1.00	783.9	665.6	855.9	851.6	850.7
APD from experimental values		**16.79%**	**−7.25%**	**−6.67%**	**−6.55%**

Table 5. Experimental and theoretical density of binary liquid system of Ethanol + 1-Octanol at 303.15 K.

Mole Fraction of Ethanol	Density (Experimental Values) kg/m^3	Theoretical Density (kg/m^3)			
		Mchaweh–Nasrifar–Mashfeghian Model (ρ_{MNM})	Hankinson and Thomson Model (ρ_{HT})	Yamada and Gunn Model (ρ_{YG})	Reid et al. Model (ρ_R)
0.00	817.2	659.5	862.7	858.1	855.2
0.13	815.9	661.6	864.3	859.7	856.9
0.24	814.6	663.3	865.2	860.7	857.9
0.33	813.4	664.4	865.6	861.2	858.5
0.55	808.6	666.3	865.2	860.9	858.5
0.70	801.2	666.9	863.5	859.3	857.2
0.81	794.1	666.9	861.4	857.2	855.5
0.89	788.8	666.5	859.3	855.1	853.7
0.96	785.6	666.0	857.3	853.0	851.9
1.00	783.9	665.6	855.9	851.6	850.7
APD from experimental values		**17.13**	**−7.46**	**−6.92**	**−6.66**

3.3. Ultrasonic Velocity Studies

Studies on ultrasonic velocity are useful for extensive applications towards the evaluation of the thermodynamic and physicochemical properties of simple, binary and ternary mixtures [49,50]. Considering the extensive reports in the literature on binary mixtures, it is understood that relatively less attention has been focused on the mixtures based on ethanol [51–53]. In the present work, the experimental ultrasonic velocities are compared with values derived through various theoretical methods: the Nomoto relation (U_N) [35], Van Dael and Vangeel relation (U_{IMR}) [36], Impedance relation (U_{IR}) [37], Rao's specific velocity relation (U_R) [38] and the Junjie relation (U_J) [39]. The experimental values, along with the theoretical values calculated using various models, are presented in Tables 6 and 7 along with standard relations [35–39].

Table 6. Experimental and theoretical ultrasonic velocity of binary liquid system of Ethanol + 1-Hexanol at 303.15 K.

Mole Fraction of Ethanol	Ultrasonic Velocity (Experimental Values) m/s	Theoretical Ultrasonic Velocity (m/s)				
		Nomoto Relation (U_N)	Van Dael and Vangeel Relation (U_{IMR})	Impedance Relation (U_{IR})	Rao's Specific Velocity Relation (U_R)	Junjie Relation (U_J)
0.00	1281.7	1193.9	1281.7	1281.7	1192.3	1281.1
0.14	1270.6	1183.6	1188.1	1261.0	1172.1	1268.1
0.28	1257.9	1172.0	1131.8	1240.8	1152.8	1253.8
0.49	1245.9	1150.6	1088.0	1210.5	1124.5	1228.7
0.64	1217.3	1129.5	1079.0	1187.0	1103.1	1205.4
0.77	1194.0	1108.9	1085.7	1168.4	1086.4	1183.9
0.87	1177.3	1088.8	1100.2	1153.2	1073.1	1163.9
0.95	1145.3	1069.0	1119.2	1140.6	1062.1	1145.1
1.00	1133.3	1056.1	1133.3	1133.3	1055.9	1133.3
APD from experimental values		7.06%	6.49%	1.34%	8.24%	0.55%

Table 7. Experimental and Theoretical Ultrasonic velocity of Binary liquid system of Ethanol + 1-Octanol at 303.15 K.

Mole Fraction of Ethanol	Ultrasonic Velocity (Experimental Values) m/s	Theoretical Ultrasonic Velocity (m/s)				
		Nomoto Relation (U_N)	Van Dael and Vangeel Relation (U_{imr})	Impedance Relation (U_{IR})	Rao's Specific Velocity Relation (U_R)	Junjie Relation (U_J)
0.00	1327.5	1234.6	1327.5	1327.5	1235.3	1327.3
0.13	1316.6	1224.8	1183.1	1303.1	1210.9	1314.1
0.24	1307.6	1214.8	1109.1	1281.8	1190.0	1300.9
0.33	1298.6	1205.5	1070.4	1264.4	1173.3	1289.0
0.55	1264.0	1177.5	1028.9	1223.1	1134.7	1255.1
0.70	1239.7	1150.2	1032.9	1193.7	1108.1	1224.3
0.81	1200.4	1123.5	1053.4	1171.6	1088.6	1196.3
0.89	1167.8	1097.6	1081.0	1154.5	1073.9	1170.9
0.96	1146.8	1073.3	1110.7	1141.3	1062.7	1148.5
1.00	1133.3	1056.1	1133.3	1133.3	1055.9	1133.3
APD from experimental values		6.79%	10.10%	1.66%	8.60%	0.33%

For the Ethanol + 1-hexanol binary liquid system, the following trend was noticed: $\Delta U_R > \Delta U_N > \Delta U_{IMR} > \Delta U_{IR} > \Delta U_J$. The calculations reveal that the APD of ultrasonic velocity is the most when using Rao's specific velocity relation [38] and is the least in Jungie's relation [39]. This leads to the conclusion that Jungie's relation is the most suitable theoretical method for estimating the ultrasonic velocity for the Ethanol + 1-hexanol binary liquid system. In the case of the Ethanol + 1-octanol binary liquid system, it was observed that deviation takes the order $\Delta U_{IMR} > \Delta U_R > \Delta U_N > \Delta U_{IR} > \Delta U_J$. The APD of ultrasonic velocity values as calculated from the Van Dael and Vangeel [36] relation were relatively higher than those predicted by Jungie's relation [39]. Thus, it can be concluded that Jungie's relation [39] is the most suitable theoretical method for estimating the ultrasonic velocity for Ethanol + 1-octanol binary liquid system.

3.4. Molecular Interaction Properties

From the experimental values of density, viscosity and ultrasonic velocity [27], various molecular interaction parameters like adiabatic compressibility, intermolecular free length, free volume, internal pressure, and viscous relaxation time were determined and are presented in Table 8.

Normally, a decrease in adiabatic compressibility indicates closed packing and decreased ionic repulsion. In the present study, the adiabatic compressibility for both systems (Ethanol + 1-Hexanol and Ethanol + 1-Octanol) increases with an increase with the concentration of ethanol. This indicates that the molecules are loosely packed in the solution. The adiabatic compressibility shows an inverse behaviour when compared to ultrasonic velocity. This indicates that there is a significant interaction between the binary liquids. This increasing trend suggests a moderate strong electrolytic nature in which the solutes tend to attract the solvent molecules. The intermolecular free length shows a similar behaviour to adiabatic compressibility. From Table 8, the free volume shows an increasing trend with the increase in the concentration of ethanol. This may be compactness due to association at a higher concentration [54]. This increasing trend is due to stronger intramolecular interaction than intermolecular interaction which can be attributed to the loose packing of molecules inside the shield, which suggests a weak molecular interaction in the components of mixtures [55]. The internal pressure is a measure of cohesive forces between the constituent molecules in liquids. It is also defined as the energy required to vaporize a unit volume of a substance. The values of internal pressure increase with an increase in

the mole fractions of ethanol. The value of internal pressure was found to be greater for the Ethanol+1-hexanol than Ethanol+1-octanol liquid system. This suggests that there is a strong interaction between the solute and solvent molecules or that there is an increase in the extent of complexation with the increase in concentration [55]. The internal pressure of a liquid reflects the molecular interaction. The dispersion of the ultrasonic speed of sound in the binary system gives information about the characteristics of relaxation time (τ), which explains the cause of dispersion. The decreasing trend of relaxation time was observed in the present case. It may be due to the structural changes occurring in the mixtures resulting in the weakening of intermolecular forces [56].

Table 8. Molecular interaction properties of binary liquid systems of Ethanol + 1-Hexanol and Ethanol + 1-Octanol at 303.15 K.

Mole Fraction of Ethanol	Adiabatic Compressibility (β) ($\times 10^{-10}$ m^2N^{-1})	Intermolecular Free Length (L_f) ($\times 10^{-11}$ m)	Free Volume (V_f) ($\times 10^{-8}$ m^3mol^{-1})	Internal Pressure (π) ($\times 10^8$ Pa)	Viscous Relaxation Time (τ) ($\times 10^{-12}$ s)
Ethanol + 1-Hexanol					
0.00	7.537	5.696	2.201	6.723	3.914
0.14	7.688	5.753	2.394	6.889	3.448
0.28	7.871	5.821	2.607	7.070	3.030
0.49	8.066	5.893	3.030	7.365	2.410
0.64	8.490	6.046	3.347	7.718	2.046
0.77	8.865	6.178	3.605	8.081	1.783
0.87	9.159	6.279	3.891	8.390	1.562
0.95	9.702	6.463	4.121	8.728	1.414
1.00	9.932	6.539	4.205	8.985	1.336
Ethanol + 1-Octanol					
0.00	6.943	5.467	1.551	6.486	6.011
0.13	7.070	5.517	1.737	6.612	5.157
0.24	7.179	5.559	1.964	6.697	4.410
0.33	7.290	5.602	2.155	6.804	3.889
0.55	7.740	5.773	2.480	7.349	3.015
0.70	8.121	5.913	2.951	7.675	2.348
0.81	8.739	6.134	3.313	8.056	1.967
0.89	9.296	6.326	3.649	8.423	1.688
0.96	9.678	6.455	4.060	8.691	1.446
1.00	9.932	6.539	4.205	8.985	1.336

3.5. Studies on Excess Parameters

In order to elucidate the nature of molecular interactions between the components of the liquid mixtures, it is of considerable interest to study the excess parameters rather than the actual values [57]. Non-ideal liquid mixtures show a significant deviation from linearity in their physical behaviour with respect to the concentration, and temperature interoperates with the presence of strong or weak interactions.

The excess values of β^E, L_f^E, τ^E and π^E are recorded in Table 9. The positive excess values represent the dispersion forces, while the negative values indicate the dipole–dipole interaction, charge transfer interaction and hydrogen bonding between the unlike molecules [58].

Table 9. Excess parameters of binary liquid systems of Ethanol + 1-Hexanol and Ethanol + 1-Octanol at 303.15K [27].

Mole Fraction of Ethanol	β^E ($\times 10^{-10}$ m^2N^{-1})	L_f^E ($\times 10^{-11}$ m)	$\pi^E \times 10^8$ Pa	$\tau^E \times 10^{-12}$ s
Ethanol + 1-Hexanol				
0.00	0.000	0.000	0.000	0.000
0.14	−0.191	−0.063	−0.157	−0.096
0.28	−0.340	−0.112	−0.288	−0.158
0.49	−0.636	−0.213	−0.458	−0.248
0.64	−0.590	−0.193	−0.463	−0.205
0.77	−0.513	−0.166	−0.381	−0.148
0.87	−0.459	−0.149	−0.298	−0.110
0.95	−0.115	−0.036	−0.148	−0.044
1.00	0.000	0.000	0.000	0.000
Ethanol + 1-Octanol				
0.00	0.000	0.000	0.000	0.000
0.13	−0.262	−0.090	−0.198	−0.245
0.24	−0.490	−0.168	−0.396	−0.465
0.33	−0.651	−0.223	−0.516	−0.561
0.55	−0.840	−0.282	−0.505	−0.435
0.70	−0.908	−0.302	−0.555	−0.400
0.81	−0.623	−0.201	−0.452	−0.259
0.89	−0.322	−0.100	−0.299	−0.139
0.96	−0.135	−0.041	−0.193	−0.076
1.00	0.000	0.000	0.000	0.000

Excess parameters have been calculated using the following relation:

$$A^E = A_{exp} - A_{id}$$

$$A_{id} = \Sigma\, A_i\, X_i$$

where A_i represents any acoustical parameter and xi is the corresponding mole fraction.

The excess values of adiabatic compressibility, free length, internal pressure and relaxation time were found to be negative in both systems (Ethanol + 1-Hexanol and Ethanol + 1-Octanol). This indicates the presence of a strong interaction between the components of the mixtures [59].

4. Conclusions

In this work, the experimental viscosity of ethanol-based binary liquid mixtures (Ethanol + 1-hexanol and Ethanol + 1-octanol at 303.15 K) was compared with a value predicted using various theoretical models. With regard to Ethanol + 1-hexanol binary liquid system, it was found that the average percentage of deviation (APD) of viscosity is more in the Hind and Bingham model and less in the Kendall and Monroe model. It was therefore concluded that the Kendall and Monroe model is the most suitable theoretical method for estimating viscosity for the Ethanol + 1-hexanol binary liquid system. Regarding the results derived for the Ethanol + 1-octanol binary liquid system, it was observed that the APD of η is more in the Hind model and Bingham model and less in the Gambrill model. From the results, it was concluded that the Gambrill model is the most suitable theoretical method for estimating the viscosity of the Ethanol + 1-octanol binary liquid system. Upon

comparing the experimental density of the binary liquid mixtures (Ethanol + 1-hexanol and Ethanol + 1-octanol at 303.15 K) by applying various theoretical models, it was inferred that the APD of the density predicted by the Mchaweh–Nasrifar–Mashfeghian model is larger and is the least in the Reid model. It was concluded that the Reid et al. model is the most suited to predict the density closest to the experimental results for both the binary liquid systems. On comparing the experimental ultrasonic velocity through values derived through various theoretical models of binary liquid mixtures (Ethanol + 1-hexanol and Ethanol + 1-octanol) at 303.15 K, it was concluded that the APD of the ultrasonic velocity for the Ethanol + 1-hexanol binary liquid system is the most in Rao's specific velocity relation and the least in Jungie's relation, indicating the best suitability of Jungie's relation for estimating the ultrasonic velocity. On applying various theoretical models for the Ethanol + 1-octanol binary liquid system, it was observed that the average percentage of deviation of the ultrasonic velocity is the most in the Van Dael and Vangeel relation and the least in Jungie's relation. Hence, Jungie's relation is the most suitable theoretical method for estimating the ultrasonic velocity for the Ethanol + 1-octanol binary liquid system.

Variation in molecular interaction parameters with the molar concentration of ethanol suggested the presence of specific solute–solvent interactions at a higher concentration, and the effect of concentration was analysed. The calculated excess values and their signs indicate the possible involvement of specific hydrogen-bonding interactions in the binary mixture components. The results of the present study provide insights and inference on knowing the best or most suited theoretical model that could predict the closest values of thermo-acoustic parameters for ethanol-based binary liquid mixtures. Importantly, the study informs the specific choice of theoretical model that could give the closest thermo-acoustic property values for ethanol-based binary mixtures, having aliphatic linear chain alcohols with varying numbers of carbons. The results achieved in this study into the ultrasonic velocity, density and viscosity of ethanol-based binary liquid mixtures are expected to justify the practical application of simple models to estimate the few important properties involved in industrial applications.

Author Contributions: R.P.: conceptualization, software; investigation and writing—original draft; A.G.: methodology; formal analysis; data curation and visualization; A.I.G.: conceptualization; validation; investigation; writing—original draft and funding acquisition; D.-E.L.: methodology, formal analysis; data curation and visualization; K.V.: methodology; validation; investigation; writing—original draft and supervision. All authors have read and agreed to the published version of the manuscript.

Funding: This work was supported by the National Research Foundation of Korea (NRF) grant funded by the Korean government (MSIT) (Nos. NRF-2018R1A5A1025137 and NRF-2022R1A2C1092289).

Institutional Review Board Statement: Not applicable.

Informed Consent Statement: Not applicable.

Data Availability Statement: Not applicable.

Acknowledgments: The authors thank Sri Chandrasekharendra Saraswathi Viswa Mahavidyalaya (SCSVMV Deemed University), Enathur, Kanchipuram, for providing facilities to carry out this research work. This work was supported by the National Research Foundation of Korea (NRF) grant funded by the Korean government (MSIT) (Nos. NRF-2018R1A5A1025137 and NRF-2022R1A2C1092289).

Conflicts of Interest: The authors declare no conflict of interest.

References

1. Parashar, R.; Azhar Ali, M.; Mehta, S.K. Excess molar volumes of some partially miscible liquid mixtures. *J. Chem. Thermodyn.* **2000**, *32*, 711–716. [CrossRef]
2. Pretorius, F.; Focke, W.W.; Androsch, R.; Toit, E.D. Estimating binary liquid composition from density and refractive index measurements: A comprehensive review of mixing rules. *J. Mol. Liq.* **2021**, *332*, 115893. [CrossRef]
3. Boli, E.; Katsavrias, T.; Voutsas, E. Viscosities of pure protic ionic liquids and their binary and ternary mixtures with water and ethanol. *Fluid Phase Equilib.* **2020**, *520*, 112663. [CrossRef]

4. Qin, X.; Yang, S.; Zhao, J.; Wang, L.; Zhang, Y.; Luo, D. Density and viscosity for the ternary mixture of 1,3,5-trimethyladamantane + 1,2,3,4-tetrahydronaphthalene + n-octanol and corresponding binary systems at T = (293.15 to 343.15) K. *J. Chem. Thermodyn.* **2022**, *168*, 106726. [CrossRef]
5. Cartes, M.; Chaparro, G.; Alonso, G.; Mejía, A. Density and viscosity of liquid mixtures formed by n-hexane, ethanol, and cyclopentyl methyl ether. *J. Mol. Liq.* **2022**, *359*, 119353. [CrossRef]
6. Li, D.; Zheng, Y.; Wang, J.; Pang, Y.; Liu, M. Volumetric properties and viscosity for the ternary system of (1-pentanol + ethylcyclohexane + methyl myristate) and corresponding binary systems at T = 293.15–323.15 K. *J. Chem. Thermodyn.* **2022**, *165*, 106660. [CrossRef]
7. Said, Z.; Cakmak, N.K.; Sharma, P.; Syam Sundar, L.; Inayat, A.; Keklikcioglu, O.; Li, C. Synthesis, stability, density, viscosity of ethylene glycol-based ternary hybrid nanofluids: Experimental investigations and model -prediction using modern machine learning techniques. *Powder Technol.* **2022**, *400*, 117190. [CrossRef]
8. Pang, F.M.; Seng, C.E.; Teng, T.T.; Ibrahim, M.H. Densities and viscosities of aqueous solutions of 1-propanol and 2-propanol at temperatures from 293.15 K to 333.15 K. *J. Mol. Liq.* **2007**, *136*, 71–78. [CrossRef]
9. Cano-Gómez, J.J.; Iglesias-Silva, G.A.; Castrejón-González, E.O.; Ramos-Estrada, M.; Hall, K.R. Density and Viscosity of Binary Liquid Mixtures of Ethanol + 1-Hexanol and Ethanol + 1-Heptanol from (293.15 to 328.15) K at 0.1 MPa. *J. Chem. Eng. Data* **2015**, *60*, 1945–1955. [CrossRef]
10. Indraswati, N.; Mudjijati; Wicaksana, F.; Hindarso, H.; Ismadji, S. Density and Viscosity for a Binary Mixture of Ethyl Valerate and Hexyl Acetate with 1-Pentanol and 1-Hexanol at 293.15 K, 303.15 K, and 313.15 K. *J. Chem. Eng. Data* **2001**, *46*, 134–137. [CrossRef]
11. Audonnet, F.; Pádua, A.A.H. Density and Viscosity of Mixtures of n-Hexane and 1-Hexanol from 303 to 423 K up to 50 MPa. *Int. J. Thermophys.* **2002**, *23*, 1537–1550. [CrossRef]
12. Domańska, U.; Żołek-Tryznowska, Z. Measurements of the density and viscosity of binary mixtures of (hyper-branched polymer, B-H2004+1-butanol, or 1-hexanol, or 1-octanol, or methyl tert-butyl ether). *J. Chem. Thermodyn.* **2010**, *42*, 651–658. [CrossRef]
13. Estrada-Baltazar, A.; Bravo-Sanchez, M.G.; Iglesias-Silva, G.A.; Alvarado, J.A.J.; Castrejon-Gonzalez, E.O.; Ramos-Estrada, M. Densities and viscosities of binary mixtures of n-decane + 1-pentanol, +1-hexanol, +1-heptanol at temperatures from 293.15 to 363.15K and atmospheric pressure. *Chin. J. Chem. Eng.* **2015**, *23*, 559–571. [CrossRef]
14. Das, K.N.; Habibullah, M.; Rahman, I.M.M.; Hasegawa, H.; Ashraf Uddin, M.; Saifuddin, K. Thermodynamic Properties of the Binary Mixture of Hexan-1-ol with m-Xylene at T = (303.15, 313.15, and 323.15) K. *J. Chem. Eng. Data* **2009**, *54*, 3300–3302. [CrossRef]
15. Saini, A.; Prabhune, A.; Mishra, A.P.; Dey, R. Density, ultrasonic velocity, viscosity, refractive index and surface tension of aqueous choline chloride with electrolyte solutions. *J. Mol. Liq.* **2021**, *323*, 114593. [CrossRef]
16. Rana, V.A.; Chaube, H.A. Relative permittivity, density, viscosity, refractive index and ultrasonic velocity of binary mixture of ethylene glycol monophenyl ether and 1-hexanol at different temperatures. *J. Mol. Liq.* **2013**, *187*, 66–73. [CrossRef]
17. Hasan, M.; Shirude, D.F.; Hiray, A.P.; Kadam, U.P.; Sawant, A.B. Densities, viscosities and ultrasonic velocity studies of binary mixtures of toluene with heptan-1-ol, octan-1-ol and decan-1-ol at 298.15 and 308.15 K. *J. Mol. Liq.* **2007**, *135*, 32–37. [CrossRef]
18. Parveen, S.; Shukla, D.; Singh, S.; Singh, K.P.; Gupta, M.; Shukla, J.P. Ultrasonic velocity, density, viscosity and their excess parameters of the binary mixtures of tetrahydrofuran with methanol and o-cresol at varying temperatures. *Appl. Acoust.* **2009**, *70*, 507–513. [CrossRef]
19. Thanuja, B.; Kanagam, C.; Sreedevi, S. Studies on intermolecular interaction on binary mixtures of methyl orange–water system: Excess molar functions of ultrasonic parameters at different concentrations and at different temperatures. *Ultrason. Sonochem.* **2011**, *18*, 1274–1278. [CrossRef]
20. Thiyagarajan, R.; Palaniappan, L. Ultrasonic investigation of molecular association in binary mixtures of aniline with aliphatic alcohols. *C. R. Chim.* **2007**, *10*, 1157–1161. [CrossRef]
21. Satheesh, B.; Sreenu, D.; Savitha Jyostna, T. Thermodynamic and spectroscopic studies of intermolecular interactions between isoamyl alcohol and monocyclic aromatic non-ideal binary liquid mixtures. *Chem. Data Collect.* **2020**, *28*, 100448. [CrossRef]
22. Venkatramanana, K.; Padmanaban, R.; Arumugam, V. Acoustic, Thermal and molecular interactions of Polyethylene Glycol (**2000**, *3000*, 6000). *Phys. Procedia* **2015**, *70*, 1052–1056. [CrossRef]
23. Mathur, V.; Arya, P.K.; Sharma, K. Estimation of activation energy of phase transition of PVC through thermal conductivity and viscosity analysis. *Mater. Today Proc.* **2021**, *38*, 1237–1240. [CrossRef]
24. Babu, P.; Prabhakara Rao, N.; Chandra Sekhar, G.; Bhanu Prakash, P. Ultrasonic studies in the ternary mixtures: Water + Iso-propanol +Pyridine at 303.15 K. *Chem. Thermodyn. Therm. Anal.* **2022**, *5*, 100032. [CrossRef]
25. Syed Ibrahim, P.S.; Chidambara vinayagam, S.; Senthil Murugan, J.; Edward Jeyakumar, J. Ultrasonic studies on ternary liquid mixtures of some 1-alkanols with meta methoxy phenol and n hexane at 313 K. *J. Mol. Liq.* **2020**, *304*, 112752. [CrossRef]
26. Srivastava, N.; Rathour, B.K.; Singh, S.; Singh, S. Thermoacoustical study of intermolecular interactions in binary liquid mixtures of benzaldehyde with methanol and ethanol. *Chem. Phys. Impact* **2023**, *6*, 100144. [CrossRef]
27. Ali, A.; Hyder, S.; Nain, A.K. Studies on molecular interactions in binary liquid mixtures by viscosity and ultrasonic velocity measurements at 303.15 K. *J. Mol. Liq.* **1999**, *79*, 89–99. [CrossRef]
28. Hind, R.K.; McLaughlin, E.; Ubbelohde, A.R. Structure and viscosity of liquids. Viscosity-temperature relationships of pyrrole and pyrrolidone. *Trans. Faraday Soc.* **1960**, *56*, 331–334. [CrossRef]

29. Kendall, J.; Monroe, K.P. The Viscosity of Liquids. II. The Viscosity-Composition Curve for ideal liquid mixtures. *J. Am. Chem. Soc.* **1917**, *39*, 1787–1802. [CrossRef]
30. Fakruddin Babavali, S.K.; Srinivasu, C.H.; Narendra, K.; Sridhar Yesaswi, C.H. Experimental and theoretical predictions of viscosity in binary liquid mixtures containing Quinoline with Arenes (Benzene, Toluene and Mesitylene) at temperature t = 303.15 K: A comparative study. *RASAYAN J. Chem.* **2016**, *9*, 544–549.
31. Nasrifar, K.; Moshfeghian, M. A saturated liquid density equation in conjunction with the Predictive-Soave–Redlich–Kwong equation of state for pure refrigerants and LNG multicomponent systems. *Fluid Phase Equilib.* **1998**, *153*, 231–242. [CrossRef]
32. Hankinson, R.W.; Thomson, G.H. A new correlation for saturated densities of liquids and their mixtures. *AIChE J.* **1979**, *25*, 653–663. [CrossRef]
33. Yamada, T.; Gunn, R.D. Saturated liquid molar volumes Rackett equation. *J. Chem. Eng. Data* **1973**, *18*, 234–236. [CrossRef]
34. Reid, R.C.; Prausnitz, J.M.; Sherwood, T.K. *The Properties of Gases and Liquids*; McGraw Hill: New York, NY, USA, 1977.
35. Nomoto, O. Empirical Formula for Sound Velocity in Liquid Mixtures. *J. Phys. Soc. Jpn.* **1958**, *13*, 1528–1532. [CrossRef]
36. Fakruddin Babavali, S.K.; Shakira, P.; Srinivasu, C.H.; Narendra, K. Comparative study of theoretical ultrasonic velocities of binary liquid mixtures containing quinoline and mesitylene at temperatures T = (303.15, 308.15, 313.15 and 318.15) K. *Karbala Int. J. Mod. Sci.* **2015**, *1*, 172–177. [CrossRef]
37. Santhi, N.; Sabarathinam, P.L.; Madhumitha, J.; Alamelumangai, G.; Emayavaramban, M. Theoretical evaluation of ultrasonic velocity in binary liquid mixtures of Alcohols + Benzene. *Int. Lett. Chem. Phys. Astron.* **2013**, *2*, 18–35. [CrossRef]
38. Rama Rao, M. Velocity of Sound in Liquids and Chemical Constitution. *J. Chem. Phys.* **1941**, *9*, 682–685. [CrossRef]
39. Junjie, Z. Calculation of Ultrasonic Velocity in Binary Liquid Mixtures of Benzene. *J. China. Univ. Sci. Technol.* **1984**, *14*, 298–299.
40. Reddick, J.A.; Bringer, W.S. *Techniques of Chemistry*, 3rd ed.; W'dey Interscience: New York, NY, USA, 1970; Volume 2.
41. Weissberger, A. *Techniques of Organic Chemistry*; Interscience Publishers, Inc.: New York, NY, USA, 1959; Volume 7.
42. Tanford, C. *Physical Chemistry of Macromolecules*; John Wiley and Sons Inc.: New York, NY, USA, 1961.
43. Monnery, W.D.; Svrcek, W.Y.; Mehrotra, A.K. Viscosity: A critical review of practical predictive and correlative methods. *Can. J. Chem. Eng.* **1995**, *73*, 3–40. [CrossRef]
44. Poling, B.E.; Prausnitz, J.M.; O'connell, J.P. *Properties of Gases and Liquids*, 5th ed.; McGraw-Hill Education: New York, NY, USA, 2001.
45. Cao, W.; Fredenslund, A.; Rasmussen, P. Statistical thermodynamic model for viscosity of pure liquids and liquid mixtures. *Ind. Eng. Chem. Res.* **1992**, *31*, 2603–2619. [CrossRef]
46. Thiyagarajan, R.; Palaniappan, L. Molecular interaction study of two aliphatic alcohols with cyclohexane. *Indian J. Pure Appl. Phy.* **2008**, *46*, 852–856.
47. Elangovan, S.; Kebede, L.; Senbeto, E.K. Intermolecular Interactions between Chlorpheniramine with 1-Butanol, 1-Pentanol, and 1-Hexanol. *Russ. J. Phys. Chem.* **2022**, *96*, S1–S7. [CrossRef]
48. Glory, J.; Naidu, P.S.; Jayamadhuri, N.; Ravindra Prasad, K. Study of Ultrasonic Velocity, Density and Viscosity in the Binary Mixtures of Benzyl Benzoate with 1-Octanol and Isophorone. *Res. Rev. J. Pure Appl. Phy.* **2013**, *1*, 5–18.
49. Wankhede, D.S.; Lande, M.K.; Arbad, B.R. Densities and Viscosities of Binary Mixtures of Paraldehyde + Propylene Carbonate at (288.15, 293.15, 298.15, 303.15, and 308.15) K. *J. Chem. Eng. Data* **2005**, *50*, 261–263. [CrossRef]
50. Challis, R.E.; Povey, M.J.W.; Mather, M.L.; Holmes, A.K. Ultrasound techniques for characterizing colloidal dispersions. *Rep. Prog. Phys.* **2005**, *68*, 1541–1637. [CrossRef]
51. Bhardwaj, C.K.; Prakash, S.; Bhardwaj, A.K. Study of nitrazepam interaction with alcohol: An ultrasonic and physiochemical investigation. *Can. J. Chem.* **2021**, *99*, 942–949. [CrossRef]
52. Srivastava, N.; Rathour, B.K.; Singh, S. Ultrasonic and Thermodynamical Study of Molecular Interactions in Binary Liquid Mixtures at Different Temperatures. *Russ. J. Phys. Chem.* **2022**, *96*, 15–26. [CrossRef]
53. Bindhani, S.K.; Roy, G.K.; Mohanty, Y.K.; Kubendran, T.R. Effect of temperature and concentration on density, viscosity and ultrasonic velocity of the pentan-1-ol + nitrobenzene mixtures. *Russ. J. Phys. Chem.* **2014**, *88*, 1255–1264. [CrossRef]
54. Naik, A.B. Densities, viscosities, speed of sound and some acoustical parameter studies of substituted pyrazoline compounds at different temperatures. *Ind. J. Pure Appl. Phys.* **2015**, *53*, 27–34.
55. Naik, A.B.; Morey, P.B. Density, viscosity, and ultrasonic measurements on liquid–liquid interactions of some binary mixtures. *Russ. J. Phys. Chem.* **2022**, *96*, 2417–2424. [CrossRef]
56. Elangovan, S.; Mullainathan, S. Intermolecular Interaction Studies in Binary Mixture of Methyl formate with Methanol at Various Temperatures. *Asian J. Chem.* **2014**, *26*, 137–141. [CrossRef]
57. Rezaei-Sameti, M.; Iloukhani, H.; Rakhshi, M. Excess thermodynamic parameters of binary mixtures of methanol, ethanol, 1-propanol, and 2-butanol + chloroform at (288.15–323.15 K) and comparison with the Flory theory. *Russ. J. Phys. Chem.* **2010**, *84*, 2023–2032. [CrossRef]
58. Fort, R.J.; Moore, W.R. Viscosities of binary liquid mixtures. *Trans. Faraday Soc.* **1966**, *62*, 1112–1119. [CrossRef]
59. Fort, R.J.; Moore, W.R. Adiabatic compressibilities of binary liquid mixtures. *Trans. Faraday Soc.* **1965**, *61*, 2102–2111. [CrossRef]

Linear Programming Model of Maximum Network Flow and Its Solution

K. Bharathi [1], T. Sundar[2],
[1]Department of Mathematics
[2]Department of Electronics and Instrumentation Engineering
[1,2]Sri Chandrasekharendra Saraswathi Viswa Mahavidyalaya,
Kanchipuram – 631561.
Tamil Nadu, India
[1]kbharathi@kanchiuniv.ac.in
[2]sundart@kanchiuniv.ac.in

ABSTRACT:

The flow network design is one of the applications with the complex network to be solved in many real-life applications. Generally, the network flow is modeled as a graph with the capacity of the edge and workplace as nodes. The objective of flow network design is to find the maximum flow value. This type of problem can be designed as a graph and many novel models are applied to solve this type of flow problem. In this, a novel method is applied to model the flow network as a linear programming design. The designed linear programming of the flow network is solved using open software and the solution was checked with the existing models of the flow network.

Keywords: Flow Network, Linear Programming, Start node, End node, Maximum flow, and Objective.

I. INTRODUCTION

Networking deals with a great section of operation research. Many problems of our daily life can be represented by the network model. There are four types of network model shortest path model, minimum spanning tree model, maximal flow model, and minimum cost capacity network model. The linear programming model is used in many varieties of complex situations in a real-world application. The application of the linear programming model is wide processed such as in business or economic situations where the existing resources are limited. The problem there will be to make use of the available resources in such a way that to maximize production or minimize the expenditure. These data can be formulated as linear programming

models. The objective of the linear programming problem is to maximize the profit and minimize the total cost. The LPP is to determine the values of the decision variables such that all the constraints are satisfied and gives the maximum or minimum value for the objective function. The maximum or minimum value of the objective function is called an Optimum value. In this paper, we have worked on maximal flow. The objective of the maximal flow problem is to find the maximum flow that can be sent from specified node source(s) to specified node sink(t) through the edges of the network. The maximum flow asks for the largest amount of flow that can be transported from one vertex (source) to another (sink). Originally the maximal flow was invented by Fulkerson and Dantzig and solved by specializing in the simplex method for the liner programming, and Ford and Fulkerson solved it by augmenting the path algorithm.

The literature on network flow problems is extensive. In the mid of 1950, Air force researchers T.E.Harris and F.S. Ross published a report studying the rail network that linked the Soviet Union to its satellite countries in eastern Europe. In 1955, Lester R.Ford and Delbert R.Fulkerson created the first known algorithm. Over the past fifty years, researchers have improved several algorithms for solving maximal-flow problems. In this paper, we have introduced to find the maximum network flow and formulated as a linear programming problem (LPP), and then solved it using open-source software.

The augmenting path method is to gradually increase the flow until the flow gets its maximum value. The increase in flow is done by increasing f: s to v of an out edge from (s, v) or decreasing f: v to s of an in the edge from v to s, till the valid edges are used. This method develops the feasibility approach to the terminating point t. With this, a way path through the edges from the start point s to the terminal point t is generally known as augmenting path. The graph N = (V, E) represents a network with a feasible path f: u to v, and c (f: u to v) is the capacity of residual. The capacity of residual is generally given as c (f: u to v) = c: u to v - f: u to v + f: v to u. The capacity of residual is an additional path of the network that travels from u to v internodes.

The network flow model is a directed type graph structure G, with the edges representing flow value through the path. The maximum capacity c: u to v exists for all edges u to v. The initial node without any input capacity is known as the source node and it's represented by s. The terminal node without any output capacity is known as the sink node and

it's represented by t. Evaluating the maximum flow capacity using feasible flow through network flow is generally known as a maximum flow problem.

II. GENERAL NETWORK FLOW MODEL APPLICATION

The network flow models are generally applied in real-world applications such as road laying networks, railway networks, commodity transport networks, and many more fields. Let us now see some of it

A. Project Selection

Considering the project of installing of fiber network to overcome the need of the companies of telecom to supply the high-speed network service in the accent of incoming revenue. This type of project is designed as a network flow model and there are many methods to solve this type of model but with many complications and complicity.

B. Transportation problem

The model of transportation of products and all verity of commodities from one or many points to other places play an important place in real-world commitments. Generally, this type of design is down as an optimization model, there exist many algorithms to solve the complicity in this application model. The model of a flow network can be formulated and feasibility can be got using many methods.

C. Assignment problem

A design of assigning the work is mostly stated as an assignment problem, which is applied in many productions filed. This assignment model is designed as a network flow with corresponding work units and the feasible path is obtained by this application of the flow network model. The vital role of the assignment model is the traveling salesman problem in the complicity to find a feasible route in the design content.

D. Maximum value flow

The model of a network with its direction represents the routes and the flow through it is specified and detrainment of the maximum flow is the needed application in the real-world situation.

The model of network flow is also applied in many fields such as shortest path problem, minimum cost flow problem, multi-commodity flows, extraction of web communities, image segmentation, telecommunication wireless, and so on.

III. DESIGN METHODOLOGY TO FIND MAXIMUM FLOW IN NETWORK MODEL

To find a feasible flow network with an optimal solution, many algorithms are stated and applied to solve the maximum flow problem. In this work, the basic concepts of the maximum flow problem and its design is discussed and the solution for it was made using open-source software and compared with the existing algorithms.

Step 1: The graphical design of the maximum flow problem is considered.

Step 2: The problem is designed as a linear programming model of the flow network.

Step 3: By giving the input as linear programming in the software the program is run.

Step 4: The output of the flow network is displayed in the description box of the software.

IV. DESIGN OF MAXIMUM FLOW NETWORK MODEL AS LINEAR PROGRAMMING MODEL

Let us consider a project which contains 6 nodes connected with 10 edges with the flow capacity of the network given as the table value

A. Table Flow Table

TABLE I. FLOW TABLE

Begin node	Terminating node	Flow Capacity
0	1	16
0	2	13
1	2	10
1	3	13
2	1	4
2	4	14
3	2	8
3	5	20
4	3	7
4	5	4

B. Network representation of the flow network is as follows

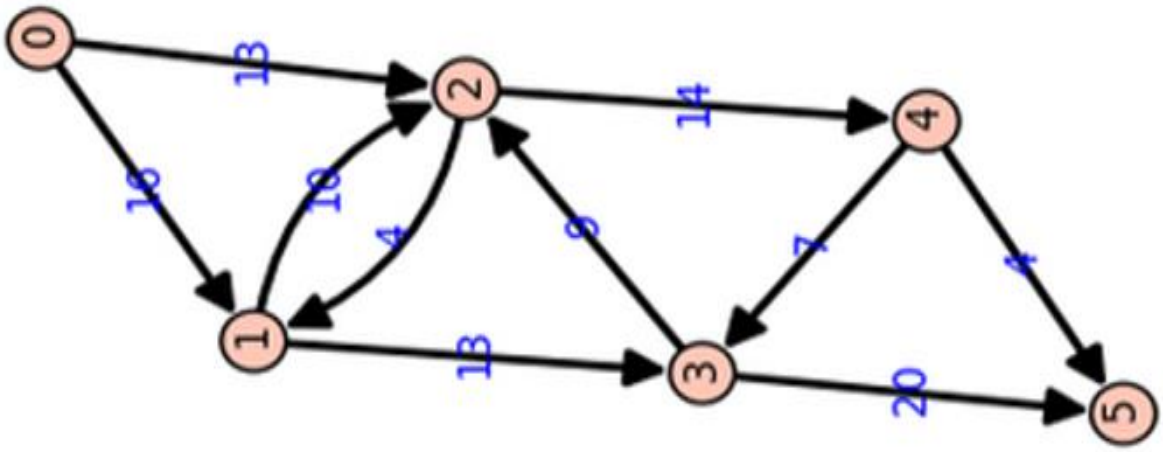

Fig. 1. Network flow

C. The design of the linear programming model of the flow network is as

The objective function is to find the maximum flow of the network the objective is to maximize, that is as follows:

$$\text{Maximize } Z = x_1 + x_2$$

The first set of constraints is derived from the flow value of the network as follows:

$$x_1 \leq 16\,, x_2 \leq 13\,, x_3 \leq 10\,,$$
$$x_4 \leq 12\,, x_5 \leq 4\,, x_6 \leq 14\,,$$
$$x_7 \leq 9\,, x_8 \leq 20\,, x_9 \leq 7, x_{10} \leq 4\,.$$

The second set of constraint is derived from the incoming and outgoing flow value of each node, the start node and the terminal node are made idle the constraints are as follows:

$$x_1 + x_5 = x_3 + x_4$$
$$x_2 + x_3 + x_7 = x_5 + x_6$$
$$x_4 + x_9 = x_7 + x_8$$
$$x_6 = x_9 + x_{10}$$

The network flow is now designed as a linear programming model, which is as follows:

Maximize $Z = x_1 + x_2$

Subject to

$x_1 \leq 16\,, x_2 \leq 13\,, x_3 \leq 10\,,$

$x_4 \leq 12\,, x_5 \leq 4\,, x_6 \leq 14\,,$

$x_7 \leq 9\,, x_8 \leq 20\,, x_9 \leq 7, x_{10} \leq 4\,.$

$x_1 + x_5 = x_3 + x_4$

$x_2 + x_3 + x_7 = x_5 + x_6$

$x_4 + x_9 = x_7 + x_8$

$x_6 = x_9 + x_{10}$

D. *The designed model of linear programming is given as input values in open-source software as follows:*

In [2]:
```
# Maximum Flow Problem

p = MixedIntegerLinearProgram(maximization=True,
                              solver = 'GLPK')

x = p.new_variable(nonnegative=True)

p.set_objective(x[1]+x[2])
```

```
p.add_constraint(x[1],max=16)
p.add_constraint(x[2],max=13)
p.add_constraint(x[3],max=10)
p.add_constraint(x[4],max=12)
p.add_constraint(x[5],max=4)
p.add_constraint(x[6],max=14)
p.add_constraint(x[7],max=9)
p.add_constraint(x[8],max=20)
p.add_constraint(x[9],max=7)
p.add_constraint(x[10],max=4)
```

```
p.add_constraint(x[1]+x[5]-x[3]-x[4],max=0)
p.add_constraint(x[2]+x[3]+x[7]-x[5]-x[6],max=0)
p.add_constraint(x[4]+x[9]-x[7]-x[8],max=0)
p.add_constraint(x[6]-x[9]-x[10],max=0)
```

```
show(p)
round(p.solve(),2),round(p.get_values(x[1]),2),
round(p.get_values(x[2]),2),
round(p.get_values(x[3]),2),
round(p.get_values(x[4]),2),
round(p.get_values(x[5]),2),
round(p.get_values(x[6]),2),
round(p.get_values(x[7]),2),
round(p.get_values(x[8]),2),
round(p.get_values(x[9]),2),
round(p.get_values(x[10]),2)
```

E. The solution is represented in the output box as follows

```
Maximization:
  x_0 + x_1
Constraints:
  x_0 <= 16.0
  x_1 <= 13.0
  x_2 <= 10.0
  x_3 <= 12.0
  x_4 <= 4.0
  x_5 <= 14.0
  x_6 <= 9.0
  x_7 <= 20.0
  x_8 <= 7.0
  x_9 <= 4.0
  x_0 - x_2 - x_3 + x_4 <= 0.0
  x_1 + x_2 - x_4 - x_5 + x_6 <= 0.0
  x_3 - x_6 - x_7 + x_8 <= 0.0
  x_5 - x_8 - x_9 <= 0.0
Variables:
  x_0 is a continuous variable (min=0.0, max=+oo)
  x_1 is a continuous variable (min=0.0, max=+oo)
  x_2 is a continuous variable (min=0.0, max=+oo)
  x_3 is a continuous variable (min=0.0, max=+oo)
  x_4 is a continuous variable (min=0.0, max=+oo)
  x_5 is a continuous variable (min=0.0, max=+oo)
  x_6 is a continuous variable (min=0.0, max=+oo)
  x_7 is a continuous variable (min=0.0, max=+oo)
  x_8 is a continuous variable (min=0.0, max=+oo)
  x_9 is a continuous variable (min=0.0, max=+oo)
(23.0, 12.0, 11.0, 0.0, 12.0, 0.0, 11.0, 0.0, 19.0, 7.0, 4.0)
```

The maximum flow value of the given network is as 23 units.

V. CONCLUSION

Solving maximum flow problem plays an important role in many of the application fields. Finding an optical flow was done using many algorithms and the feasibility is reached. Here we have studied the existing algorithms and solved the problem using open-source software. Evaluation of the maximum flow network is done using open-source software and the results are given. By using open-source software, the time conception of evaluation is minimized.

REFERENCES

[1] Iraschko, R.R., Path Restorable Networks, Ph.D. Dissertation, University of Alberta, spring, 1997.

[2] Iraschko, R.R., MacGregor, M. H., Grover, W. D., "Optimal Capacity Placement for Path Restoration in Mesh Survivable Networks", Proc. IEEE ICC '96, June 1996.

[3] A. ´Custi´c, R. Zhang, and A. P. Punnen, "The quadratic minimum spanning tree problem and its variations," *Discrete Optimization*, vol. 27, no. 4, pp. 73–87, 2018.

[4] L. R. Ford, JR. and D.R. Fulkerson, "Maximal Flow Through a Network". Rand Corporation, Santi Monica, California. September 20, 1955.

[5] A. Fischer and F. Fischer, "An extended approach for lifting clique tree inequalities," *Journal of Combinatorial Optimization*, vol. 30, no. 3, pp. 489–519, 2015.

[6] A. Fischer and C. Helmberg, "The symmetric quadratic travelling salesman problem," *Mathematical Programming A*, vol. 142, no. 1-2, pp. 205–254, 2013.

[7] A. Fischer, F. Fischer, G. J¨ager, J. Keilwagen, P. Molitor, and I. Grosse, "Exact algorithms and heuristics for the quadratic travelling salesman problem with an application in bioinformatics," *Discrete Applied Mathematics*, vol. 166, pp. 97–114, 2014.

[8] Anderson, L. B., Atwell, R. J., Barnett, D. S., & Bovey, R. L. "Application of the maximum flow problem to sensor placement on urban road networks for homeland security", Homeland Security Affairs, 3(3), 1-15. Retrieved February 15, 2011.

[9] Ford LR Jr, Fulkerson DR. l957. A simple algorithm for finding maximal network flow and application to the Hitchcock problem. Canadian Journal of Mathematics, 9: 210-218 Zhang WJ. 2012.

[10] U. Pferschy and R. Stanek, "Generating subtour elimination constraints for the TSP from pure integer solutions," *Central European Journal of Operations Research,* vol. 25, no. 1, pp. 231–260, 2017.

[11] B. Rostami and F. Malucelli, "Lower bounds for the quadratic minimum spanning tree problem based on reduced cost computation," *Computers and Operations Research,* vol. 64, pp. 178–188, 2015.

[12] Sherman, Jonah (2013). "Nearly Maximum Flows in Nearly Linear Time". Proceedings of the 54th Annual IEEE Symposium on Foundations of Computer Science. pp. 263–269. arXiv:1304.2077

[13] K.Bharathi, "Optimal Sequence for Travelling Salesman using Graph Structure". *International Journal of Scientific Research in Engineering and Management (IJSREM),* ISSN: 2582-3930, Volume: 04 Issue: 04 ,1-6, April -2020.

[14] Bharathi, K and Vijayalakshmi, C, "A Framework for the Design and Analysis of an Evolutionary Algorithm for Multi Travelling Salesman Problem", *Indian Journal of Science and Technology,* vol. 9(48), pp. 1-4, 2016.

[15] Bharathi, K and Vijayalakshmi, C, "Multi-Objective Transportation Problem Using Add On Algorithm", *International Journal of Pure and Applied Mathematics,* vol. 109(10), pp. 99-107, 2016.

MATHEMATICS 2023. Vol. 33. Issue 1. Pp. 119–129.

MSC2020: 31D05, 60J45

© *V. R. Manivannan, M. Venkataraman*

Δ-FUNCTIONS ON RECURRENT RANDOM WALKS

If a random walk on a countable infinite state space is reversible, there are known necessary and sufficient conditions for the walk to be recurrent. When the condition of reversibility is dropped, by using discrete Dirichlet solutions and balayage (concepts familiar in potential theory) one could partially retrieve some of the above results concerning the recurrence and the transience of the random walk.

Keywords: parabolic networks, Dirichlet solutions, balayage, recurrent random walks.

DOI: 10.35634/vm230108

Introduction

A random walk $\{N, P = [p(a,b)]\}$ where N is a countable infinite state space and $P = [p(a,b)]$ is a matrix of a transition probabilities $\{p(a,b)\}$ is recurrent if the walk starting at a state e returns to e infinitely often. If the random walk is reversible (that is, there exists a function $\phi(x) > 0$ such that $\phi(a)p(a,b) = \phi(b)p(a,b)$ for any pair of states a, b) then there are known necessary and sufficient conditions for the random walk to be recurrent, proved by using methods from normed spaces. But when the random walk is not reversible, these methods are not of use. Many problems in a random walk are solved by considering it as a reversible Markov chain. We show that the reversible condition can be ignored by using potential theoretic techniques for some random walk problems. Many authors have investigated random walks in an infinite network using the Laplace operator, recall S. McGuinness [1], V. Anandam [2, 3], K. Abodayeh, V. Anandam [4, 5], C. St. J. A. Nash–Williams [6], T. Lyons [7], W. Woess [8], J. M. Cohen et al. [9], F. Colonna, M. Tjani [10], J. M. Cohen et al. [11]. In [6], Nash–Williams explained a random walk on an electrical network with the help of probabilistic methods.

Later in [7], T. Lyons studied the Royden criterion in Riemann surfaces, giving a necessary and sufficient condition for a reversible countable state Markov chain to be transient. V. Anandam [2] studied random walks in an infinite network without reversible conditions and proved the Nash–Williams criterion by using potential theoretic methods. In [12], V. Anandam and M. Damlakhi studied these potential theoretic methods in finite networks with the help of perturbed Laplace operators. K. Abodayeh, V. Anandam in [13, 14] investigated Schrödinger networks and their Cartesian product and supersolutions of discrete Schrödinger equations. In [15], N. Nathiya, Ch. Amulya Smyrna studied the developments of infinite Schrödinger networks in the Euclidean spaces. In [16], V. Anandam studied recurrent or transient random walk on an infinite tree with the help of reversibility condition and transition probabilities matrix. Whereas in this article, we have developed the potential theoretic methods without the condition of reversibility. With the help of this condition, we have studied the potential theoretic methods on infinite random walks. For example, among other results, it is shown that the random walk $\{N, P = [p(a,b)]\}$, reversible or not, is recurrent if in the associated infinite network $\{N, p(a,b)\}$ there exists a function $v(a) \geq 0$ outside a finite set such that $(1-p)v(a) \geq 0$ and $\lim\limits_{n\to\infty} v(a) = \infty$, or if every function $s(a) \geq 0$ on N such that $(1-p)s(a) \geq 0$ is constant, by making extensive use of Dirichlet solutions and balayage.

§ 1. Infinite network

In this section, an abridged version of potential theory on infinite graphs, relevant to the study of random walks, is given. It is mainly taken from [3]. Let N be an infinite graph with a countable infinite number of vertices and countable number of edges. If a and b are two vertices joined by an edge, say that a and b are neighbours denoted by $a \sim b$. The graph is connected if for any two vertices a and b, there exists a path $\{a = a_0, a_1, \ldots, a_n = b\}$, $a_i \sim a_{i+1}$ for $0 \leq i \leq n-1$; if $a = b$ and $n \geq 3$ in this path, say that there is a self-loop at the vertex a; say that the graph is locally-finite if every vertex has only a finite number of neighbours. A collection of real numbers $t(a,b) \geq 0$ defines a set of transition indices $\{t(a,b)\}$ on the graph, provide that $t(a,b) > 0$ if and only if $a \sim b$, $t(a,b)$ and $t(b,a)$ need not have the same value. An infinite graph N that is connected, locally finite, without self-loops and provided with a set of transition indices $\{t(a,b)\}$ is here referred to as an infinite network $\{N, t(a,b)\}$.

Let A be a subset of N. A vertex $a \in A$ is an interior vertex of A if all the neighbours $b \sim a$ are also in A. Let $\overset{\circ}{A}$ denote the collection of all the interior vertices of A, the set $\partial A = A \setminus \overset{\circ}{A}$ is referred to as the boundary of A. If $u(a)$ is a real-valued function on A, the Laplacian at a vertex $a \in \overset{\circ}{A}$ is defined as $\Delta u(a) = \sum_{b \sim a} t(a,b)\,[u(b) - u(a)]$. A real-valued function $u(a)$ on A is said to be upper Δ-function on A if $\Delta u(a) \leq 0$ at every vertex $a \in \overset{\circ}{A}$ and lower Δ-function on A if $\Delta u(a) \geq 0$ at every vertex $a \in \overset{\circ}{A}$, and Δ-function on A if it is both upper Δ-function and lower Δ-function on A. A non-negative upper Δ-function $p(a)$ on A is called a basis function if it has the following property: for any lower Δ-function $v(a)$ on A such that $v(a) \leq p(a)$, one should have $v(a) \geq 0$.

§ 2. Some properties of upper Δ-functions

1. If $u_n(a)$ is a sequence of upper Δ-functions on A and if $u(a) = \lim_{n\to\infty} u_n(a)$ exists and is real-valued, then $u(a)$ is upper Δ-function on A, also $\Delta u(a) = \lim_{n\to\infty} \Delta u_n(a)$.

2. If $\{v_i(a)\}$ is the family ψ of all upper Δ-functions on A majorized by on upper Δ-function $u(a)$ on A, then the family ψ is upper-directed and $h(a) = \sup_{\psi} v_i(a)$ is a Δ-function $u(a)$ on A. It is easy to remark that $p(a) = u(a) - h(a)$ is a basis function on A. Consequently, one can assert: if $u(a)$ is an upper Δ-function on A majorizing a lower Δ-function then $u(a)$ is the sum of a basis function $p(a)$ on A and its greatest Δ-function minorant $h(a)$; this decomposition as the sum of a basis function and the greatest Δ-function minorant is also unique. This is usually referred to as the Riesz decomposition.

3. **Dirichlet solution:** Many properties (like condenser principle, balayage, reduced functions etc.) in the study of basis functions on an infinite network appear as solutions to problems which are actually variations of a generalized Dirichlet problem. We shall refer to the following result [3, Theorem 3.1.7] as a

   Generalized Dirichlet solution: Let F be a subset in the network $\{N, t(a,b)\}$ and $A \subset \overset{\circ}{F}$. Suppose $f(a)$ is a real-valued function defined on F/A such that $v \leq f \leq u$ on F/A where u is an upper Δ-function on F and v is a lower Δ-function on F. Then there exists a function $h(a)$ on F such that $v \leq h \leq u$ on F; $h(a) = f(a)$ on F/A; and $\Delta u(a) = 0$ at every vertex in $\overset{\circ}{A}$. Moreover, h can be so chosen that if h_1 is another such function on F having these three properties, then $h_1 \leq h$. However if the set A contains only a finite number of vertices, then the solution $h(a)$ is uniquely determined.

4. **Reduced functions and balayage:** Suppose $s(a) \geq 0$ is an upper Δ-function on a subset A and $E \subset A$. Let ψ be the family of all the non-negative upper Δ-functions $u(a)$ on A which majorize $s(a)$ on E. Then $\left(R_s^E(x)\right)_A = \inf_{u \in \psi} u(a)$ is referred to as (the reduced function in the case of potential theory on topological spaces) the balayage of $s(a)$ on E in the subset A. We leave out A when it is the whole set N.

   Note that $v(a) = \left(R_s^E(a)\right)_A$ is a non-negative upper Δ-function on A such that $v(a) \leq s(a)$ on A; $v(a) = s(a)$ on E; and $\Delta v(a) = 0$ if $a \in A/E$. If there exists a basis function $p(a)$ on A such that $s(a) \leq p(a)$ on A, then $v(a)$ is a basis function on A.

5. **Parabolic and hyperbolic networks:** In the study of lower Δ-functions, upper Δ-functions in the Euclidean case, there is a marked difference between $\mathbb{R}^2$ and $\mathbb{R}^n, n \geq 3$, because of the fact that any non-negative upper Δ-function in $\mathbb{R}^2$ is constant (recall Liouville's Theorem) while non-constant positive upper Δ-functions exist in $\mathbb{R}^n, n \geq 3$ (recall the Newtonian gravitational kernel in $\mathbb{R}^3$). However, there are many similarities also in these two cases since the potential theory is based on the logarithmic kernel $\log \frac{1}{|a-b|}$ in $\mathbb{R}^2$ while in $\mathbb{R}^3$ it is based on the Newtonian Kernel $\frac{1}{|a-b|}$.

To consider these two different cases in the context of an infinite network $\{N, t\}$, let us say that it is a parabolic network if any non-negative upper Δ-function on N is constant and it is a hyperbolic network if there are non-constant positive upper Δ-functions (and hence positive basis functions) on N. There are various distinguishing properties to differentiate between these two types of networks. One such is given now by using the Dirichlet solution.

Let e be a fixed vertex in N. Let $\{A_n\}$ be a sequence of finite sets such that $e \in \overset{\circ}{A}_1$, $A_n \subset \overset{\circ}{A}_{n+1}$ for $n \geq 1$ and $N = \cup_n A_n$. Let $h_n(a)$ be the Dirichlet solution in A_n with boundary values 1 at e and 0 on ∂A_n, then extended by 0 outside A_n. Then $\{h_n\}$ is an increasing sequence of bounded functions on N, $0 \leq h_n(a) \leq 1$. Let $h(a) = \lim_{n \to \infty} h_n(a)$. The function $h \equiv 1$ if and only if N is a parabolic network. Otherwise it is hyperbolic; notice that in this case $h(a) = R_1^e(a)$.

§ 3. Random walks

A random walk $\{N, P = [p(a,b)]\}$ behaves in some case (when the matrix P is irreducible) similar to an infinite network $\{X, p(a,b)\}$ with the restriction $\sum_{b \sim a} p(a,b)u(b)$. A real-valued function $u(a)$ is said to be upper Δ-function if $Pu(a) \leq u(a)$ for all a. If $u(a)$ is a function such that $u(a) > -\infty$ for all $a \in N$, $Pu(a) \leq u(a)$ is finite at one vertex c, then $u(a)$ is real-valued on N and consequently upper Δ-function. For $u(c) \geq Pu(c)$ implies that $u(a)$ is real-valued for all $a \sim c$; this leads to the conclusion that $u(a)$ is real-valued on N since N is connected.

We write $-\Delta = (I - P)$. The infinite network $\{N, p(a,b)\}$ associated with the random walk $\{N, P\}$ is referred to as a parabolic network if every positive upper Δ-function in $\{N, p(a,b)\}$ is constant; if there exists a non-Δ-function positive upper Δ-function on $\{N, p(a,b)\}$, then it is referred to as a hyperbolic network.

Let us start with a time-homogeneous Markov chain that is a discrete-time stochastic process $\{N_n\}$, $n = 0, 1, 2, \ldots$, where N_n takes values in the state space N with a countable infinite states [17]. For any two states a, b the transition probability from a to b is denoted by $p(a,b) = \text{Prob}\{N_1 = b, N_0 = a\}$. Thus, the set N with the transition numbers $p(a,b)$ can be considered as an infinite network in which a and b are neighbours if and only if $p(a,b) > 0$; at this stage N may or may not be a connected graph. Denote by P the infinite matrix of the transition probabilities $\{p(a,b)\}$. In $\{N, p(a,b)\}$, just as $p(a,b)$ represents the probability that the walker starting at the state b reaches the state a, $p^n(a,b)$ represents the probability that the walker

starting at b reaches a in n steps. Actually $p^n(a,b)$ is the entry in the a^{th} column and the b^{th} row of the matrix p^n. Take $p^0 = I$. Let us assume that given any two states a and b, there exist integers m and n such that $p^m(a,b) > 0$ and $p^n(b,a) > 0$; in this case the matrix P is referred to as irreducible. When P is irreducible, the infinite graph $\{N, p(a,b)\}$ is actually connected so that it is an infinite network in the earlier sense. When the matrix P is irreducible, we also refer to $\{N,P\} = \{N, P = [p(a,b)]\}$ as a random walk with the state space N and the transition probability matrix P determined by the process $\{N_n\}$.

Definition 1. *An irreducible Markov chain* $\{N_n\}$ *on* N *is said be recurrent* if for each state a, the chain returns to a infinitely often. That is, $\mathrm{Prob}\{N_n = a \text{ for infinitely many } n\} = 1$.

Since the transition probabilities matrix is assumed to be irreducible, then starting from a state b the walker can reach any other state a in finite steps. Consequently certain variations in the above definition can be proposed:

(i) suppose e is a fixed state and a is any other state; then $\{N_n\}$ is recurrent if and only if the walker starting from a reaches e infinitely often;

(ii) if the irreducible chain visits a state infinitely often, then it also visits every other state in N infinitely often.

Definition 2. *An irreducible Markov chain* $\{N_n\}$ *on* N *is called transient* if it is not recurrent. Thus, transient means that the chain visits any state only a finite number of times and then wanders off to the state at infinity.

Thus, the division of random walks into two groups, recurrent and transient, depends on the situation whether the Markov chain $\{N_n\}$ returns to any starting state infinitely often or only a finite number of times. This distinction is manifested in different forms in the classification of random walks as shown below and we also interpret these results in the context of infinite networks associated with the respective random walks.

The following passage up to the proof of Proposition 4 is mainly based on Lawler [17, Section 2.2]. Fix a state e and assume that $N_0 = e$. Consider the random variable R which gives the total number of visits to e including the initial visit. Write $R = \sum\limits_{n=0}^{m} \chi\{N_n = e\}$ where χ is the characteristic function. When the chain is recurrent, R is identically ∞. That is, if $R_m = \sum\limits_{n=0}^{m} \chi\{N_n = e\}$, then $R_m \to \infty$ when $m \to \infty$. Now the expectation is $E(R_m) = \sum\limits_{n=0}^{\infty} \mathrm{Prob}\{N_n = e\} = \sum\limits_{n=0}^{m} p^n(e,e)$. Hence in the case of recurrence $\sum\limits_{n=0}^{\infty} p^n(e,e) = \infty$.

Note that $R < \infty$ with probability 1 if the chain is transient. In this case the expectation of R is $E(R) = E\left[\sum\limits_{n=0}^{\infty} \chi\{N_n = e\}\right] = \sum\limits_{n=0}^{\infty} \mathrm{Prob}\{N_n = e\} = \sum\limits_{n=0}^{\infty} p^n(e,e)$.

Proposition 1. *The Markov chain is transient if and only if* $\sum\limits_{n=0}^{\infty} p^n(e,e) < \infty$.

P r o o f. From the above narrative, if $\sum\limits_{n=0}^{\infty} p^n(e,e) < \infty$ then the chain cannot be recurrent. Conversely, assume that the chain is transient. That is, the chain $\{N_n\}$ returns to e only a finite number of times. Let q be the probability of the first return of $\{N_n\}$ to e. Note that $q \neq 1$ since the chain is transient: if $q = 1$ then with probability 1 the chain always returns to e and by continuing we see that the probability is 1 for the chain to returns to e infinitely often; that is the chain is recurrent.

In the case of transience, $R = 1$ if and only if the chain never returns to e, hence the probability is $1 - q$; and $R = m$ if and only if the chain returns $(m-1)$ times and does not return for the m^{th} time, hence the probability is $q^{m-1}(1-q)$. Consequently, $E(R) = \sum\limits_{m=1}^{\infty} m \cdot \text{Prob}\{R = m\} = \sum\limits_{m=1}^{\infty} m\,[q^{m-1}(1-q)] = \frac{1}{1-q} < \infty$. Comparing this with the earlier expression for $E(R)$ in the case of transience, we conclude that the Markov chain is transient if and only if

$$\sum_{n=0}^{\infty} p^n(e,e) < \infty. \qquad \square$$

Remark 1. For any state c, the walker can reach e from c in a finite number of steps. Thus, the nature of transience does not depend on the choice of the initially fixed state e. Consequently, the Markov chain $\{N_n\}$ is transient if and only if $\sum\limits_{n=0}^{\infty} p^n(c,c) < \infty$ for any state c. Instead of the circuit probabilities like $p^n(c,c)$, we shall now take up the consideration of $p^n(a,b)$ which is the probability that the walker starting at the state N reaches the state b in n steps. For this, it is easier to consider $\{N, P = [p(a,b)]\}$ either as a random walk or an infinite network as the occasion demands.

Writing $p^n(a,b)$ as $p_b^n(a)$, remark that

$$P\,[p_b^n(a)] = \sum_c p(a,c)p_b^n(c) = \sum_c p(a,c)p^n(c,b) = p^{n+1}(a,b) = p_b^{n+1}(a),$$

since $p_b^n(a)$ denotes the probability that the walker starting from the state a reaches the state b in n steps, then the expression $G_b(a) = \sum\limits_{n=0}^{\infty} p_b^n(a)$ represents the expected number of visits to the state b starting from the state a.

Proposition 2. *If the random walk $\{N, P = [p(a,b)]\}$ is transient, then the infinite network $\{N, p(a,b)\}$ associated with it is hyperbolic.*

P r o o f. We shall actually show that $G_b(a)$ is the Green basis function on the network $\{N, p(a,b)\}$ with Δ-function support at $\{b\}$.

Choose a vertex b in the network N. If $G_b(a) = \sum\limits_{n=0}^{\infty} p_b^n(a)$, then $P\,[G_b(a)] = \sum\limits_{n=1}^{\infty} p_b^n(a) \leq$ $\leq G_b(a)$ so that $G_b(a)$ is a positive upper Δ-function in the network $\{N, p(a,b)\}$.

The function $G_b(a)$ is actually a basis function. For that note that when $G_b(a)$ is real-valued, we can write $G_b(a) - P\,[G_b(a)] = \delta_b(a)$ which is the column vector with entry 1 when $b = a$ and 0 in other entries. Consequently, $-\Delta\,[G_b(a)] = \delta_b(a)$.

If $h \geq 0$ is a Δ-function such that $h(a) \leq G_b(a)$, then we have $h(a) = P^m h(a) \leq$ $\leq P^m\,[G_b(a)] = \sum\limits_{n=m}^{\infty} p_b^n(a)$ which tends to 0 when $m \to \infty$; this shows that $h \equiv 0$. Hence $G_b(a)$ is a basis function which in this case is the Green basis function having $\{b\}$ as its Δ-function support. $\square$

Remark 2. The above theorem can be reformulated: A random walk $\{N, P = [p(a,b)]\}$ is recurrent if the associated infinite network $\{N, p(a,b)\}$ is parabolic. Conversely, if the Markov chain is reversible, then the parabolicity of the network implies that the random walk is recurrent. ("Reversible" means that there exists a real-valued function $\phi(a) > 0$ such that $\phi(a)p(a,b) = \varphi(b)p(b,a)$ for any two states a, b.) This converse can be deduced [2, Theorem 3.3] from McGuinness [1, p. 90]. See the very important papers of Nash–Williams [6] and Lyons [7] in this context.

§ 4. Infinite trees

A connected graph is called a tree if there is no cycle in it, that is there is no closed path $\{a_1, a_2, \ldots, a_n, a_1\}$ with $n \geq 3$. Thus, in an infinite tree T, if a, b are any two vertices then there exists a unique path connecting a to b. Suppose a random walk $\{T, P = [p(a,b)]\}$ is defined in the infinite tree T.

Fix a vertex e in T. Then for any a in T, if $\{e, a_1, a_2, \ldots, a_n = a\}$ is the unique path connecting e to a, write $\phi(a) = \frac{p(e,a_1)p(a_1,a_2)\ldots p(a_{n-1},a)}{p(a,a_{n-1})p(a_{n-1},a_{n-2})\ldots p(a_1,e)}$. Note that if $b \sim a$, then $\phi(a)p(a,b) = \phi(b)p(b,a)$. Hence $\{T, P\}$ is reversible, which leads to the conclusion: The random walk $\{T, P = [p(a,b)]\}$ on the infinite tree T is recurrent if and only if the associated network $\{T, p(a,b)\}$ is parabolic.

Proposition 3. *Let $\{N, P = [p(a,b)]\}$ be a random walk. Suppose there exists a function v defined outside a finite set A in N such that $(I-P)v(a) \geq 0$ at every $a \in N/A$ and $\lim\limits_{a\to\infty} v(a) = \infty$. Then the random walk is recurrent.*

P r o o f. With the existence of such a function $v(a)$, the network $\{N, p(a,b)\}$ has to be parabolic. Otherwise, for each vertex $b \in N$ there exists the Green basis function $G_b(a)$ which is bounded and $(I-P)G_b(a) = \delta_b(a)$. Choose a large finite set E, $E_0 \supset A$. Let h be the Dirichlet solution on E with boundary values v on ∂E. Let v_1 be the function on N such that $v_1 = h$ on E and $v_1 = v$ on (N/E). Define for $a \in N$, $v_2(a) = v_1(a) + \sum\limits_{b\in\partial E} \Delta V_1(b) G_b(a)$.

Then for $a \in \overset{\circ}{\partial E}$, $(I-P)v_2(a) = 0$; for $a \in (N/E)$, $(I-P)v_1(a) \geq 0$; for $a \in \partial E$, $(I-P)v_2(a) = (I-P)v_1(a) + (-)(I-P)v_1(a) = 0$. Thus, $(I-P)v_2(a) \geq 0$ on N. Now $G_b(a)$ is bounded on N, so that $\lim\limits_{a\to\infty} v_2(a) = \infty$. But this is not possible by the Minimum Principle for v_2. Consequently, the assumption that $\{N, p(a,b)\}$ is not parabolic is invalid. So the random walk $\{N, P\}$ is recurrent.

Let us consider now a random walk $\{T, P = [p(a,b)]\}$ on an infinite tree T. Fixing a vertex $e \in T$, let us measure distance from e. Remark that T is reversible and that for any $a \in T$, $|a| = n$, there is one neighbour $\tilde{a}$, $|\tilde{a}| = n-1$; other neighbours b_i are at a distance $|b_i| = n+1$. □

Proposition 4. *Let $\{T, P = [p(a,b)]\}$ be a random walk on an infinite tree. Measure distances in T from a fixed vertex e. If $p(a,\tilde{a}) \geq \frac{1}{2}$ for all a, then $\{T, P\}$ is recurrent. If $p(a,\tilde{a}) < \frac{1}{2}$, then $\{T, P\}$ is transient.*

P r o o f. Consider the function $f(n) = \left(\frac{\alpha}{1-\alpha}\right)^n$, $0 < \alpha < 1$, at any a, $|a| = n \geq 1$, we have $(I-P)f(n) = -\left[1 - 2p(a,\tilde{a})\right] \frac{2\alpha-1}{1-\alpha} \left[\frac{\alpha}{1-\alpha}\right]^n$.

1. Suppose $p(a,\tilde{a}) > \frac{1}{2}$ for all a. Then take $1 > \alpha > \frac{1}{2}$. In this case $\frac{\alpha}{1-\alpha} > 1$. Hence $(I-P)f(n) > 0$ outside e, and $f(n) \to \infty$ at the point at infinity. Hence by Proposition 3, $\{T, P\}$ is recurrent.

2. Suppose $p(a,\tilde{a}) < \frac{1}{2}$ for all a. Then take $0 < \alpha < \frac{1}{2}$. Hence $(I-P)f(n) > 0$. At e $(I-P)f(e) = -\left[\frac{\alpha}{1-\alpha} - 1\right] > 0$. Hence $f(n)$ is a positive upper Δ-function tending to 0 at infinity, hence a basis function, so that $\{T, P\}$ is transient. (Remark 2 following Proposition 2.)

3. The case $p(a,\tilde{a}) = \frac{1}{2}$: for the function $s(a) = n$ when $|a| = n \geq 1$, $(I-P)s(a) > 0$; moreover, $s(a) \to \infty$. Hence $\{T, P\}$ is recurrent.

Let $\{N, p(a,b)\}$ be the infinite network associated with the random walk $\{N, P = [p(a,b)]\}$. Let us recall the notion of reduced functions in the network [3]. If $s(a)$ is a non-negative upper Δ-function defined on a set E and A is a subset in the interior E^0 of E, then $\left[R_s^A(a)\right]_E = \inf_{u \in \Im} u(a)$ where $\Im$ is the family of non-negative upper Δ-functions $u(a)$ on E such that $u(a) \geq s(a)$ on A. □

Example 1. Let T be a homogeneous tree of degree 2 and the transition probability $p(a, \tilde{a}) = \frac{q+1}{2}$. Consider a function $s(a) = 2^{-1+|a|}$. Note that for any vertex a in T, $|a| = n \geq 1$. Here $|a|$ represents the distance between the root vertex.

P r o o f.

$$\begin{aligned}\Delta s(a) &= \frac{q+1}{2}[2^{-1+(n-1)} - 2^{-1+n}] + \frac{q-1}{2}[2^{-1+(n+1)} - 2^{-1+n}] \\ &= \frac{q+1}{2}[2^{-1+n-1} - 2^{-1+n}] + \frac{q-1}{2}[2^{-1+n+1} - 2^{-1+n}] \\ &= \frac{q+1}{2}[2^{n-2} - 2^{-1+n}] + \frac{q-1}{2}[2^n - 2^{-1+n}] \leq 0.\end{aligned}$$

If $p(a, \tilde{a}) \geq \frac{1}{2}$ for all a, then $\{T, P\}$ is recurrent. If $p(a, \tilde{a}) < \frac{1}{2}$, then $\{T, P\}$ is transient. □

Lemma 1. *Let E be a finite set $e \in \overset{\circ}{E}$. Then $[R_1^e(a)]_E$ is the Dirichlet solution in E with boundary values 1 at e and 0 at each vertex in ∂E.*

P r o o f. Let $\varphi(a)$ be the unique Dirichlet solution on E with boundary values 1 at e and 0 on ∂E. Then $\varphi(a) \geq [R_1^e]_E$ on E. Since $R_1^e(a)$ is a non-negative upper Δ-function on E with values 1 at e and 0 on ∂E, by the construction of the Dirichlet solution we have $\varphi(a) \geq [R_1^e(a)]_E$. This proves $\varphi(a) = [R_1^e(a)]_E$ on E. □

Lemma 2. *Let $e \in \overset{\circ}{E}$ where E is a finite set. Then the probability that the walker starting at a state $a \in \overset{\circ}{E}$ goes outside $\overset{\circ}{E}$ before ever coming back to e is $1 - [R_1^e(a)]_E$.*

P r o o f. Let $\varphi(a)$ be the probability that the walker starting at a reaches e before visiting any state in ∂E. Then $\varphi(e) = 1$, $\varphi(c) = 0$ for $c \in \partial E$; moreover, for any $a \in \overset{\circ}{E}$, we have $\varphi(a) = \sum_{b \sim a} p(a,b)\varphi(b)$. This means $(I - P)\varphi(a) = 0$. That is, $\varphi(a)$ is harmonic on E with boundary values $\varphi(e) = 1$, $\varphi(c) = 0$ on ∂E. Hence by the above lemma 1, $\varphi(a) = [R_1^e(a)]_E$. This shows that the walker starting at $a \in \overset{\circ}{E}$ goes outside $\overset{\circ}{E}$ before ever coming to e with the probability $1 - \varphi(a) = 1 - [R_1^e(a)]_E$. □

Theorem 1. *In the random walk $\{N, P = [p(a,b)]\}$, the probability that the walker starting at the state a goes off to infinity A without visiting e is $1 - \varphi(a) = 1 - [R_1^e(a)]$ which is defined with reference to the associated network $\{N, p(a,b)\}$.*

P r o o f. Let $\{E_n\}$ be an increasing sequence of finite sets such that $N = \cup E_n$. For any a in N, if $a \in E_m$ then $[R_1^e(a)]_n$ (which represents the reduced function with respect to the finite set E_n) is defined for $n \geq m$ and is an increasing sequence of upper Δ-functions. Since $[R_1^e(a)]_n \leq R_1^e(a)$, then $v(a) = \sup_n [R_1^e(a)]_n$ is an upper Δ-function on N and $v(a) \leq R_1^e(a)$. On the other hand, since $v(a)$ is an upper Δ-function on N and $v(e) = 1$, we have $v(a) \geq R_1^e$ also. Thus, $R_1^e(a) = v(a) = \lim_{n \to \infty} [R_1^e(a)]_n$.

Now the probability that the walker starting at the state x and going off to infinity A without visiting e is the limiting value of $1 - [R_1^e(a)]_n$ when $n \to \infty$ which is $1 - R_1^e(a)$. □

Corollary 1. *In the random walk* $\{N, P = [p(a,b)]\}$*, the probability that the walker starting at* e*, after leaving* e *never returns to* e *is* $(I-P)R_1^e$.

P r o o f. The probability (from the above Theorem 1) is

$$\sum_{b\sim e} p(e,b)\,[1-R_1^e(b)] = \sum_{b\sim e} p(e,b)\,[R_1^e(e)-R_1^e(b)] = -\Delta\,[R_1^e(e)] = (I-P)R_1^e(e). \qquad \square$$

Some remarks on the reduced function $R_1^e(a)$ in the infinite network $\{N, p(a,b)\}$.

1. The network N is parabolic if and only if $R_1^e \equiv 1$ on N.

2. The network N is hyperbolic if and only if $R_1^e(a)$ is a basis function on N.

3. As in [3, Section 3.2], for each $e_i \sim e$, denote by $[e, e_i]$ the subset $[e, e_i] = \{a\colon$ there exists a path joining a to e that passes through $e_i\}$; e_i and e are assumed to be in $[e, e_i]$. Note that if e_i, e_j ate two neighbours of e, then either $[e, e_i]$ and $[e, e_j]$ are two subsets having e as the only common vertex or $[e, e_i] = [e, e_j]$. The subset $[e, e_i]$ is called an S-domain if 0 is the only bounded function $h(a)$ on $[e, e_i]$ such that $h(e) = 0$ and $-\Delta h(c) = (I-P)h(c) = 0$ for any $c \neq e$. A subset $[e, e_j]$ is called a P-domain if it is not an S-domain. If a set $[e, e_i]$ contains only a finite number of vertices, then it is necessarily an S-domain. The network $\{N, p(a,b)\}$ is parabolic if and only if all the subsets $[e, e_i]$ are S-domains. It is hyperbolic if and only if at least one $[e, e_i]$ is a P-domain; in this case there may be other subsets that are S-domains.

4. If the random walk $\{N, P = [p(a,b)]\}$ is transient, it has been seen that $G_e(a) = \sum_{n=0}^{\infty} p^n(a,e)$ represents the expected number of visits to the state e starting from the state a. The function $G_e(a)$ can also be interpreted as the Green function in the hyperbolic network $\{N, p(a,b)\}$ with Δ-function support at e. Now (see [3, Corollary 3.3.7]), $G_e(a) \leq G_e(e)$ for all $a \in N$; in fact, $G_e(a) = G_e(e)R_1^e(a)$.

5. It can also be mentioned that in the case of a transient random walk, if A is a finite set in N, then R_1^A denotes the probability that the walker starting at the state a to reaches a state in A before wandering off to infinity.

Funding. We thank the referee for very useful comments. The first author acknowledges the support given by the Vellore Institute of Technology through the Teaching cum Research Associate fellowship (VIT/HR/2019/5944 dated 18th September 2019).

REFERENCES

1. McGuinness S. Recurrent networks and a theorem of Nash–Williams, *Journal of Theoretical Probability*, 1991, vol. 4, issue 1, pp. 87–100. https://doi.org/10.1007/BF01046995
2. Anandam V. Some potential-theoretic techniques in non-reversible Markov chains, *Rendiconti del Circolo Matematico di Palermo*, 2013, vol. 62, issue 2, pp. 273–284. https://doi.org/10.1007/s12215-013-0124-8
3. Anandam V. *Harmonic functions and potentials on finite or infinite networks*, Berlin: Springer, 2011. https://doi.org/10.1007/978-3-642-21399-1
4. Abodayeh K., Anandam V. Potential-theoretic study of functions on an infinite network, *Hokkaido Mathematical Journal*, 2008, vol. 37, issue 1, pp. 59–73. https://doi.org/10.14492/hokmj/1253539587

5. Anandam V., Abodayeh K. Non-locally-finite parahyperbolic networks, *Memoirs of The Graduate School of Science and Engineering, Shimane University. Series B: Mathematics*, 2014, vol. 47, pp. 19–35. https://ir.lib.shimane-u.ac.jp/en/28650
6. Nash–Williams C. St. J. A. Random walk and electric currents in networks, *Mathematical Proceedings of the Cambridge Philosophical Society*, 1959, vol. 55, issue 2, pp. 181–194. https://doi.org/10.1017/S0305004100033879
7. Lyons T. A simple criterion for transience of a reversible Markov chain, *The Annals of Probability*, 1983, vol. 11, issue 2, pp. 393–402. https://doi.org/10.1214/aop/1176993604
8. Woess W. Random walks on infinite graphs and groups — a survey on selected topics, *Bulletin of the London Mathematical Society*, 1994, vol. 26, issue 1, pp. 1–60. https://doi.org/10.1112/blms/26.1.1
9. Cohen J. M., Colonna F., Singman D. The distribution of radial eigenvalues of the Euclidean Laplacian on homogeneous isotropic trees, *Complex Analysis and its Synergies*, 2021, vol. 7, issue 2, article number: 21. https://doi.org/10.1007/s40627-021-00071-2
10. Colonna F., Tjani M. Essential norms of weighted composition operators from reproducing kernel Hilbert spaces into weighted-type spaces, *Houston Journal of Mathematics*, 2016, vol. 42, no. 3, pp. 877–903. https://zbmath.org/?q=an:1360.47004
11. Cohen J. M., Colonna F., Singman D. A global Riesz decomposition theorem on trees without positive potentials, *Journal of the London Mathematical Society*, 2007, vol. 75, issue 1, pp. 1–17. https://doi.org/10.1112/jlms/jdl001
12. Anandam V., Damlakhi M. Perturbed Laplace operators on finite networks, *Revue Roumaine de Mathématiques Pures et Appliquées*, 2016, vol. 61, no. 2, pp. 75–92. https://zbmath.org/?q=an:1399.35147
13. Abodayeh K., Anandam V. Schrödinger networks and their Cartesian products, *Mathematical Methods in the Applied Sciences*, 2020, vol. 44, issue 6, pp. 4342–4347. https://doi.org/10.1002/mma.7034
14. Abodayeh K., Anandam V. Quasi-bounded supersolutions of discrete Schrödinger equations, *Applied Mathematical Sciences*, 2016, vol. 10, no. 34, pp. 1693–1704. https://doi.org/10.12988/ams.2016.63111
15. Nathiya N., Amulya Smyrna Ch. Infinite Schrödinger networks, *Vestnik Udmurtskogo Universiteta. Matematika. Mekhanika. Komp'yuternye Nauki*, 2021, vol. 31, issue 4, pp. 640–650. https://doi.org/10.35634/vm210408
16. Anandam V. Random walks on infinite trees, *Revue Roumaine de Mathématiques Pures et Appliquées*, 2020, vol. 65, no. 1, pp. 75–82. https://zbmath.org/7340511
17. Lawler G. F. *Introduction to stochastic processes*, New York: Chapman and Hall/CRC, 2006. https://doi.org/10.1201/9781315273600

Received 09.09.2022

Accepted 30.01.2023

Varadha Raj Manivannan, Department of Mathematics, School of Advanced Sciences, Vellore Institute of Technology University, Vellore, 632014, India.
ORCID: https://orcid.org/0000-0002-1258-8409
E-mail: varadharaj.m219@gmail.com

Madhu Venkataraman, Assistant Professor, Department of Mathematics, School of Advanced Sciences, Vellore Institute of Technology University, Vellore, 632014, India.
ORCID: https://orcid.org/0000-0002-9036-3336
E-mail: madhu.riasm@gmail.com

Citation: V. R. Manivannan, M. Venkataraman. Δ-functions on recurrent random walks, *Vestnik Udmurtskogo Universiteta. Matematika. Mekhanika. Komp'yuternye Nauki*, 2023, vol. 33, issue 1, pp. 119–129.

МАТЕМАТИКА 2023. Т. 33. Вып. 1. С. 119–129.

В. Р. Маниваннан, М. Венкатараман

Δ-функции на рекуррентных случайных блужданиях

Ключевые слова: параболические сети, решения Дирихле, выметание, рекуррентные случайные блуждания.

УДК 519.21, 531.26

DOI: 10.35634/vm230108

Если случайное блуждание на бесконечном счетном пространстве состояний обратимо, то известны необходимые и достаточные условия для того, чтобы это блуждание было рекуррентным. Если отбросить условие обратимости, то, используя дискретные решения Дирихле и выметание (понятия, известные из теории потенциала), можно частично установить некоторые из приведенных выше результатов, касающихся повторяемости и переходности случайного блуждания.

Финансирование. Мы благодарим рецензента за очень полезные комментарии. Первый автор выражает признательность за поддержку, оказанную Веллорским технологическим институтом в рамках стипендии Teaching cum Research Associate (VIT/HR/2019/5944 от 18 сентября 2019 года).

СПИСОК ЛИТЕРАТУРЫ

1. McGuinness S. Recurrent networks and a theorem of Nash–Williams // Journal of Theoretical Probability. 1991. Vol. 4. Issue 1. P. 87–100. https://doi.org/10.1007/BF01046995
2. Anandam V. Some potential-theoretic techniques in non-reversible Markov chains // Rendiconti del Circolo Matematico di Palermo. 2013. Vol. 62. Issue 2. P. 273–284. https://doi.org/10.1007/s12215-013-0124-8
3. Anandam V. Harmonic functions and potentials on finite or infinite networks. Berlin: Springer, 2011. https://doi.org/10.1007/978-3-642-21399-1
4. Abodayeh K., Anandam V. Potential-theoretic study of functions on an infinite network // Hokkaido Mathematical Journal. 2008. Vol. 37. Issue 1. P. 59–73. https://doi.org/10.14492/hokmj/1253539587
5. Anandam V., Abodayeh K. Non-locally-finite parahyperbolic networks // Memoirs of The Graduate School of Science and Engineering, Shimane University. Series B: Mathematics. 2014. Vol. 47. P. 19–35. https://ir.lib.shimane-u.ac.jp/en/28650
6. Nash–Williams C. St J. A. Random walk and electric currents in networks // Mathematical Proceedings of the Cambridge Philosophical Society. 1959. Vol. 55. Issue 2. P. 181–194. https://doi.org/10.1017/S0305004100033879
7. Lyons T. A simple criterion for transience of a reversible Markov chain // The Annals of Probability. 1983. Vol. 11. Issue 2. P. 393–402. https://doi.org/10.1214/aop/1176993604
8. Woess W. Random walks on infinite graphs and groups — a survey on selected topics // Bulletin of the London Mathematical Society. 1994. Vol. 26. Issue 1. P. 1–60. https://doi.org/10.1112/blms/26.1.1
9. Cohen J. M., Colonna F., Singman D. The distribution of radial eigenvalues of the Euclidean Laplacian on homogeneous isotropic trees // Complex Analysis and its Synergies. 2021. Vol. 7. Issue 2. Article number: 21. https://doi.org/10.1007/s40627-021-00071-2
10. Colonna F., Tjani M. Essential norms of weighted composition operators from reproducing kernel Hilbert spaces into weighted-type spaces // Houston Journal of Mathematics. 2016. Vol. 42. No. 3. P. 877–903. https://zbmath.org/?q=an:1360.47004
11. Cohen J. M., Colonna F., Singman D. A global Riesz decomposition theorem on trees without positive potentials // Journal of the London Mathematical Society. 2007. Vol. 75. Issue 1. P. 1–17. https://doi.org/10.1112/jlms/jdl001
12. Anandam V., Damlakhi M. Perturbed Laplace operators on finite networks // Revue Roumaine de Mathématiques Pures et Appliquées. 2016. Vol. 61. No. 2. P. 75–92. https://zbmath.org/?q=an:1399.35147

13. Abodayeh K., Anandam V. Schrödinger networks and their Cartesian products // Mathematical Methods in the Applied Sciences. 2020. Vol. 44. Issue 6. P. 4342–4347. https://doi.org/10.1002/mma.7034
14. Abodayeh K., Anandam V. Quasi-bounded supersolutions of discrete Schrödinger equations // Applied Mathematical Sciences. 2016. Vol. 10. No. 34. P. 1693–1704. https://doi.org/10.12988/ams.2016.63111
15. Nathiya N., Amulya Smyrna Ch. Infinite Schrödinger networks // Вестник Удмуртского университета. Математика. Механика. Компьютерные науки. 2021. Т. 31. Вып. 4. С. 640–650. https://doi.org/10.35634/vm210408
16. Anandam V. Random walks on infinite trees // Revue Roumaine de Mathématiques Pures et Appliquées. 2020. Vol. 65. No. 1. P. 75–82. https://zbmath.org/7340511
17. Lawler G. F. Introduction to stochastic processes. New York: Chapman and Hall/CRC, 2006. https://doi.org/10.1201/9781315273600

Поступила в редакцию 09.09.2022

Принята к публикации 30.01.2023

Маниваннан Варадха Радж, Школа передовых наук, кафедра математики, Веллорский технологический институт, Веллуру, Тамилнад, 632014, Индия.
ORCID: https://orcid.org/0000-0002-1258-8409
E-mail: varadharaj.m219@gmail.com

Венкатараман Мадху, доцент, Школа передовых наук, кафедра математики, Веллорский технологический институт, Веллуру, Тамилнад, 632014, Индия.
ORCID: https://orcid.org/0000-0002-9036-3336
E-mail: madhu.riasm@gmail.com

Цитирование: В. Р. Маниваннан, М. Венкатараман. Δ-функции на рекуррентных случайных блужданиях // Вестник Удмуртского университета. Математика. Механика. Компьютерные науки. 2023. Т. 33. Вып. 1. С. 119–129.

Linear Algebra and its Applications 680 (2024) 208–219

Contents lists available at ScienceDirect

Linear Algebra and its Applications

journal homepage: www.elsevier.com/locate/laa

A perturbed averaging operator on finite graphs

Varadha Raj Manivannan [a,*], Victor Anandam [b]

[a] *Department of Mathematics, School of Advanced Sciences, Vellore Institute of Technology, Vellore - 632 014, Tamil Nadu, India*
[b] *Ramanujan Institute for Advanced Study in Mathematics, University of Madras, Chepauk, Chennai 600 005, India*

ARTICLE INFO

Article history:
Received 11 November 2022
Received in revised form 4 August 2023
Accepted 30 September 2023
Available online 12 October 2023
Submitted by R. Brualdi

MSC:
15A18
31C20
31C05

Keywords:
Finite graphs
Superharmonic functions
Perron-Frobenius theorem
Greatest eigenvalue

ABSTRACT

On a finite random walk $\{X, p(x,y)\}$, an averaging operator A is defined by $Au(x) = \sum p(x,y)u(y)$ and its perturbation is $A_\varphi u(x) = Au(x) - \varphi(x)u(x)$, where $\varphi(x)$ is a real-valued function on the states of X. The properties of the solutions and the supersolutions of $A_\varphi u(x) = 0$ are studied which fall into three categories depending on the greatest eigenvalue (a term made precise) of the non-symmetric matrix representing A_φ. Relative to the operator A_φ, the Dirichlet-Poisson solution, the Green function, the Equilibrium Principle and the Condenser problem are investigated.

1. Introduction

Potential theory on Euclidean spaces $\mathbb{R}^n$ has been developed in two different ways. One, define the Dirichlet norm, the inner product and use Banach space-Hilbert space

* Corresponding author.
E-mail addresses: varadharaj.m219@gmail.com (V.R. Manivannan), vanandam@hotmail.com (V. Anandam).

https://doi.org/10.1016/j.laa.2023.09.029
0024-3795/

techniques to introduce potential functions as projections, based on the Dirichlet Principle, see Deny [14]. The other way is to start with harmonic and superharmonic functions (functions with mean-value and super mean-value properties), introduce the Harnack property, Minimum principle and discuss the solutions to the Dirichlet problem which leads to the notion of potentials as non-negative superharmonic functions having 0 as the greatest harmonic minorant, see Bauer [5], Brelot [10] and Constantinescu and Cornea [13].

When we discuss discrete potential theory in the context of finite or infinite weighted graphs, the above dichotomy reappears. In the two cases of electrical networks, with conductances on branches as weights and reversible random walks, with transition probabilities as weights, a Dirichlet norm can be defined; in these cases the results are proved as in the first development of classical potential theory mentioned above, see [3,8,16–18]. In the paper [12] of Carmona, Encinas and Mitjana, admissible potentials and effective resistances on a finite weighted graph with symmetric conductances are considered by using the Dirichlet principle and potential-theoretic methods as in the first development mentioned above.

In this note, we leave out the symmetric conductances requirement and follow discrete potential-theoretic methods suggested by the second development indicated above.

Consider an irreducible matrix which determines a finite network $\{X = \{V, E\}, t(x, y)\}$ made up of a finite graph X and a set of non-symmetric weights $\{t(x, y)\}$ on the edges $[x, y] : t(x, y) \geq 0, t(x, y) > 0$ if and only if $[x, y]$ is an edge, $t(x, y)$ and $t(y, x)$ need not be the same. The combinatorial Laplacian $\mathcal{L}$ is given by $\mathcal{L}u(x) = \sum_{y \sim x} t(x, y)[u(x) - u(y)], y \sim x$, $y \in V; x \in V$; denoting that $[x, y]$ is an edge. If $\varphi(x)$ is any real-valued function on X, then by using Perron-Frobenius Theorem as in [2,4,7], $\varphi(x) = c - \frac{\mathcal{L}\xi(x)}{\xi(x)}, \xi(x) > 0$ for any $x \in X$; this representation is unique in the sense that c is the smallest eigenvalue of the matrix representing the perturbed Laplace operator $\mathcal{L}_\varphi$, defined by $\mathcal{L}_\varphi u(x) = \mathcal{L}u(x) + \varphi(x)u(x)$; and $\xi(x)$ is the normalized eigenfunction with all its entries positive, associated to c and $\sum_x \xi(x) = 1$.

This suggests a natural classification of the networks $\{X, t(x, y), \varphi(x)\}$ depending on whether $c = 0$, $c > 0$ or $c < 0$. We carry out this classification here, leading to an appropriate function theory in each of these three cases. It is helpful to note that when $\varphi(x) = \lambda$ is a constant, the solutions of the Laplace ($\lambda = 0$), the Schrödinger ($\lambda > 0$) and the Helmholtz ($\lambda < 0$) operators respectively lay a foundation for our research in developing three different function theories on $\{X, t(x, y), \varphi(x)\}$ based on the smallest eigenvalue c of $\mathcal{L}_\varphi$.

2. Preliminaries

To emphasize the non-symmetry of the conductances, we shall use the writing in the study of random walks. A finite perturbed random walk $X_\varphi = \{X = \{V, E\}, p(x, y), \varphi(x)\}$ consists of a finite graph X, a set $\{p(x, y)\}$ is transition proba-

bilities it satisfies that $\sum_{y\in X} p(x,y) = 1$ for any $x \in X$, and a function $\omega(x) > 0$ on the states in X. We do not require the random walk to be reversible: that is, there may not be any function $\omega(x) > 0$ such that $\omega(x)p(x,y) = \omega(y)p(y,x)$ for any pair of states x, y. The averaging operator A is defined as $Au(x) = \sum_y p(x,y)u(y) = (I - \mathcal{L})u(x)$, where $\mathcal{L}$ is the combinatorial Laplacian operator of the finite network $\{X, p(x,y)\}$. Thus, if $C(V)$ is the family of real-valued functions on X, $A : C(V) \to C(V)$ is linear, $Af \geq 0$ if $f \geq 0$ and if f_n is a sequence in $C(V)$ tending to f in $C(V)$ then $Af_n \to Af$.

A real-valued function $s(x)$ is said to be superharmonic (harmonic, subharmonic respectively) if $As(x) \leq s(x)$, $(As(x) = s(x)$, $As(x) \geq s(x)$respectively). For a real-valued function $\varphi(x)$ on X, write $A_\varphi u(x) = Au(x) - \varphi(x)u(x)$ and say that $u(x)$ is φ-superharmonic if and only if $A_\varphi u(x) \leq 0$. Thus, φ-superharmonic is the same as superharmonic when $\varphi \equiv 1$. For any real-valued function $f(x)$ on X, write $f(x) = f^+(x) + f^-(x)$ where $f^+(x) = \max(f(x), 0)$ and $f^-(x) = -\min(f(x), 0)$. We define the dirac delta function on $E \subset X$, is, for any $y \in X$, $\delta_y(x) = \begin{cases} 1 & x \in E \\ 0 & \text{otherwise} \end{cases}$.

Proposition 2.1. *If $u(x), v(x)$ are φ-superharmonic functions on X, then $\inf(u, v)$ also is φ-superharmonic.*

Proof. Let $s(x) = \inf(u(x), v(x))$. At a state z in X, suppose $s(z) = u(z)$. Then,

$$\begin{aligned} A_\varphi s(z) &= As(z) - \varphi(z)s(z) \\ &= As(z) - \varphi(z)u(z) \\ &\leq Au(z) - \varphi(z)u(z) \\ &= A_\varphi u(z) \leq 0. \quad \square \end{aligned}$$

Lemma 2.2. *If $s(x) \geq 0$ is a φ-superharmonic function on X such that $s(z) = 0$ for some state z. Then $s(x) = 0$ for all x.*

Proof. $As(z) \leq \varphi(z)s(z) = 0$, hence $\sum_{y\sim x} p(z,y)s(y) = 0$ so that $s(y) = 0$ for any $y \sim z$. Then by connectedness of X, we find $s = 0$. $\square$

Proposition 2.3. *Let $f(x)$ be a real-valued function on X. Let $\mathfrak{F}$ be the family of all φ-superharmonic functions $s(x)$ on X such that $s(x) \geq f(x)$. If there exists a positive φ-superharmonic function $v(x)$ on X, then $\mathfrak{F}$ is non-empty and $\inf_{s\in\mathfrak{F}} s(x)$ is φ-superharmonic.*

Proof. Since $v(x) \geq \alpha > 0$ on X, if $f(x) \leq \beta$ then $f(x) \leq \frac{\beta}{\alpha}v(x)$, hence the family is non-empty. If $s_n(x)$ is a sequence of φ-superharmonic function such that $s(x) = \lim_n s_n(x)$ exists and is real-valued then it is easy to see that $s(x)$ is φ-superharmonic. Now, if

$u, v \in \mathfrak{F}$, then $\inf(u, v) \in \mathfrak{F}$. Hence $\mathfrak{F}$ is a lower directed family of φ-superharmonic functions. Since X is finite we can extract a decreasing sequence $s_n(x)$ from $\mathfrak{F}$ so that $\inf_{s\in\mathfrak{F}} s(x) = \lim_n s_n(x)$ for every x in X, which is φ-superharmonic on X. □

Proposition 2.4. *Let $s(x)$ be a φ-superharmonic function on X. Let $\mathfrak{F}$ be the family of all φ-subharmonic functions $v(x)$ on X such that $v(x) \leq s(x)$. If $\mathfrak{F}$ is non-empty, then $h(x) = \sup_{v\in\mathfrak{F}} v(x)$ is φ-harmonic on X. Moreover, if h' is any φ-harmonic function such that $h' \leq s$, then $h' \leq h$.*

Proof. With obvious changes, from Proposition 2.3, we see that $h(x)$ is a φ-subharmonic function. It remains to show that $h(x)$ is φ-harmonic on X. For that we use the method known as the Poisson modification. Let z be any state in X. Then $\varphi(z)h(z) \leq \sum_{y\sim z} p(z, y)h(y)$. Consider the function $u(x)$ on X such that $u(x) = \begin{cases} h(x) & \text{if } x \neq z \\ \frac{1}{\varphi(z)} \sum p(z, y)h(y) & \text{if } x = z. \end{cases}$ Then $s(x) \geq u(x) \geq h(x)$ on X; $u(x)$ is φ-harmonic at the state z since $\varphi(z)u(z) = \sum_{y\sim z} p(z, y)h(y) = \sum_{y\sim z} p(z, y)u(y) = Au(z)$; and $u(x)$ is φ-subharmonic on X so that $u \in \mathfrak{F}$. Consequently $u(x) = h(x)$ on X which means that $h(x)$ is φ-harmonic at $x = z$. Since the state z is chosen arbitrarily we conclude that $h(x)$ is φ-harmonic on X. Suppose now h' is a φ-harmonic function, $h' \leq s$. Then $h' \in \mathfrak{F}$ so that $h' \leq h$ on X. □

Remark 1.

(1) In the above Proposition 2.4, the function $h(x)$ is known as the greatest φ-harmonic minorant of $s(x)$.
(2) **φ-potentials:** A φ-superharmonic function $s(x) \geq 0$ is termed a φ-potential if and only if its greatest φ-harmonic minorant is 0.
(3) **Riesz decomposition:** Let $h(x)$ be the greatest φ-harmonic minorant of a φ-superharmonic function $s(x) \geq 0$. Then $p(x) = s(x) - h(x)$ is a φ-potential. Thus $s(x) = p(x) + h(x)$ which in the classical case is known as the Riesz decomposition of $s(x)$. This decomposition of $s(x)$ as a φ-potential and a non-negative φ-harmonic function is unique in the sense that if $s(x)$ is the sum of any other φ-potential $p_1(x)$ and a φ-harmonic function $h_1(x)$ then $p(x) = p_1(x)$ and $h(x) = h_1(x)$.

We can look at the operator A_φ as a perturbation of A. In fact, in a finite network $\{X, c(x, y)\}$ in which the conductances $c(x, y)$ are symmetric, Carmona, Encinas and Mitjana [11] consider the Schrödinger operator $\mathcal{L}_q$ defined by $\mathcal{L}_q(u) = \mathcal{L}(u) + qu$ for any $u \in X$, where $\mathcal{L}$ is the combinatorial Laplacian operator and q is a potential function on X such that the Schrödinger operator $\mathcal{L}_q$ is positive semidefinite. They investigate among other nice results the relation between the lowest eigenvalue λ of $\mathcal{L}_q$ when $\lambda \geq 0$ and

the existence of q-superharmonic functions and q-harmonic functions; also the Dirichlet Principle is invoked to obtain solutions to the Dirichlet-Poisson problem and to prove the existence of the Green function on a subset of X. For similar considerations in a symmetric infinite network, see Yamasaki [19].

In the present case where the conductances in $\{X, p(x,y), \varphi(x)\}$ are not necessarily symmetric, we start with a unique representation for any real-valued function $\varphi(x)$, by using the Perron-Frobenius Theorem in [15]: Let $M = (m_{ij})$ be a positive matrix, that is $m_{ij} > 0$ for all entries. Then some of the important points of the Perron theorem are:

(1) If ρ is the spectral radius of "m", then $\rho > 0$ is a simple eigenvalue of "m", with an associated eigenvector $\xi(x)$ having all its entries positive.
(2) If λ is any eigenvalue of m different from ρ, then $|\lambda| < \rho$.
(3) Any eigenvector other than $\xi(x)$ contains entries of different sign.

Frobenius extended the above results to the case when M is a non-negative matrix that is irreducible also.

Let $\varphi(x)$ be a real-valued function. Define $A_\varphi u(x) = Au(x) - \varphi(x)u(x)$. The operator A_φ, when $\varphi = 1, \varphi > 1, \varphi < 1$, generalizes the classical Laplace, Schrödinger, Helmholtz operators respectively. Then for $\beta > 0$ large, the matrix representing $A_\varphi + \beta I$ has all its entries non-negative. Hence (by Perron-Frobenius Theorem) there is the eigenvalue α (largest in the sense that if λ is any other eigenvalue then $|\lambda| < \alpha$) which is simple and its associated eigenvector $\xi(x)$ has all its entries positive. We fix $\xi(x)$ uniquely with the restriction $\sum_x \xi(x) = 1$. $(A_\varphi + \beta I)\xi(x) = \alpha\xi(x)$. Hence $A_\varphi \xi(x) = k\xi(x)$, where $k = \alpha - \beta$; that is $A\xi(x) - \varphi(x)\xi(x) = k\xi(x)$ so that $\varphi(x) = \frac{A\xi(x)}{\xi(x)} - k$.

Proposition 2.5. *The constant k is the largest eigenvalue of A_φ in the sense that if σ is any other eigenvalue of A_φ, then Re $\sigma < k$.*

Proof. Suppose $A_\varphi \mu(x) = \sigma\mu(x)$. Then $(\beta I + A_\varphi)\mu(x) = (\beta + \sigma)\mu(x)$. Since α is the largest eigenvalue of $\beta I + A_\varphi$ by Perron-Frobinius, $|\beta + \sigma| < \alpha$. Hence $\beta + \text{Re}\sigma = \text{Re}(\beta + \sigma) \leq |\beta + \sigma| < \alpha$, so that Re $\sigma < \alpha - \beta = k$. □

3. Finite random walks and φ-potentials

In this section, we consider $\varphi(x) = \frac{A\xi(x)}{\xi(x)} - k$, for any $x \in X$, when $k < 0$. In this case $\varphi(x) > \frac{A\xi(x)}{\xi(x)} > 0$. Since the largest eigenvalue k is negative, 0 is not an eigenvalue of A_φ, hence A_φ is invertible so that $A_\varphi[h(x)] = 0$ for any $h(x)$ implies that $h(x) = 0$. This means that there is no non-zero solution to the equation $A_\varphi u(x) = 0$.

However, since $A_\varphi \xi(x) = A\xi(x) - \left[\frac{A\xi(x)}{\xi(x)} - k\right]\xi(x) = k\xi(x) < 0$, the function $\xi(x)$ is a positive φ-superharmonic function. Since there is no non-zero φ-harmonic function on X, the function $\xi(x) > 0$ is a φ-potential on X. Remark also that any φ-superharmonic

function s on X is non-negative: because, for a large positive constant α, $-s(x) \leq \alpha\xi(x)$; here the left side is φ-superharmonic and the right side a φ-potential. Hence $-s(x) \leq 0$ on X. In fact, every φ-superharmonic function on X is a φ-potential.

Proposition 3.1. *The largest eigenvalue $k < 0$ if and only if $\varphi(x) > \frac{A\mu(x)}{\mu(x)}$ for some $\mu(x) > 0$.*

Proof. When $k < 0, \varphi(x) = \frac{A\xi(x)}{\xi(x)} - k > \frac{A\xi(x)}{\xi(x)}$. On the other hand suppose $\varphi(x) > \frac{A\mu(x)}{\mu(x)}$ for some $\mu(x) > 0$. Then

$$\begin{aligned}
\frac{A\xi(x)}{\xi(x)} - k &> \frac{A\mu(x)}{\mu(x)} \\
k\xi(x)\mu(x) &< \mu(x)A\xi(x) - \xi(x)A\mu(x) \\
&= \sum_y p(x,y)[\mu(x)\xi(y) - \xi(x)\mu(y)]
\end{aligned}$$

so called Doob transform,

$$\begin{aligned}
&= \sum_y p(x,y)\xi(x)\xi(y)\left[\frac{\mu(x)}{\xi(x)} - \frac{\mu(y)}{\xi(y)}\right] \\
&= \bar{\mathcal{L}}\left[\frac{\mu(x)}{\xi(x)}\right],
\end{aligned}$$

where $\bar{\mathcal{L}}$ is the combinatorial Laplacian of the finite network $\{X, \bar{t}(x,y) = p(x,y)\xi(x)\xi(y)\}$. Hence if we assume $k \geq 0$ then we should have $\bar{\mathcal{L}}\left[\frac{\mu(x)}{\xi(x)}\right] > 0$ so that $\frac{\mu(x)}{\xi(x)}$ is a constant λ and $0 = \bar{\mathcal{L}}[\lambda] > 0$. This contradiction shows that $k < 0$. □

Proposition 3.2. *For any real-valued function $u(x)$ on X, $A_\varphi[u(x)] = \xi(x)\{-\tilde{\mathcal{L}}[\frac{u(x)}{\xi(x)}] + k[\frac{u(x)}{\xi(x)}]\}$, where $\tilde{\mathcal{L}}$ is the combinatorial Laplacian of $\{X, t(x,y) = p(x,y)\frac{\xi(y)}{\xi(x)}\}$.*

Proof.

$$\begin{aligned}
A_\varphi[u(x)] &= Au(x) - \left[\frac{A\xi(x)}{\xi(x)} - k\right]u(x) \\
&= \sum_y p(x,y)\xi(y)\left[\frac{u(y)}{\xi(y)} - \frac{u(x)}{\xi(x)}\right] + ku(x) \\
&= \xi(x)\left\{\sum_y p(x,y)\frac{\xi(y)}{\xi(x)}\left[\frac{u(y)}{\xi(y)} - \frac{u(x)}{\xi(x)}\right] + k\left[\frac{u(x)}{\xi(x)}\right]\right\} \\
&= \xi(x)\left\{-\tilde{\mathcal{L}}\left[\frac{u(x)}{\xi(x)}\right] + k\left[\frac{u(x)}{\xi(x)}\right]\right\}. \quad \square
\end{aligned}$$

Consequences:

(1) If $p(x)$ is an $\tilde{\mathcal{L}}$-potential, then $p(x)\xi(x)$ is a φ-potential.

Proof. Since $k < 0$, for any $s(x) \geq 0, A_\varphi[s(x)] \leq -\xi(x)\tilde{\mathcal{L}}\left[\frac{s(x)}{\xi(x)}\right]$. Take $s(x) = p(x)\xi(x)$. If $v(x) \geq 0$ is φ-subharmonic, $v(x) \leq s(x)$ then we show that $v = 0$ to conclude that $s(x)$ is a φ-potential. Now, $0 \leq A_\varphi[v(x)] \leq -\xi(x)\tilde{\mathcal{L}}\left[\frac{v(x)}{\xi(x)}\right]$ so that $\frac{v(x)}{\xi(x)}$ is $\tilde{\mathcal{L}}$-subharmonic, majorized by $\frac{s(x)}{\xi(x)} = p(x)$ which is an $\tilde{\mathcal{L}}$-potential. Hence $\frac{v(x)}{\xi(x)} = 0$. □

(2) If $A_\varphi[s(x)] = 0$, then $s(x) = 0$ for all x.

Proof. From the above Proposition 3.2, $0 = A_\varphi[s(x)] = \xi(x)\{-\tilde{\mathcal{L}}[\frac{s(x)}{\xi(x)}] + k[\frac{s(x)}{\xi(x)}]\}$. Hence $\tilde{\mathcal{L}}\left[\frac{s(x)}{\xi(x)}\right] = k\left[\frac{s(x)}{\xi(x)}\right]$. If $\frac{s(x)}{\xi(x)} \neq 0$, then it would mean that $k < 0$ is an real eigenvalue of $\tilde{\mathcal{L}}$, by the contradiction since all the eigenvalues of $\tilde{\mathcal{L}}$ are non-negative. Hence $s = 0$. □

Green Function: Since A_φ is invertible, given any function $f(x)$ on X, there exists a unique solution $u(x)$ such that $A_\varphi[u(x)] = f(x)$, (Poisson equation). In particular, if we take $f(x) = -\delta_y(x)$ where y is a fixed state, then there exists a unique function $g_y(x)$ such that $A_\varphi[g_y(x)] = -\delta_y(x)$. The φ-superharmonic function $g_y(x)$ is known as the Green function of $\{X, p(x,y), \varphi(x)\}$ with pole at the state y.

Proposition 3.3. *When $k < 0$, any real-valued function $f(x)$ on X is the difference of two φ-potentials on X.*

Proof. Let $s_1(x) = \sum_z [A_\varphi f(z)]^+ g_z(x)$ and $s_2(x) = \sum_z [A_\varphi f(z)]^- g_z(x)$. Then $s_1(x), s_2(x)$ are two φ-potentials. Write $s(x) = s_2(x) - s_1(x)$. If $h(x) = f(x) - s(x)$, then $A_\varphi[h(x)] = A_\varphi[f(x)] - [A_\varphi f(x)]^- + [A_\varphi f(x)]^+ = 0$; since $k < 0$, then $h = 0$, leading to the conclusion that $f(x)$ is a difference of two φ-potentials. □

Lemma 3.4. *Let F be a proper subset of X. Let $f(x)$ be a real-valued function on $X \setminus F$. Then there exists a unique function $s(x)$ on X such that $A_\varphi[s(x)] = 0$ for $x \in F$ and $s(x) = f(x)$ for $x \in X \setminus F$.*

Proof. Since $\xi(x) > 0$ is φ-superharmonic on X, we can take a φ-superharmonic function $u(x) > 0$ on X such that $u(x) \geq f(x)$ on $X \setminus F$. Let $v(x) = \begin{cases} u(x) & \text{on } F \\ f(x) & \text{on } X \setminus F. \end{cases}$ Then $A_\varphi[v(x)] \leq 0$ for each $x \in F$. Let $\mathfrak{F}$ be the family of all functions $v(x)$ on F such that $A_\varphi[v(x)] \leq 0$ at every $x \in F$ and $v(x) = f(x)$ on $X \setminus F$. Let $s(x) = \inf_{v \in \mathfrak{F}} v(x)$. Then (as in Proposition 2.4) $A_\varphi[s(x)] = 0$ at every $x \in F$ and $s(x) = f(x)$ on $X \setminus F$.

To prove the uniqueness of solution, it is enough to show that if $A_\varphi[s(x)] = 0$ on F and $s(x) = 0$ on $X \setminus F$, then $s = 0$ on X. By the construction given above, when $A_\varphi[s(x)] = 0$ on F and $s(x) = 0$ on $X \setminus F$, we have obtained $s(x) = \inf_{v \in \mathfrak{F}} v(x)$, where $\mathfrak{F}$ consists of functions $v(x)$ such that $A_\varphi v(x) \leq 0$ on F and $v(x) = 0$ on $X \setminus F$. In particular the function $v = 0$ on X is in $\mathfrak{F}$ and hence $s(x) \leq 0$. Proceeding similarly, since $A_\varphi[-s(x)] = 0$ on F and $-s(x) = 0$ on $X \setminus F$, then $-s(x) \leq 0$. Consequently $s = 0$. □

Theorem 3.5 *(Dirichlet-Poisson). Let F be a subset of X. Let $\mu(x)$ and $\psi(x)$ be two functions defined on F and $X \setminus F$ respectively. Then there exists a unique function $s(x)$ on X such that $A_\varphi[s(x)] = \mu(x)$ on F and $s(x) = \psi(x)$ on $X \setminus F$.*

Proof. When $F = X$ or ϕ, the theorem can be interpreted accordingly. Let $u(x) = \sum_{z \in F} \mu(z) g_z(x)$, where $g_z(x)$ is the Green function with pole at z. Then $u(x)$ is a function on X such that $A_\varphi[u(x)] = -\mu(x)$ when $x \in F$ and $A_\varphi[u(x)] = 0$ when $x \in X \setminus F$, assuming F is a proper subset of X. Let $f(x) = u(x) + \psi(x)$ when $x \in X \setminus F$. Then by Lemma 3.4 above, there exists a unique function $v(x)$ on X such that $A_\varphi[v(x)] = 0$ on F and $v(x) = f(x)$ on $X \setminus F$. Let $s(x) = v(x) - u(x)$ on X. Then on F, $A_\varphi[s(x)] = A_\varphi[v(x)] - A_\varphi[u(x)] = 0 + \mu(x)$ and on $X \setminus F$, $s(x) = f(x) - u(x) = \psi(x)$. The uniqueness of the solution $s(x)$ is seen as before. □

Remark 2. In a finite network $\{X, c(x, y)\}$ with symmetric conductances, let $\mathcal{L}_q u(x) = \mathcal{L}u(x) + q(x)u(x)$, where $q(x) \geq 0$ and $\mathcal{L}$ is the combinatorial Laplacian. Bendito, Carmona, Encinas [6], using the Equilibrium Measures have studied boundary value problems and symmetric Green functions including the Dirichlet-Poisson problem and have given various applications.

4. Finite random walks without φ-potentials

In this section, we have some properties of finite random walks when $k = 0$. From the previous section, we have in this case $A_\varphi[u(x)] = -\xi(x)\tilde{\mathcal{L}}\left[\frac{u(x)}{\xi(x)}\right]$ for any real-valued function $u(x)$ on X. Consequently,

(1) The constant λ is an eigenvalue of A_φ with associated eigenfunction $\mu(x)$ if and only if $-\lambda$ is an eigenvalue of $\tilde{\mathcal{L}}$ with associated eigenfunction $\frac{\mu(x)}{\xi(x)}$.

Proof. $A_\varphi[\mu(x)] = \lambda\mu(x)$ if and only if $\tilde{\mathcal{L}}\left[\frac{\mu(x)}{\xi(x)}\right] = -\lambda\left[\frac{\mu(x)}{\xi(x)}\right]$. □

(2) Any φ-superharmonic function on X is proportional to $\xi(x)$.

Proof. Suppose $A_\varphi u(x) \leq 0$. Then $\tilde{\mathcal{L}}\left[\frac{u(x)}{\xi(x)}\right] \geq 0$, hence $\frac{u(x)}{\xi(x)}$ is a constant. □

Theorem 4.1. *If F is a proper subset of X and $u(x), v(x)$ are two real-valued functions on X such that $u(x) \geq v(x)$ on F and $A_\varphi u(x) \leq A_\varphi v(x)$ on $X \setminus F$, then $u(x) \geq v(x)$ on X.*

Proof. Since $A_\varphi[u(x)] = -\xi(x)\tilde{\mathcal{L}}\left[\frac{u(x)}{\xi(x)}\right]$, from the assumptions we have $\frac{u(x)}{\xi(x)} \geq \frac{v(x)}{\xi(x)}$ on F and $\tilde{\mathcal{L}}\left[\frac{u(x)}{\xi(x)}\right] \geq \tilde{\mathcal{L}}\left[\frac{v(x)}{\xi(x)}\right]$ on $X \setminus F$. Hence [1, Theorem 2.2.3], $\frac{u(x)}{\xi(x)} \geq \frac{v(x)}{\xi(x)}$ on X, proving the theorem. □

Since $A_\varphi[u(x)] = -\xi(x)\tilde{\mathcal{L}}\left[\frac{u(x)}{\xi(x)}\right]$, like in the above theorem, many of the properties of A_φ can be proved by using the properties of $\tilde{\mathcal{L}}$ as given in [1, Section 2.2]. For example:

(1) If F is a proper subset of X, $u(x) \geq 0$ on F and $A_\varphi[u(x)] \leq 0$ on $X \setminus F$, then $u(x) \geq 0$ on X. As a result, $u(x) = 0$ on F and $A_\varphi u(x) = 0$ on $X \setminus F$ would imply that $u = 0$ on X.
(2) (Dirichlet-Poisson) Let F be a proper subset of X and $f(x), g(x)$ two real-valued functions on F and $X \setminus F$ respectively. Then there exists a unique function $u(x)$ on X such that $A_\varphi[u(x)] = f(x)$ on F and $u(x) = g(x)$ on $X \setminus F$.
(3) (Green function on F) For any y in the proper subset F of X, there exists a unique function $G_y^F(x) \geq 0$ on X such that $A_\varphi\left[G_y^F(x)\right] = -\delta_y(x)$ on F and $G_y^F(x) = 0$ on $X \setminus F$.
(4) (Equilibrium Principle) See Bendito, Carmona, Encinas [6] for a similar result defining the Equilibrium measures in a finite network with symmetric conductances: Let F be a proper subset of X. Then given $f \geq 0$ on F, there exists a unique function $u(x) \geq 0$ on X such that $A_\varphi u(x) = -f(x)$ on F and $u = 0$ on $X \setminus F$. Moreover if $f > 0$ then $u > 0$ on F.
(5) (Condenser Principle) Let A and B be two non-empty disjoint subsets of X. Let $F = X \setminus (A \cup B) \neq \phi$. Then there exists a unique function $v(x)$ on X such that $0 \leq v(x) \leq \xi(x)$ on X,

$$\begin{aligned} v(x) = 0 \quad &\text{and} \quad A_\varphi[v(x)] \geq 0 \quad \text{if} \quad x \in A, \\ v(x) = \xi(x) \quad &\text{and} \quad A_\varphi[v(x)] \leq 0 \quad \text{if} \quad x \in B, \\ &\text{and} \quad A_\varphi[v(x)] = 0 \quad \text{if} \quad x \in F. \end{aligned}$$

5. The case when the greatest eigenvalue is positive

(1) There is no positive φ-superharmonic function on X.

Proof. Suppose $v(x) > 0$ and $A_\varphi v(x) \leq 0$. Then

$$0 \geq Av(x) - \varphi(x)v(x)$$

$$
\begin{aligned}
&= Av(x) - \left[\frac{A\xi(x)}{\xi(x)} - k\right] v(x) \\
-k\xi(x)v(x) &\geq \xi(x)Av(x) - v(x)A\xi(x) \\
&= \xi(x)\sum_y p(x,y)v(y) - v(x)\sum_y p(x,y)\xi(y) \\
&= \sum_y p(x,y)[\xi(x)v(y) - v(x)\xi(y)] \\
&= \sum_y p(x,y)\xi(x)\xi(y)\left[\frac{v(y)}{\xi(y)} - \frac{v(x)}{\xi(x)}\right]
\end{aligned}
$$

Now consider the finite network $\{X, t(x,y)\}$ where $t(x,y) = p(x,y)\xi(x)\xi(y)$. If the combinatorial Laplacian operator of this network is $\bar{\mathcal{L}}$, then we have $-\bar{\mathcal{L}}\left[\frac{v(x)}{\xi(x)}\right] \leq -k\xi(x)v(x) < 0$ so that $\frac{v(x)}{\xi(x)}$ is a constant λ and we should have $0 = \bar{\mathcal{L}}\left[\frac{v(x)}{\xi(x)}\right] < 0$, a contradiction. So, we conclude that there is no positive φ-superharmonic function on X, if $k > 0$. □

Lemma 5.1. *The constant λ is an eigenvalue of A_φ with associated eigenfunction $s(x)$ if and only if $(k - \lambda)$ is an eigenvalue of $\tilde{\mathcal{L}}$ with associated eigenfunction $\left[\frac{s(x)}{\xi(x)}\right]$ where $\tilde{\mathcal{L}}$ is the combinatorial Laplacian operator in the finite network $\{X, t(x,y) = \frac{\xi(y)}{\xi(x)}p(x,y)\}$.*

Proof.

$$
\begin{aligned}
&\text{If} \quad A_\varphi s(x) = \lambda s(x), \text{then} \\
As(x) - \left[\frac{A\xi(x)}{\xi(x)} - k\right] s(x) &= \lambda s(x) \\
\xi(x)\Delta s(x) - s(x)A\xi(x) &= (\lambda - k)s(x)\xi(x) \\
\sum_y p(x,y)\frac{\xi(y)}{\xi(x)}\left[\frac{s(y)}{\xi(y)} - \frac{s(x)}{\xi(x)}\right] &= (\lambda - k)\left[\frac{s(x)}{\xi(x)}\right] \\
-\tilde{\mathcal{L}}\left[\frac{s(x)}{\xi(x)}\right] &= (\lambda - k)\left[\frac{s(x)}{\xi(x)}\right].
\end{aligned}
$$

Hence, if $s(x)$ is an eigenfunction associated to the eigenvalue λ of A_φ, then $\left[\frac{s(x)}{\xi(x)}\right]$ is an eigenfunction associated to the eigenvalue $(k - \lambda)$ of $\tilde{\mathcal{L}}$. To prove the converse, reverse the argument. □

Consequences: Since the real part of any non-zero eigenvalue of $\tilde{\mathcal{L}}$ is positive, the constant k may or may not be an eigenvalue of $\tilde{\mathcal{L}}$.

(a) Suppose k is not an eigenvalue of $\tilde{\mathcal{L}}$.

(1) Then 0 is not an eigenvalue of A_φ. Hence there is no non-zero solution for the equation $A_\varphi u(x) = 0$.
(2) (Poisson) The matrix A_φ is invertible. Hence for any real-valued function $f(x)$ on X, there is a unique solution $u(x)$ such that $A_\varphi[u(x)] = f(x)$.
(3) (Logarithmic kernel) In particular, for any fixed state y in X there exists a unique function $g_y(x)$ such that $A_\varphi[g_y(x)] = -\delta_y(x)$. This function $g_y(x)$ cannot be non-negative (as in the case of the logarithmic potential in $\mathbb{R}^2$).

(b) Suppose k is an eigenvalue of $\tilde{\mathcal{L}}$.
(1) Note that k is an eigenvalue of $\tilde{\mathcal{L}}$ if and only if non-zero $A_\varphi-$ solutions exist on X.

Proof. By the Lemma 5.1, k is an eigenvalue of $\tilde{\mathcal{L}}$ if and only if 0 is an eigenvalue of A_φ, if and only if there exists a non-zero function $h(x)$ such that $A_\varphi[h(x)] = 0$. □

(2) If $s(x)$ is an eigenfunction associated to k (for the operator $\tilde{\mathcal{L}}$), then $u(x) = s(x)\xi(x)$ is a solution to the equation $A_\varphi[u(x)] = 0$.

Proof. If $\tilde{\mathcal{L}}[s(x)] = ks(x)$, then $A_\varphi[s(x)\xi(x)] = -\xi(x)\tilde{\mathcal{L}}[s(x)] + k\xi(x)s(x) = 0$. □

(3) Any non-zero solution $u(x)$ of the equation $A_\varphi[u(x)] = 0$ has both positive and negative entries.

Proof. This can be seen from the properties of the eigenfunctions associated to non-zero eigenvalues of the combinatorial Laplacian operator, see Biyikoglu, Leydold, Stadler [9]. Alternately we can prove it as follows: Suppose $A_\varphi[u(x)] = 0$. Then $Au(x) = \varphi(x)u(x)$. A simplification as before gives $\tilde{\mathcal{L}}\left[\frac{u(x)}{\xi(x)}\right] = k\left[\frac{u(x)}{\xi(x)}\right]$. Hence if all the entries of $u(x)$ are of the same sign, then $\tilde{\mathcal{L}}\left[\frac{u(x)}{\xi(x)}\right]$ is positive or negative. Hence $u(x) = \lambda\xi(x)$ for some constant λ, leading to the contradiction $A_\varphi[\xi(x)] = 0$ when $k > 0$. □

Remark 3. From the above results, we have the following:

(1) For any x, $k + \varphi(x) \geq \sigma > 0$. For, $\varphi(x) = \frac{A\xi(x)}{\xi(x)} - k = \left[\sum_y p(x,y)\frac{\xi(y)}{\xi(x)}\right] - k$.
(2) There exists a function $\mu(x) > 0$ such that $A_\varphi[\mu(x)] \leq 0$ if and only if $k \leq 0$.
(3) If $\varphi(z) \leq 0$ for some state z, then there is no function $\mu(x) > 0$ such that $A_\varphi[\mu(x)] \leq 0$, that is there is no positive φ-superharmonic function on X.

Declaration of competing interest

The authors declare that they have no conflict of interest.

Data availability

No data was used for the research described in the article.

Acknowledgement

We thank the referee for very useful comments. The first author acknowledges the support given by the Vellore Institute of Technology, Vellore through the Teaching cum Research Associate fellowship (VIT/HR/2019/5944 dated 18th September 2019).

References

[1] V. Anandam, Harmonic Functions and Potentials on Finite or Infinite Networks, UMI Lecture Notes, vol. 12, Springer, 2011.
[2] V. Anandam, M. Damlakhi, Perturbed Laplace operators on finite networks, Rev. Roum. Math. Pures Appl. 61 (2016) 75–92.
[3] A. Ancona, Théorie du Potentiel sur les Graphs et les Variétés, Springer Lecture Notes in Math., vol. 1427, 1990.
[4] C. Araúz, A. Carmona, A.M. Encinas, Dirichlet to Robin maps on finite networks, Appl. Anal. Discrete Math. 9 (2015) 85–102.
[5] H. Bauer, Harmonische Räume und Ihre Potentialtheorie, Lecture Notes in Math., vol. 22, Springer, 1966.
[6] E. Bendito, A. Carmona, A.M. Encinas, Equilibrium measure, Poisson kernel and effective resistance on networks, in: V.A. Kaimanovich, K. Schmidt, W. Woess (Eds.), Random Walks and Geometry, Walter de Gruyter, Berlin, 2004, pp. 363–376.
[7] E. Bendito, A. Carmona, A.M. Encinas, Potential theory for Schrödinger operators on finite networks, Rev. Mat. Iberoam. 21 (2015) 771–818.
[8] E. Bendito, A. Carmona, A.M. Encinas, J.M. Gesto, M. Mitjana, Kirchhoff indexe of a networks, Linear Algebra Appl. 432 (2010) 2278–2292.
[9] T. Biyikoglu, J. Leydold, P.F. Stadler, Laplacian Eigenvectors of Graphs. Perron-Frobenius and Faber-Krahn Type Theorems, Springer Lecture Notes in Mathematics, vol. 1915, 2007.
[10] M. Brelot, Les étapes et les aspects multiples de la théorie du potentiel, in: L' Enseignement Mathématique, vol. XVIII, 1972, pp. 1–36.
[11] A. Carmona, A.M. Encinas, M. Mitjana, Perturbations of discrete elliptic operators, Linear Algebra Appl. 468 (2015) 270–285.
[12] A. Carmona, A.M. Encinas, M. Mitjana, Resistance distances in extended or contracted networks, Linear Algebra Appl. 576 (2019) 5–34.
[13] C. Constantinescu, A. Cornea, Potential Theory on Harmonic Spaces, Springer-Verlag, 1972.
[14] J. Deny, Méthodes Hilbertiennes en Théorie du Potentiel, C.I.M.E., I Ciclo, Stresa, 121–201, Edizioni Cremonese, Rome, 1970.
[15] F. Gantmacher, The Theory of Matrices, vol. 2, AMS Chelsea Publishing, 2000.
[16] M. Keller, D. Lenz, R.K. Wojciechowski, Graphs and Discrete Dirichlet Spaces, Grundlehren der Mathematischen Wissenschaften, vol. 358, Springer, 2021.
[17] P.M. Soardi, Potential Theory on Infinite Networks, Springer Lecture Notes in Mathematics, vol. 1590, 1994.
[18] M. Yamasaki, Discrete potentials on an infinite network, Mem. Fac. Sci. Shimane Univ. 13 (1979) 31–44.
[19] M. Yamasaki, The equation $\Delta u = qu$ on an infinite network, Mem. Fac. Sci. Shimane Univ. 21 (1987) 31–46.